DOCTORAL THESIS

Development of high performance analytical method for DNA fragments by capillary electrophoresis with electrokinetic supercharging preconcentration

（動電過給前濃縮キャピラリー電気泳動法による DNA 断片の高性能分析法の
開発）

XIAOXUE YE

HIROSHIMA UNIVERSITY

NOVEMBER 2013

CONTENTS

Chapter 3: High sensitive analysis of rare earth elements

Chapter 4: High sensitive analysis of DNA fragments by EKS-CGE

ABSTRACT

Development of high performance analytical method for DNA fragments by capillary electrophoresis with electrokinetic supercharging preconcentration

Capillary electrophoresis (CE) has became a popular separation tool after the past decades of successful development. With recognized advantages of inherent instrumental simplicity, rapid analysis, minor sample and solvent consumption in comparison with chromatographic techniques, CE has matured as an established separation technique in several application areas from large biomolecules to small inorganic ions. However, analysts in many industrial and environmental laboratories continue to impede the CE as a routine tool due to the predominance of HPLC, as well as personal inexperience and suspicion of CE. The latter issue is mostly related to insufficient concentration sensitivity which is suffering from minute sample volumes (at the nl level) and short light pathways (typically 25 - 100 µm) for photometric detection. To address this drawback of CE, many efforts of CE developers have been focused on in-line preconcentration techniques. To obtain high sensitivity, it is essential to introduce a large amount of sample, then well focused into a sharp zone prior to separation.

Electrokinetic supercharging (EKS) is an in-line preconcentration technique which implies an extended electrokinetic injection to introduce a great amount of analyte and followed by a tITP stacking step to refocus the injected analytes into a narrow zone. Rare-earth metal ions were used as model analytes to develop a simplified EKS system by a system-induced terminator and optimize electrode setting for a larger amount of analytes. Since the low sensitivity of CGE hinders many applications of DNA analysis

where the sample concentration is usually very low, it was expected that such a advanced EKS system could be proposed in DNA analysis.

In Chapter 1, general introduction of CE including the developing history, wide applications from small ions to biomolecular, basic principles and instrumentation.

In Chapter 2, fundamental studies to understand the formation of terminator zone were undertaken by 2D computer simulation, and this information can be used for designing a simplified EKS mode. Furthermore, to introduce more analyte ions at the injection stage for better sensitivity, the relationship between the electrode configuration and the effective electric field has been discussed.

In chapter 3 and 4, the advanced EKS system and was successfully adopted for the analysis of rare-earth elements and DNA fragments, respectively. In the analysis of DNA fragments by CGE, when the co-ion of BGE took over the role of leading ion, the EKS setup was further simplified. To to amass more analyte ions within the effective electric field, the electrode configuration and position related to capillary end was modified in both CAPI-3300 and Agilent HP^{3D} CE systems whose electrode settings were quite different.

In Chapter 5, as a result of applying a high voltage during injection, very dilute DNA fragments (below 0.2 mg/L) could be damaged in aqueous solution during EKI. By exploring the factors affecting the damage during EKI, it is practical that injection voltage should be kept as low as possible especially for the dilute DNA sample (sub mg/L).

In Chapter 6, after the considerable research for improving the accuracy of the method, factors like electrode configuration and BGE carry-over were investigated. Finally, a nice reproducibility were obtained by optimization. As the important practical implications of this study, all the results were also useful for other analytes by CE.

In Chapter 7, conclusions of this dissertation were described finally.

ABBREVIATIONS

BGE	background electrolyte
CE	capillary electrophoresis
CEC	capillary electrochromatography
CGE	capillary gel electrophoresis
CIEF	capillary isoelectric focusing
CITP	capillary isotachophoresis
CZE	capillary zone electrophoresis
$D_{e/c}$	distance between the electrode and capillary end
EKI	electrokinetic sample injection
EKS	electrokinetic supercharging
EOF	electroosmotic flow
FASI	field-amplified sample injection
HEC	hydroxyethyl cellulose
HPMC	hydroxypropyl methyl cellulose
IEF	isoelectric focusing
ITP	isotachophoresis
LE	leading electrolyte
LIF	laser-induced fluorescence
LOD	limit of detection
MBE	moving boundary electrophoresis

MCE	microchip electrophoresis
MECC	micellar electrokinetic capillary chromatography
MEKC	micellar electrokinetic chromatography
MS	mass spectrometry
PCR	polymerase chain reaction
pI	isoelectric point
RE	rare-earth metal ion
SDS	dodecyl sulfate
SE	supporting electrolyte
TBE	Tris-Boric acid-EDTA
TE	terminating electrolyte
tITP	transient isotachophoresis
Tris	tris(hydroxymethyl) aminomethane
V_{inj}	injection voltage
Vt	injection voltage multiplied by injection time
ZE	zone electrophoresis

Chapter 1: General introduction

1.1 History and applications of electrophoresis

1.1.1 Historical background of electrophoresis

Electrophoresis has been defined as the differential movement of ionized species by attraction or repulsion in an electric field. In practical terms, a positive (anode) and negative (cathode) electrode are placed in a solution containing ions. Then, when a voltage is applied across the electrodes, solute ions of different charge, i.e., anions and cations, will move through the solution towards the electrode of opposite charge.

At the beginning of (in the early) 19th century, Ferdinand Frederic Reuss observed that colloidal clay particles could migrate when an electric field was applied to the solution [1]. These observations are considered to be the origins of what we now call electrophoresis which suggested by Michaelis in 1909 [2]. The name of electrophoresis is derived from the Greek elektron meaning amber (i.e. electric) and phore meaning bearer [3].

Electrophoresis hadn't use as a separation technique until 1937, when Tiselius was able to separate the five most abundant proteins in human serum with relative ease and quantify their levels [4]. Based on such moving boundary electrophoresis (MBE), Tiselius was awarded a Nobel Prize in 1948 for his pioneering work on protein separation by electrophoresis.

Although MBE was performed by Tiselius, the separation efficiency still limited due to the thermal diffusion and convection and so only low voltages can be used. Later, improvements came up to against with convection in 1950s, many anti-convective media, such as starch polyacrylamide and agarose gel, have been used in traditional electrophoresis to reduce diffusion

and limit convective transport. Rather than charged molecules moving freely through solutions, the new methods used solid or gel matrices to separate compounds into discrete and stable bands (zones); Tiselius dubbed these methods "zone electrophoresis"(ZE). The analytes are completely separated from each other in ZE, while in MBE, only the heads and tails represent clean zones. In 1955, the discovery of starch gels that has the excellent resolving power was a major improvement in the electrophoresis of proteins [5]. Smithies separated haptoglobins in sera on slabs of starch gels. The starch gels soon yielded place to polyacrylamide gels which introduced by Raymond and Weintraub in 1959 [6]. They developed the polyacry lamide gel electrophoresis technique, which has been refined to produce a highly porous matrix for biological study. Owing to introduce starch gel and acrylamide gel as an electrophoretic substrate, zone electrophoresis was widespread in biochemistry.

Isoelectric focusing (IEF) was developed by Svensson in the early 1960s [7]. IEF involves the migration behavior of ampholytic molecules in immobilized pH gradient gel. Proteins can be positively charged or negatively charged in a pH region depending on its isoelectric point (pI) and so will migrate towards the cathode (negative) or anode (positive). When they migrate through the medium, their overall charge will decrease until reaches the pH region (at their pI) where they have no net charge. As a result, the proteins focused into sharp stationary bands with each protein positioned at a point in the pH gradient corresponding to its pI. At the beginning of 1970s, especially due to the introduction of the analytical counterpart in polyacrylamide gels [8], IEF enjoyed such a marked growth as to soon become a leading separation technique in all fields of biological sciences.

The method spread slowly until the advent of effective zone electrophoresis methods in the 1940s and 1950s, which used filter paper or gels as supporting media. By the 1960s, increasingly sophisticated gel

electrophoresis methods made it possible to separate biological based on minute physical and chemical differences, helping to drive the rise of molecular biology. Gel electrophoresis and related techniques became the basis for a wide range of biochemical methods, such as protein fingerprinting, Southern blot and similar blotting procedures, DNA sequencing, and many more.

1.1.2 Development of CE

The major bugbear with all electrophoresis is the generation of Joule heat with its many detrimental effects on the electrophoretic separations and resolution. This deficiency is effectively got over by the introduction of capillary electrophoresis (CE).

CE was firstly done by Hjerten who used a glass tube with a rather large diameter (1-3 mm) as the separation channel and subsequent detection of the separated compounds by ultraviolet absorption [9]. In his communication, separation of serum proteins, inorganic and organic ions, peptides, nucleic acids, viruses, and bacteria are described. A new trail in CE was done by Virtanen, who is the first to exploit the anti-convective properties of stationary narrow bore tubes of 0.2-0.5 mm ID and 50-100 mm length.

CE did not become popular until 1981, when Jorgenson and Lucaks reported the high-resolution power of capillary zone electrophoresis (CZE) [10]. They demonstrated that by increasing the surface to the volume ratio, e.g. using a capillary with only 75 μm I.D., the heat generated by electrophoresis was readily lost. Very high voltages could then be employed to enable high speed analyses with on-line detection and both exceptional resolution, and enhanced sample sensitivity. By applying voltages up to 30 kV across 1 m long open silica capillary equipped with a fluorimetric detector, they separated and detected fluorescamine derivatized a mino acids and peptides. The efficiency of the separation reached the limits of the theoretical model where diffusion was considered as the only dispersion effect.

Very short after Jorgenson's first publication, by adding surfactants to the background electrolyte (BGE), Terabe introduced a novel variant in 1984, which called micellar electrokinetic chromatography (MEKC) [11]. When the surfactant like SDS at the concentration above its critical micellar concentration (ca. 8.2 mM), the micelles formed. Although the efficiency of MEKC is a little below that of CZE with typically N < 200 000 plates/m, it is the only electrophoretic mode that both charged and un-charged molecules can be separated at the same time.

In 1983 Hjertén filled he capillary (150 μm ID) with polyacrylamide gel, which so called so called capillary gel electrophoresis (CGE), to eliminate adsorption of proteins to the capillary inner wall and had proven to be quite efficient in separation of proteins [12]. In 1987, Cohen and Kager use elastic quartz capillaries successfully separated DNA fragments, proteins and oligomeric RNA by CGE [13]. In 1990 Lux and Yin developed the Column preparation techniques, pretreat the inner wall of capillary with linear polymer matricesinside and initiated polymerization by γ ray, which have achieved particularly efficiency on the separation of DNA and RNA [14, 15]. Then CGE combined with laser induced fluorescence became the preferred method for DNA sequencing due to its nice LOD comparing with plate electrophoresis [16]. Conventional IEF process was also transferred into the capillary system by Hjertén [17].

With the deepening of the capillary electrophoresis, other separation modes, such as capillary isoelectric focusing (CIEF), capillary isotachophoresis (CITP), and capillary electrochromatography (CEC), were also introduced. From 1989, after availability of the first commercial apparatus and the use of high sensitive on-line detector, the practices and theories of CE are blooming all over the world.

The development of theoretical study also greatly promotes the further improvement and application of CE. Roberts et al. and Giddings et al. quantitatively analyzed the factors affecting peak dispersion [18, 19]. Andreev

et al. proposed a mathematical model, which discussed influence of electroosmotic flow (EOF) on the efficiency of CE [20]. Gas et al. proposed a mathematical model to describe the simulation of peak profiles in capillary zone electrophoresis taking wall adsorption into account [21].

Although numerous developments have been made in CE, the technique is still in a developing and growing stage. Undoubtedly, as more researchers use CE and disseminate results, it will become a standard technique in the separation science.

1.1.3 Applications of CE

After a steady growth in 1990s, CE has been widely used many fields. Routine methods were established in numbers of applications including pharmaceuticals, analysis of DNA, proteins, peptides, chiral compounds, clinical samples, and small ions.

1.1.3.1 In biotechnology field

DNA analysis

Now CE replaced slab gel electrophoresis to become the dominant technique in DNA analysis. DNA analysis included the analysis of base, nucleosides, nucleotides, oligonucleotides, ssDNA, dsDNA (DNA fragments and PCR products). CZE and micellar electrokinetic capillary chromatography (MECC) were usually used for separation of base, nucleosides, nucleotides and oligonucleotides, and CGE could be used for DNA fragments analysis. Different sizes of DNA fragments have the similar electrophoretic mobilities since each increase in size is accompanied by a corresponding increase in negative charges. So separation by mobility is difficult, but which is achieved

by using sieving matrix. DNA analysis of the major applications of the CE, CE - MS was applied to DNA analysis long ago [22].

Proteins analysis

As the complexity of the protein, the separation of the protein is consistent with challenging topic. The emergence of CE found a new way for proteins analysis, and it has been used for this purpose for over three decades. The analysis is complex also due to the different purpose. Molecular weight determination is one of the significant works in biochemical studies, SDS-CGE model is usually used for this. CE is superior to other methods such as ultracentrifugation, mass spectrometry, gel exclusion chromatography, due to its advantages of less sample consumption (several nl), easy Automation and accuracy. CIEF commonly used in the determination of the isoelectric point of the protein.

1.1.3.2 Environment analysis

In recent years, CE also showed fast development trend in environmental analysis, and increasingly used in the separation and detection of real samples from the environment. The main sources of environmental samples are water, soil and air. The detection of water quality is one of the most widely application of CE. CE uses water medium which is very close to the organisms, plants and natural background, which can avoid some sample treatment processes and shorten the separation period.

Detection of heavy metal ions in real sample can provide many important informations for environmental monitoring. Comparing with traditional methods including atomic absorption, ion chromatography, liquid chromatography (HPLC), electrochemical method, and mass spectrometry, CE has the

advantages of small solvent consumption, high separation efficiency and simple operation and received increasing recognition.

1.2 Principles of CE

1.2.1 Electrophoresis theory

The theory that governs electrophoresis is directly applicable to CE and can be dealt with very briefly, with reference to a few equations. Electrophoresis is the movement or migration of ions or solutes under the influence of an electric field. Separation by electrophoresis is based on differences in solute velocity. The velocity of an ion can be expressed as:

$$\upsilon = \mu_e E \qquad (1.1)$$

Where υ is ion migration velocity (ms^{-1}), μ_e is electrophoretic mobility (m^{2}V^{-1}s^{-1}) and E is electric field strength (Vm^{-1}).

The electric field is simply a function of the applied voltage divided capillary length (in volts/cm). The mobility of an ion in a given medium, which is constant, is characteristic of the ion. It is determined by the electric force that acts in favour of motion, balanced by its frictional drag through the medium acts against motion. Due to the balance of these forces, during electrophoresis is a steady state. Therefore, the mobility is a constant for a given ion under a given set of conditions. The equation describes the mobility in terms of physical parameters:

$$\mu_e = \frac{q}{6\pi\eta r} \qquad (1.2)$$

Where q is the ion charge, η is the solution viscosity and r is the ion radius. The charge on the ion is fixed for fully dissociated ions, such as strong acids or small ions, but can be affected by pH changes in the case of weak acids or bases. The ion radius can be affected by the counter-ion present or by any complexing agents used. From this equation it is evident that small, but highly charged species confer greater mobility, whereas large, but minimally charged species confer lower mobility.

The electrophoretic mobility is probably the most important concept to understand in electrophoresis. This is because electrophoretic mobility is a characteristic property for any given ion or solute and will always be a constant. What is more, it is the defining factor that decides migration velocities. This is important, because different ions and solutes have different electrophoretic mobilities, so they also have different migration velocities at the same electric field strength. It follows that, because of differences in electrophoretic mobility, it is possible to separate mixtures of different species by using electrophoresis.

1.2.2 Electroosmotic flow (EOF)

A vitally important feature of CE is the bulk flow of liquid in the capillary and is a consequence of the surface charge on the interior capillary wall. As shown in Fig. 1.1, the surface of the inside of a typical uncoated fused-silica capillary has ionisable silanol groups, which are in contact with the buffer during CE. These silanol groups readily dissociate, giving the capillary wall a negative charge. Therefore, when the capillary is filled with buffer, counterions (cations, in most cases), which build up near the surface to maintain charge balance, form the double-layer and create a potential difference very close to the wall. This is known as the zeta potential.
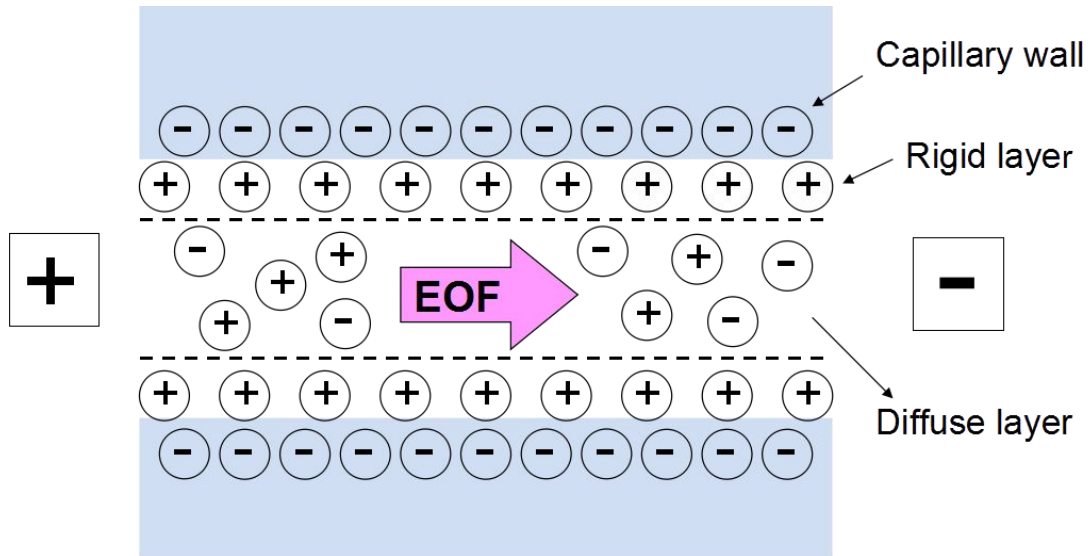
Figure 1.1: EOF due to Applied Voltage

When a voltage is applied across the capillary, cations forming the diffuse double-layer are free to migration towards the cathode, carrying the bulk solution with them. The magnitude of the EOF can be expressed in the terms of mobility by:

$$\mu_{EOF} = \frac{\varepsilon\zeta}{\eta} \qquad (1.3)$$

Where μ_{EOF} is the mobility of EOF, ε is dielectric constant, ζ is zeta potential and η is solution viscosity, respectively.

The zeta potential is essentially determined by the surface charge on the capillary wall. Since this charge is strongly pH dependent, the magnitude of the EOF varies with pH. At high pH, where the silanol groups are predominantly deprotonated, the EOF mobility will be significantly greater than at low pH

where they become protonated. The zeta potential is also dependent on the ionic strength of the buffer, as described by double-layer theory. Increased ionic strength results in double-layer compression, decreased zeta potential, and reduced EOF.
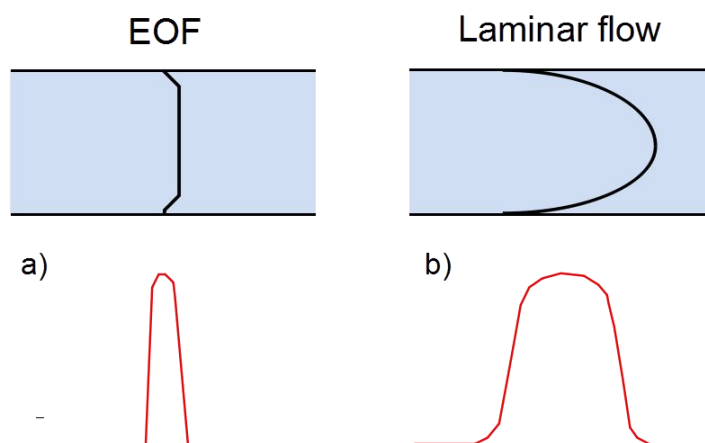
Figure 1.2: Flow profile and corresponding solute zone

A further key feature of EOF is the flat profile of the flow, as depicted in Figure 1.2. The flow is nearly uniform because the driving force of the flow is uniformly distributed along the capillary and there is no pressure drop within the capillary. The flat profile of EOF is beneficial since it minimizes zone broadening, leading to high separation efficiencies that allow separations on the basis of mobility differences as small as 0.05 %. This is in contrast to that generated by pressure which yield a parabolic or laminar flow profile due to shear force at the wall.

1.2.3 Analytical parameters

1.2.3.1 Mobility and migration time

The time required for a solute to migrate to the point of detection is called the "migration time", and is given by the quotient of migration distance and velocity. The migration time and other experimental parameters can be used to calculate the apparent solute mobility using:

$$\mu_a = \mu_e + \mu_{EOF} = \frac{l}{tE} = \frac{lL}{tV} \qquad (1.4)$$

Where l, E, L, t and V represents as effective capillary length (to the detector), electric field, total capillary length, migration time and applied voltage, respectively. In the presence of EOF, the measured mobility is called the apparent mobility, μ_a. The effective mobility, μ_e, can be extracted from apparent mobility by independently measuring the EOF using a neutral marker (e.g. DMSO, mesityl oxide, and acetone) that moves at a velocity equal to the EOF. There are significant relationships between analyte and solute mobility. The database of mobility and pKa of calculated 500 ions was almost compiled by Hirokawa [23] which may give the important information in the computer simulation of CE.

1.2.3.2 Dispersion

Separation in electrophoresis is based on differences in solute mobility that necessary to resolve two zones and is dependent on the length of the zones. Dispersion should be controlled because it increases zone length and the mobility difference necessary to achieve separation. As we know, dispersion in CE can have a number of contributors including longitudinal diffusion, Joule heating, injection length, sample adsorption, mismatched conductivities of sample and buffer, unleveled buffer reservoir and detector cell size. The total variance of dispersion contributed by these sources be given to:

$$\sigma_T^2 = \sigma_{DIF}^2 + \sigma_{INJ}^2 + \sigma_{TEMP}^2 + \sigma_{ADS}^2 + \sigma_{DET}^2 + \sigma_{Electrodispersion}^2 + ... \quad (1.5)$$

Where the subscripts refer to diffusion, injection, temperature gradients, adsorption, detection, and electrodispersion, respectively.

1.2.4 Separation efficiency and Resolution

Separation in CE is primarily described by efficiency that is often expressed in number of theoretical plates, N. Under ideal conditions the sole contribution to solute-zone broadening in CE can be considered to be longitudinal diffusion (along the capillary). Thus the equation for theoretical plate number is:

$$N = \frac{\mu_e Vl}{2DL} = \frac{\mu_e El}{2D} \quad (1.6)$$

Where D is the diffusion coefficient of an analyte. In practice, the theoretical plate number can be determined directly from an electropherogram:

$$N = 5.54 \left(\frac{t}{W_{1/2}}\right)^2 \quad (1.7)$$

Where t is migration time, $W_{1/2}$ is temporal peak width at half height. The measured efficiency in equation 1.5 is usually lower than the calculated efficiency, equation 1.4. This is because the theoretical calculation accounts only for zone broadening due to longitudinal diffusion.

Resolution of sample components is the ultimate goal in separation science. The resolution of two components can be expressed as:

$$R = \frac{2(t_2 - t_1)}{W_1 + W_2} \qquad (1.8)$$

Where t represents migration time, w is base line peak width (in time) and subscripts 1 and 2 refer to the two solutes.

1.3 Instrumental and operational aspects of CE

1.3.1 Typical CE separation system

The instrumentation required for CE is simple in design, as shown in Fig. 1.3 illustrates. A CE apparatus consists of the following main parts: (1) devices for fixing the capillary; (2) devices for interchanging the capillaries; (3) electrodes connected to a high-voltage power supply; (4) devices for sampling; (5) the detector. For a typical CE experiments, firstly we should fill the capillary with electrolyte, then remove the inlet buffer reservoir and replace it with sample vial. The Second step is loading the sample by applying either voltage or pressure. After replacing the buffer reservoir, an electric potential is applied across the capillary and the separation is performed. Optical (UV-visible or fluorometric) detection of separated analytes can be achieved directly through the capillary way near the opposite end.
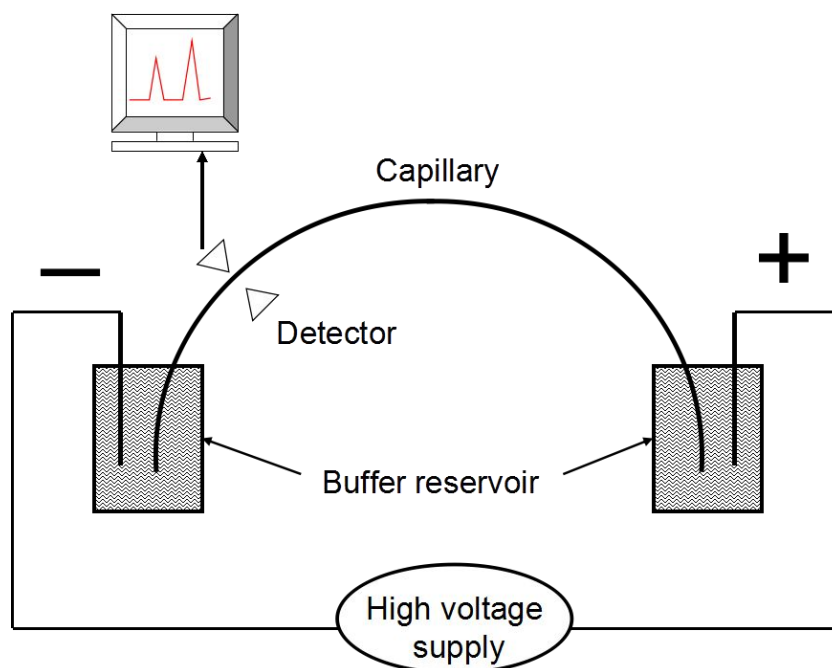
Figure 1.3: Schematic of a typical CE instrument

1.3.2 Sample injection

In CE only minute volumes of sample are loaded into the capillary in order to maintain high efficiency. Usually, the sample plug length should be less than 1 or 2 % of the total length of the capillary. The two most common injection methods are hydrodynamic and electrokinetic.

Hydrodynamic injection

Hydrodynamic sample injection is the most widely used method. It can be accomplished by application of pressure at the injection end of capillary, vacuum at the exit end of the capillary, or by siphoning action obtained by elevating the injection reservoir relative to the exit reservoir. The volume of sample loaded can be calculated by Hagen-Poiseuille equation:

$$\mathrm{Volume} = \frac{\Delta P d^4 \pi t}{128 \eta L}$$

<div align="right">(1.9)</div>

Where *ΔP* is pressure difference across the capillary, *d* id capillary inside diameter, *t* is injection time, *η* is buffer viscosity and *L* is the total length of capillary. If sensitivity is not limiting, the smallest injection lengths possible should be used. However, injection reproducibility is usually diminished with short injection times due to instrumental limitations.

Electrokinetic injection

Electrokinetic injection is performed by replacing the injection-end vial with the sample vial and applying the voltage. During the injection, analyte enters the capillary by both migration and pumping action of the EOF. A unique property of electrokinetic injection is that the quantity loaded is dependent on the mobility of the individual solutes. Discrimination occurs for ionic species since the more mobile ions are loaded to greater extent than those that are less mobile. The quantity injected, Q (g or moles), can be calculated by the equation:

$$Q = \frac{(\mu_e + \mu_{EOF}) V \pi r^2 C t}{L}$$

<div align="right">(1.10)</div>

Where μ_e represents the electrophoretic mobility of the analyte, μ_{EOF} is EOF mobility, *V* is voltage, *r* is capillary radius, *C* is analyte concentration, *t* is injection time and *L* is the total length of capillary. Although electrokinetic injection is generally not as reproducible as hydrodynamic injection, it is requires no additional device and is advantageous when viscous media or gels are employed in the capillary.

1.3.3 Separation

Capillary and capillary conditioning

The used capillaries are normally fused silica capillaries, which are coated with a protective layer of polyimide to make them strong and easy to handle. Before use, a small portion of this coating is removed to form an optial window for detection. Most commonly, capillaries are 25-100 cm long with 50 or 75 µm I.D..

Power supply

In most common case, the power supply can provide up to about 30 kV DC. Stable regulation of the voltage is required to maintain high migration time reproducibility. It is better to control the generated current in the range of 10 - 100 µA by selecting the electrolyte ionic strength, since operations with currents above this level may cause unstable and irreproducible operating conditions. The over current affects separation due to Joule heating which alter buffer viscosity and migration time. Many commercial instruments are possible to do operation by constant voltage (most common), constant current or constant power modes.

1.3.4 Detection

CE has many potential detection methods, such as optical absorption, electrochemical, conductivity, and chemical luminescence, phosphorescence, fluorescence, mass spectrometry, etc. So far, the UV-visible absorption is most common among these methods.

UV-visible absorption

UV-visible detection is widely used in CE because of its nearly universal detection nature. The detection wavelength below 200 nm to through the visible spectrum is available. The high efficiency observed in CE is due to the on-column detection which is quilt convenient, only need to remove on a flexible transparent protective coating near the outlet end of the capillary, so that the optical path can be aligned with the transparent parts. The separation is still going on while passing the detection window. As with all optical detectors, the width of the detection region should be shall relative to the solute zone width to maintain high resolution.

Laser-induced fluorescence (LIF)

Since capillary diameter is small (tens to hundreds μm), volume of on-Column detection cell is only tens to hundreds nL, when conventional UV detection method cannot meet the high sensitivity requirements, high sensitive detection method is required. LIF is extremely sensitive and can even achieve single-molecule detection level. But the detector is more complex and expensive comparing with UV-visible absorption, and usually sample derivatization is required. Currently, LIF has been widely used in analysis of amino acids, drugs, DNA and protein.

1.4 Research project and purpose

Insufficient concentration sensitivity is an inherent limitation of CE analysis, suffering from minute sample volumes and short light pathways for photometric detection. Applying an individual stacking technique does not always afford a requested increase in sensitivity, especially when the

quantification of ultra-low analytes is the target. To meet this challenge, it is essential to introduce a large amount of sample to be then well focused into a sharp zone prior to separation. However, the existing high-sensitivity methodology came across certain critical conditions, e.g. injection of a high-conductivity solution and water plug before sample introduction [8] or an hour-long injection time [24]. These might hinder its practical implementation. EKS is a powerful and practical online preconcentration approach combining electrokinetic sample injection (EKI) with transient ITP (tITP) applied for various analytes. The merit of EKS is that tITP step could remedy the shortcoming of EKI, an overloaded long sample zone could be effectively refocused implies an extended electrokinetic injection to introduce a great amount of analyte followed by a tITP stacking step to refocus the injected analytes into a narrow zone.

Our group has been performing a systematic research on improving the concentration power of EKS. The following studies demonstrated that the electrode configuration and position significantly affect the efficiency and reproducibility of sample injection [25, 26] EKS and optimized electrode configuration applied for analysis of rare-earth elements, which is highly improve the sensitivity. In addition, the information of a system-induced terminator (i.e. the hydrogen ion) was used to design a simplified EKS mode.

The low sensitivity of CGE hinders many applications of DNA analysis where the sample concentration is usually very low. Therefore, we try to proven potentially universal applicability of EKS in DNA analysis. But the most difficult point is the viscous BGE will reduce the mobility of leading ion. But it was found that by using an ultralow-viscosity not only the sieving ability was kept by additive of mannitol, but also EKS performance was promoted due to the generated leading ion of borate polyanion in TBE buffer for ITP preconcentration.

During the DNA analysis by CE, it was found that DNA fragments were decomposed during EKI. It is well known that either high-energy ionized

particle or lower energy electrons (less than 1 eV to 20 eV) also induced single- and double-strand breaks in DNA via dissociative electron attachment [27]. In order to show the possibility of DNA damage by high V_{inj} and propose a optimal injection voltage, the different injection conditions were discussed in analysis of DNA step ladder samples.

On the other hand, in DNA analysis the high diluted sample contamination by a viscous background electrolyte (BGE), carried unintentionally by the capillary or the electrode (along with the contamination from laboratory environment), significantly impairs injection efficiency. To reduce the contamination, the capillary and the electrode should be rinsed thoroughly by pure water before sampling. Therefore considerable research to addressing these issues and the optimized experimental procedure to improve injection efficiency and gain good EKS repeatability were discussed in this study.

1.5 Reference

[1] Reuss, F. F., *Memoires de la Société Imperiales de Naturalistes de Moskou* 1809, 2, 327-337.

[2] Michaelis, L., *BioChem. Zeitschrift* 1909, 16, 81-86.

[3] Righetti, P. G., *J Chromatogr. A* 2005, 1079, 24-40.

[4] Tiselius, A., Trans. Faraday Soc. 1937, 33, 524-531.

[5] Smithies, O., *Biochem. J.* 1955, 61, 629-641.

[6] Raymond, S., Weintraub, L. S., *Science* 1959, 130, 711-711.

[7] Sevensson, H*., Acta. Chem. Scand.* 1961, 15, 325-341.

[8] Righetti, P. G., Drysdale, J. W., *Biochim. Biophys. Acta* 1971, 236, 17-28.

[9] Hjertén, S., *Chromatogr. Rev.* 1967, 9, 122-219.

[10] Jorgenson, J. W., Lukacs, K. D., *Clin. Chem.* 1981, 27, 1551-1553.

[11] Terabe, S., Otsuka, K., Ichikawa, K., Tsuchiya, A., Ando, T., *Anal. Chem.* 1984, 56, 111-113.

[12] Hjertén, S., *J. Chromatogr.* A 1983, 270, 1-6.

[13] Cohen, A. S., Karger, B. L., *J. Chromatogr.* 1987, 397, 409-417.

[14] Lux, J. A., Yin, H. Y., Schomburg, G., *J. High Resolut. Chromatogr.* 1990,13, 436-437.

[15] Lux, J. A., Yin, H. Y., Schomburg, G., *Chromatographia* 1990, 30, 7-15.

[16] Drossman, H., Luckey, J. A., Kostichka, A. J., D'Cunha, J. Smith, L. M., *Anal. Chem.* 1990, 62, 900-903.

[17] Dovichi, N. J., *Electrophoresis* 1997, 18, 2393-2399.

[18] Roberts, G. O., Rhodes, P. H., Snyder, R. S., *J. Chromatogr. A* 1989, 480, 35-67.

[19] Giddings, J.C., *J. Chromatogr. A* 1989, 480, 21-33.

[20] Andreev, V. P., Lisin, E. E., *Electrophoresis* 1992, 13, 832-837.

[21] Bohuslav, G., Milan, Š., Andreas, R., Ernst, K., *Electrophoresis* 1995, 16, 958-967.

[22] Wolf, S. M., Vouros, P., *Anal. Chem.* 1995, 67, 891-900.

[23] Hirokawa, T., Nishimo, M., Kiso, Y., *J. Chromatogr. A* 1983, 271, D1-D106.

[24] Breadmore, M. C., *Electrophoresis* 2008, 29, 1082-1091.

[25] Hirokawa, T., Koshimidzu, E., Xu, Z. Q., *Electrophoresis* 2008, 29, 3786-3793.

[26] Xu, Z. Q., Koshimidzu, E., Hirokawa, T., *Electrophoresis* 2009, 30, 3534-3539.

[27] Berdys, J., Anusiewicz, I., Skurski, P., Simons, J., *J. Am. Chem. Soc.* 2004, 126, 6441-6447.

Chapter 2: Optimization of injection process

2.1 Introduction

As a popular separation tool, CE exhibits its flexible capabilities in a diversity of application areas (from small ions to biomolecules), with recognized advantages of high resolution and analytical speed. CE is also an environment friendly analytical tool due to its minimum consumption of sample and chemicals. However, because of minute sample amounts and short light-path (i.e. id of capillary) when using UV absorption detection, conventional CE has a shortcoming of low concentration sensitivity in comparison with HPLC and ICP, which have been commonly applied in industrial and environmental fields for routine analysis. To address this drawback of CE, various high-sensitivity methods have been developed in the past decades [1, 2] for in-, on- and off-line preconcentration.

In these in-line preconcentration approaches, including electrokinetic supercharging (EKS)-CZE [3, 4], electrokinetic sample injection (EKI) is widely used to enrich a low concentration sample in a very simple and effective way when the conductivity of sample is much lower than that of BGE. Chien and Burgi contributed many initial studies on EKI to elucidate the stacking mechanism and to quantify the injected amounts [5, 6]. In EKI, the sample introduction process is driven by a combined effect of electrophoretic mobility and EOF [3] and has an intrinsically stacking character when the sample is dilute (as in field amplified sample injection).

As described in our recent related study [7], the efficiency of EKI is strongly related to the electrode configuration and setting, and the injected sample amount can be increased over ten times by extending the distance between an electrode and a capillary end ($D_{e/c}$). From computer simulation [9],

it was found that the distribution of non-uniform electric field in the sample vial determined the injected amount. By using conventional electrode configuration (with short distance), the effective electric field is limited in a small volume of the sample stocked in a vial. Therefore, most of analytes could not be introduced into the capillary in spite of long injection time. This is because the dispersion velocities of the analytes are much smaller than the electrophoretic velocity. The longer the $D_{e/c}$, the greater amount of sample was introduced. Based on computer simulation, we described the dynamic change of the analyte concentration, nonuniform potential, pH and counter ion concentration at two electrode configurations, capillary inside and parallel to the electrode.

2.2 Electrokinetic supercharging

2.2.1 Transient isotachophoretic stacking

In basic tITP arrangement, the sample is introduced between LE and terminating electrolyte (TE), matching the condition that the mobility of analyte (μ_A) is lower than that of the leader (μ_L) but higher than that of terminator (μ_T). Under such circumstances, sample ions are always kept in close between the supporting electrolytes and separated as adjoining successive zones. Other features of ITP process are that the LE, sample, and TE exist in a steady-state with the same migration velocity, and the sample zone is not diluted by the BGE and broadened during the temporary ITP stage. Furthermore, the concentration of analytes would be adjusted and increased according to Kohlrausch regulating function [8]. This follows from a simple equation:

$$C_A = KC_L \qquad (2.1)$$

Where subscript A and L refer to the analyte and LE, respectively. For strong

electrolyte systems consisting of univalent compounds, the following K is determined by the ionic mobilities of the analyte, the counter-ion of BGE (μ_Q), and the leader:

$$K = \frac{\mu_A(\mu_L + \mu_Q)}{\mu_L(\mu_A + \mu_Q)} \qquad (2.2)$$

Accordingly, tITP presents a familiar sample preconcentration approach combined with zone electrophoresis [9–14].

2.2.2 Modes of transient isotachophoresis

The functions of a stacker could perform the additional electrolyte(s), a macro component(s) of the sample and/or the co-ion of the BGE, operating in a single- or a coupled-capillary arrangement [15]. As already stated above, the most common mode of tITP is when the LE and TE are introduced before and after the sample zone independently from the sample and BGE (Fig. 2.1). In some cases, however, it is practical to involve only one supporting electrolyte, TE or (LE), if the co-ion of BGE may take over the role of LE (or TE), as displayed by traces a2 and a3, respectively. The three modes shown in Fig. 3a are called separation medium-induced tITP [16,17]. When the major constituent in the sample is used as a leading or a terminating ion, the BGE's co-ion simultaneously take the complementary part in attaining tITP. Occasionally, two macro components could work as leader and terminator to achieve stacking of co-existing micro constituents. Such sample-induced types of tITP are assembled in Fig. 2.1b [18–21]. From common sense, the leading stacker as the ion of highest mobility should be introduced before the sample zone and the terminator. The fact that this is not always true and the leader could also be placed after the sample zone or even mixed with the terminator

comes from our studies [22,23]. In experiments aimed on the preconcentration of the lanthanide cations, the leading ion, i.e. K$^+$, was injected after the sample. Such a tITP mode can be understood as the ion of leading type enters the sample zone, rapidly migrates and becomes accumulated before it due to encountering the high potential gradient in this zone. Fig. 2.2 is a simulated representation of a given tITP system. While this preconcentration process mayhave some limitations, the stacking mechanism was found to be an intrinsic tITP.
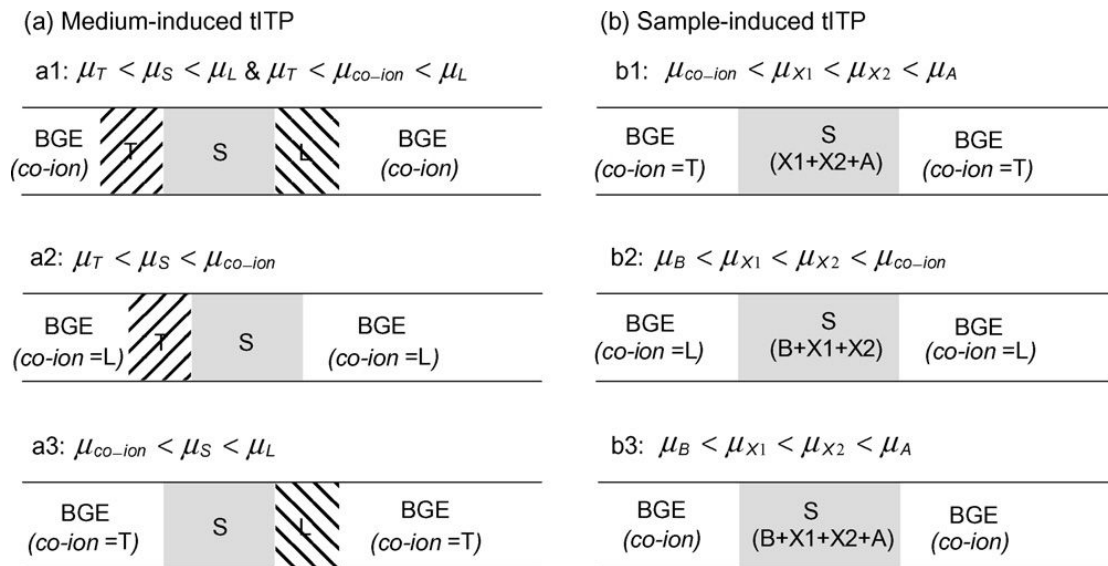

(a) Medium-induced tITP

a1: $\mu_T < \mu_S < \mu_L$ & $\mu_T < \mu_{co-ion} < \mu_L$

| BGE (co-ion) | T | S | L | BGE (co-ion) |

a2: $\mu_T < \mu_S < \mu_{co-ion}$

| BGE (co-ion =L) | T | S | BGE (co-ion =L) |

a3: $\mu_{co-ion} < \mu_S < \mu_L$

| BGE (co-ion =T) | S | L | BGE (co-ion =T) |

(b) Sample-induced tITP

b1: $\mu_{co-ion} < \mu_{X1} < \mu_{X2} < \mu_A$

| BGE (co-ion =T) | S (X1+X2+A) | BGE (co-ion =T) |

b2: $\mu_B < \mu_{X1} < \mu_{X2} < \mu_{co-ion}$

| BGE (co-ion =L) | S (B+X1+X2) | BGE (co-ion =L) |

b3: $\mu_B < \mu_{X1} < \mu_{X2} < \mu_A$

| BGE (co-ion) | S (B+X1+X2+A) | BGE (co-ion) |

Fig. 2.1: Different modes of tITP, and the relationship between the effective mobilities: (a) medium-induced; (b) sample-induced. L = leading electrolyte; S = sample; T = terminating electrolyte.
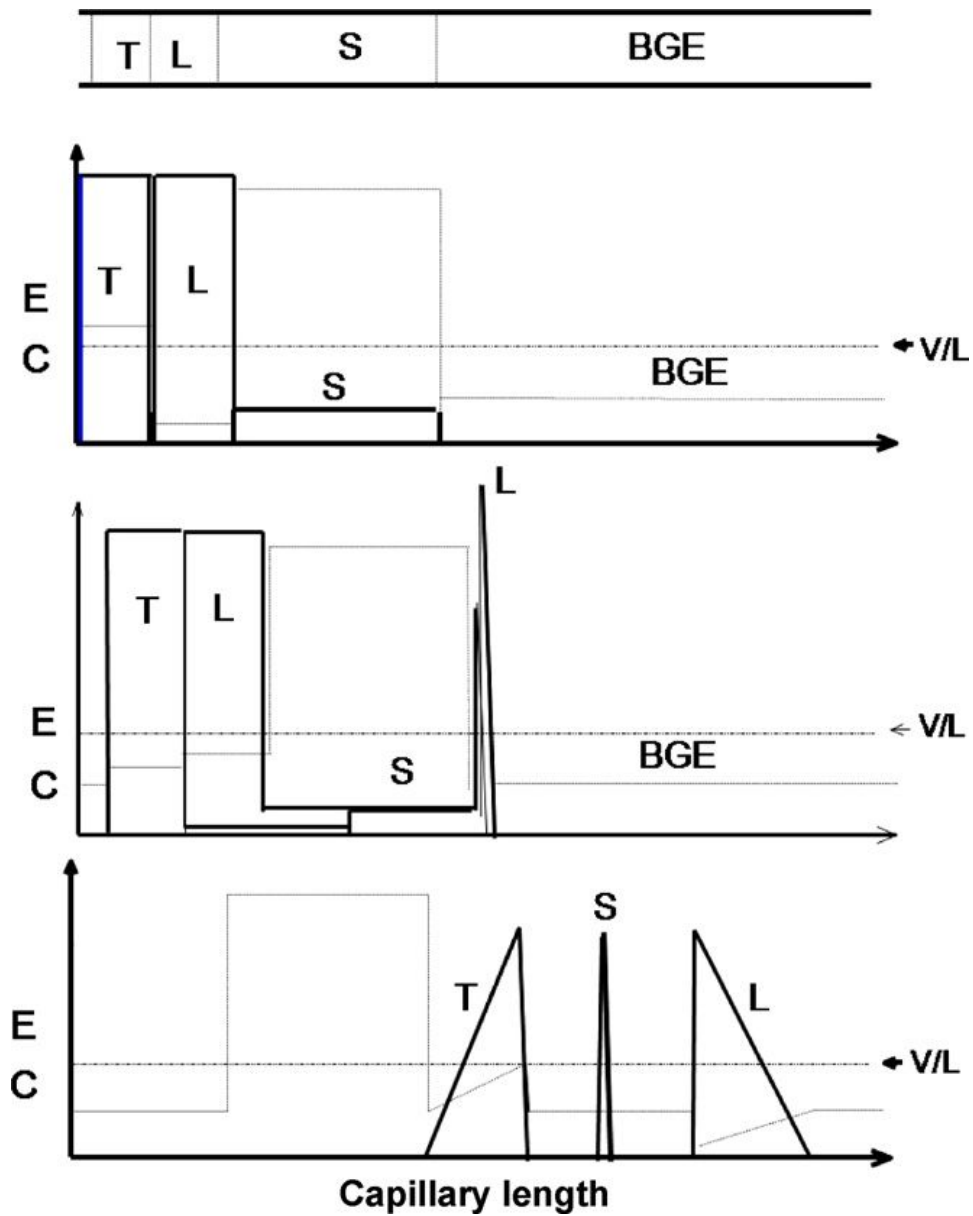
Fig. 2.2: tITP preconcentration and zone electrophoretic separation with LE added after the sample zone. Designations: L, S, and T, as in Fig. 2.1; V/L, average potential gradient along the capillary. Dashed and solid lines are profiles of potential gradient (E) and concentration (C), respectively.

2.2.3 Computer simulation [3]

For computer simulation, SIMUL (Version 4) by Gaš [24] and CFD-ACE (Version 6.6, CFDRC, Huntsville, AL, USA) were used. The former was for one-dimensional simulation. Although the latter software enabled threedimensional simulation, a two-dimensional model was used in this study to reduce calculation time. The mobilities of the analytes were $50×10^{-5}$ (m50$^+$), $40×10^{-5}$ (m40$^+$), $30×10^{-5}$ (m30$^+$), $20×10^{-5}$ (m20$^+$), $10×10^{-5}$ (m10$^+$), and 0 (m0) $cm^2V^{-1}s^{-1}$. For the simulation by SIMUL, m50$^+$, m30$^+$, and m10$^+$ were used. The counter ion of the simulated sample was 0.1mM acetic acid in both cases. The used SE was a mixture of 30mM creatinine (m_0= $37.2×10^{-5}$ $cm^2V^{-1}s^{-1}$, pKa = 4.828) and 30 mM acetic acid (m_0 = $42.4×10^{-5}$, pK_a = 4.756). The L was a mixture of 30 mM potassium hydroxide and 60mM acetic acid (pH 4.8). All simulations were carried out using PCs (Pentium Xeon, 2 GHz clock).

Computer simulation was carried out using two models: In the first model for the SIMUL program, infinite volume was assumed for the sample reservoir to see the difference of preconcentration and separation behavior between simple EKI and EKS. Simulation was continued up to 600 s in migration time under a constant current of 200 A/m^2 (1.58 μA for a capillary with 100 μm ID). The other simulation condition for SIMUL was that capillary length L = 10 cm, injection plug length of L was 0.5 cm, and the space step was 0.002 cm. Operational procedure for EKS-CZE is shown schematically in Fig. 2.3. After filling the separation capillary with the supporting electrolyte (SE) for CZE, the L was filled. Then the sample was electrokinetically injected for a certain time (opposite reservoir was filled with SE) and then the T was filled. Migration started after replacing both reservoirs with those containing SE. SIMUL was used for the simulation of the EKI stage (stage 2 in Fig. 2.3) using various analytes. Due to the limitation in the number of treatable ionic species in SIMUL, a mixture of three analytes (mixture 1) was simulated containing 0.01 mM m50$^+$, m30$^+$, and m10$^+$. The counterion was 0.1 mM acetic acid (pH 4.73).
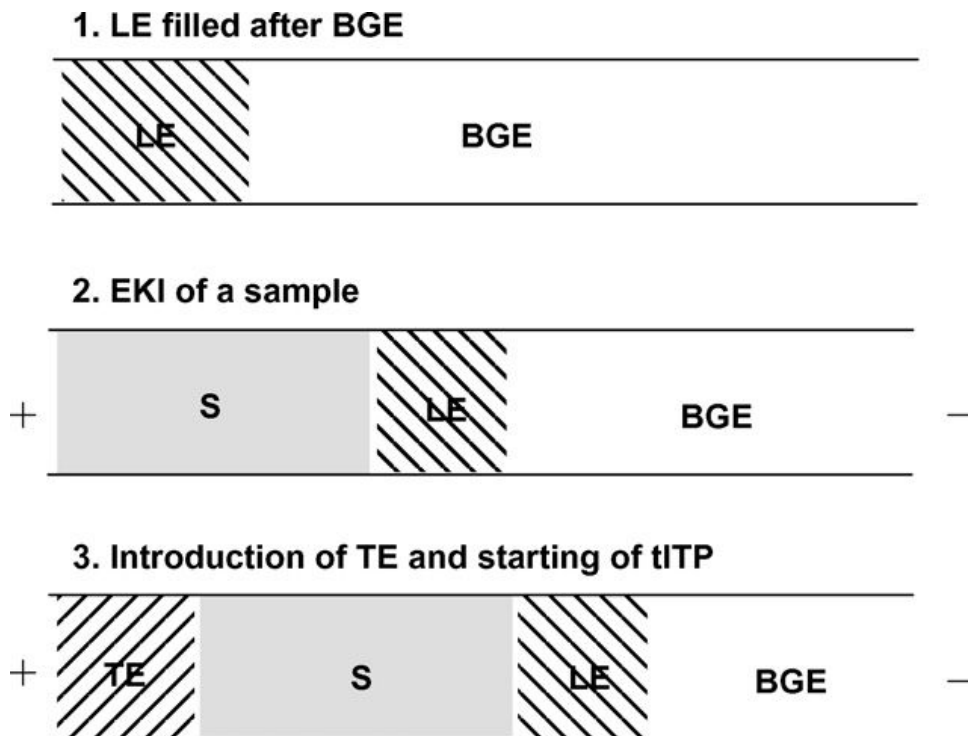
Figure 2.3: Operation of EKS. SE, supporting electrolyte for CZE; L, leading electrolyte; S, sample plug; T, terminating electrolyte. Both reservoirs are not shown in this scheme. After these three steps tr-ITP-CZE started.

EOF was not considered in the simulation by SIMUL. In this simulation, there was no limitation of the volume of the sample reservoir. That is, the sample mixture was fed continuously during simulation. Fig. 2.4 shows the preconcentration behavior of the mixture. Obviously 0.01 mM analyte was concentrated up to 10–20 mM according to isotachophoretic regulation (in the manner of moving boundary electrophoresis at this stage). In the present simulation, the maximum concentration (migration time) reached was 24.2 mM (124 s), 18.8 mM (134 s), and 10.1 mM (594 s) for m50$^+$, m30$^+$ and m10$^+$, respectively, although such high concentrations may not be reached in the

actual experiments depending on the sample volume. Formation of sharp and concentrated peaks could be expected for the analytes with a wide range of mobilities by the existence of the L zone containing high mobility of L ion (K^+ in this case). These zones are further concentrated by introducing the T zone during the tr-ITP process and the zones will be detected in CZE mode at the point of detection. The tr-ITP process after EKS is very important as will be demonstrated later.
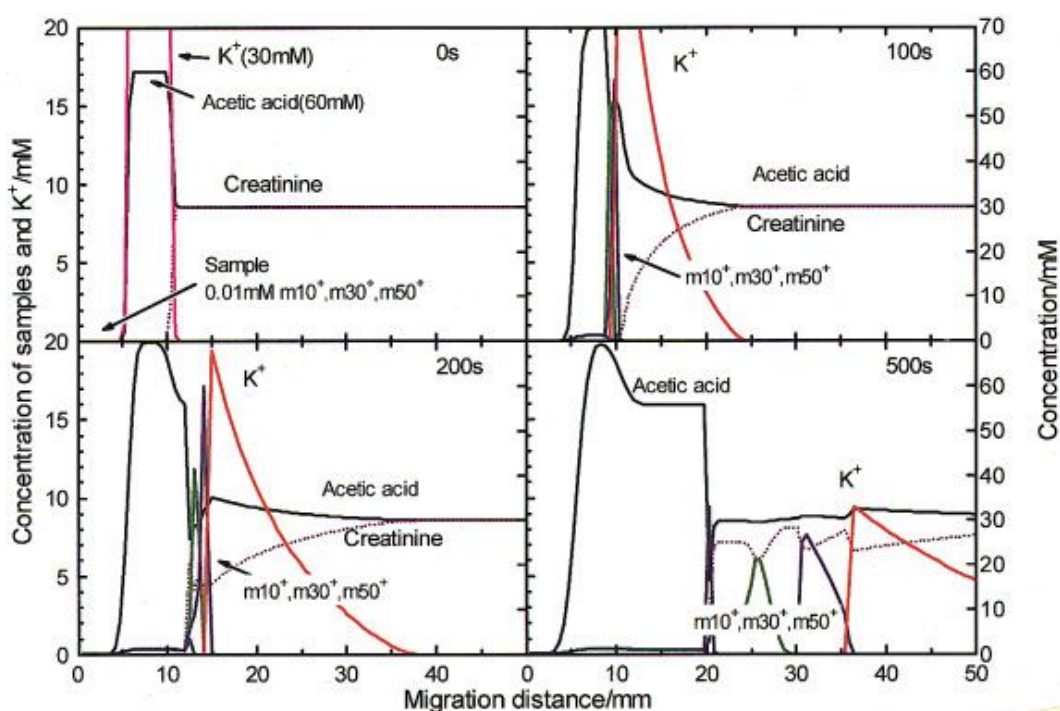

Figure 2.4: Simulated time dependence of the analytes (0.01mM m50$^+$, m30$^+$, m10$^+$ with 0.1 mM acetic acid) in EKS. Time shows migration time under constant current of 200 A/m^2. SE, 30mM creatinine 30mM acetic acid, L, 30mM K^+ + 60mM acetic acid. SIMUL (Version 4) was used for simulation.

2.2.4 Electrokinetic injection

When L was not introduced to the capillary (simple EKI), contrarily to EKS,

the preconcentration behavior greatly depends on the mobility of the analytes. The maximum concentration (migration time) reached was 1.96 mM (40 s), 2.93 mM (60 s), and 10.1 mM (250 s) for m50$^+$, m30$^+$ and m10$^+$, respectively. Figure 3 shows the EKI process of mixture. Obviously from Fig. 2.5, the frontal zone of a high mobility component (m50$^+$) is broadened gradually due to the electromigration dispersion keeping the maximum concentration. A low mobility component (m10$^+$) showed better preconcentration behavior, which can be attributed to the fact that the co-ion in SE (creatinine in this case, effective mobility was 20×10^{-5} cm^{2}V^{-1}s^{-1}) played the role of leading ion in the present system. When the other co-ion with larger mobility is used, better preconcentration behavior can be expected by simple EKI.
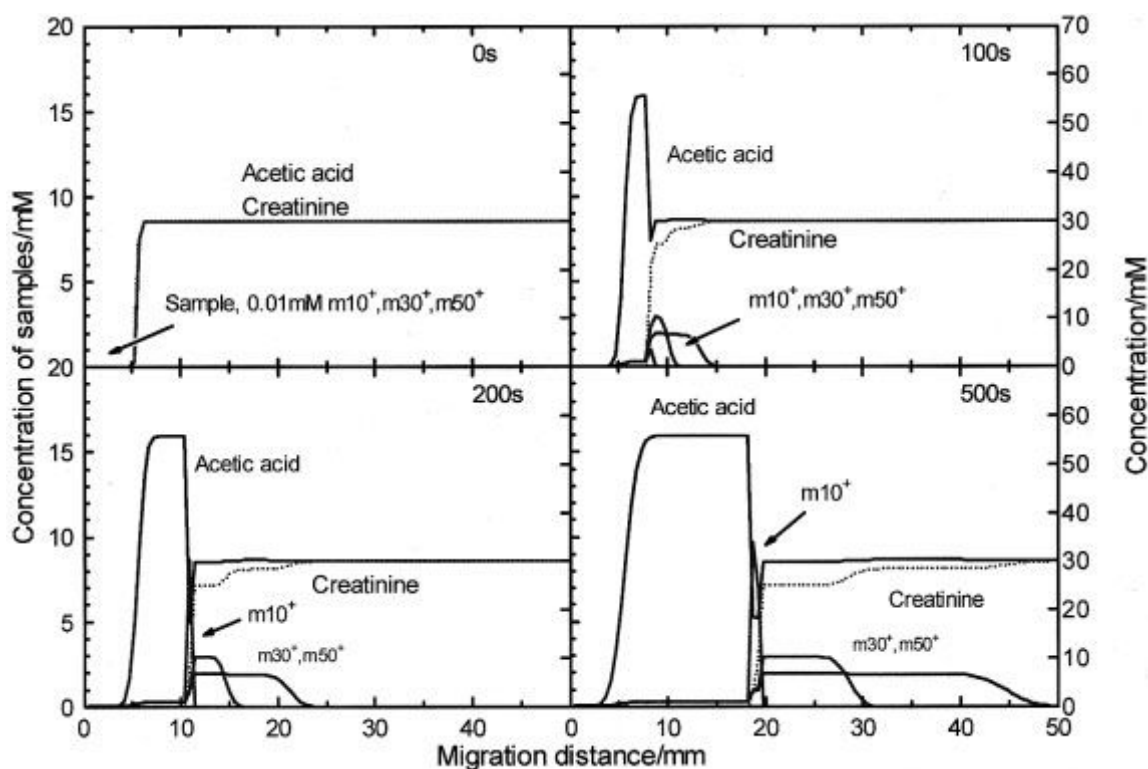

Figure 2.5: Simulated time dependence of the analytes (0.01 mM m50 , m30 , m10 with 0.1 mM acetic acid) in EKI. Simulation conditions as in Fig. 2.4.

2.3 Effects of electrode configuration and setting [7]

2.3.1 Non-uniform electrical potential distribution

The capillary filled with the BGE was dipped in the sample solution placed into the vial with the electrode and then the analytes were injected by EKI. The movement of analytes during EKI procedure has two components that take place simultaneously: (i) the analytes in the sample vial move to the capillary end and (ii) the gathered analytes enter the capillary to achieve EKI. Many efforts focused on the latter step were done to improve the effect of stacking and to quantify the amount injected [1, 25]. The analytes move toward the capillary end owing to the electrical potential distributed between the electrode and the capillary end. In other words, the analytes being outside of the effective field may not be injected. Thus, not all of the sample stocked in the vial can be injected due to the potential distribution. This phenomenon would determine the efficiency of EKI and therefore the sensitivity of CZE analysis. The non-uniform potential distribution in the electrolyte solution is significantly influenced by the electrode position such as the inserted length and the relative distance with regard to the capillary end. Quantification of such electrical potential distribution is a very complex mathematical and physical task, which needs the aid of computer simulation.

When using the hollow electrode (Fig. 2.6), the capillary could be directly inserted into the electrolyte solution through the electrode. As well known, it is a familiar type applied with Agilent HP^{3D} CE system (shown in Fig. 2.7). Two conditions were simulated with the capillary end being 500 mm shorter and 500 mm longer than the electrode end, respectively. The relationship between relative injected amount and time is displayed in Fig. 2.8A and B, where the results apparently show that a minor difference in electrode setup but caused significantly different EKI performance. In Fig. 2.8 A, the sample introduction

was saturated rapidly within 1–2 s, the relative injected amount of m50 kept at a constant level of only 0.09% (1.1 pmol) of the whole molar amount in the reservoir (1.25 nmol) despite increasing the injection time. The molar amount of 1.1 pmol is slightly larger than the amount initially held in the projected part of cylindrical electrode (see Fig. 2.8A). This means that very few analytes in the sample vial were introduced into the capillary when the capillary end was hidden in the electrode, due to the effective electrical potential distributed in a small range inside the electrode. The analytes in the outside of the range would not be moved to the capillary end within such a short time because of very weak electric field strength outside the electrode and also slow diffusion of the analytes at such a low concentration.
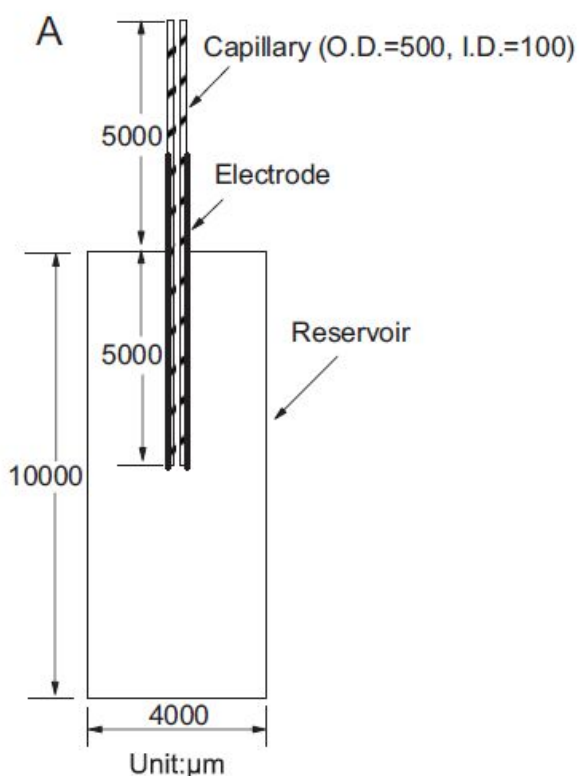

Figure 2.6: Sketches of two simulated electrode configurations: a model with a capillary inserted in a hollow electrode. The dimensions were just as marked.

2.3.2 Computer Simulation of electrical potential distribution

On the other hand, configuration with the capillary end longer than the electrode leads to a wider distribution of the electric potential in the solution. Consequently, larger molar amount was introduced, as shown in Fig. 2.8B. The injected amount was related to increase with time, but it was limited obviously from the curvature of plots in Fig. 2.8B. In our simulation, 4.4 % (54.7 pmol) of the initial amount of m50 in the reservoir was introduced in 5 s, and 13% (164 pmol) of m50 was injected for 50 s. Two simulated conditions in this model illustrated importance of the distance between the ends of capillary and electrode. Thus, the electrode setting should be carefully controlled when using EKI. As wasdemonstrated, due to different distribution of the electrical potential, the relative injected amounts under conditions shown in Fig. 2.8A and B were virtually independent of and slightly dependent on the sample volume, respectively, that was proved by simulation as well (data not shown).

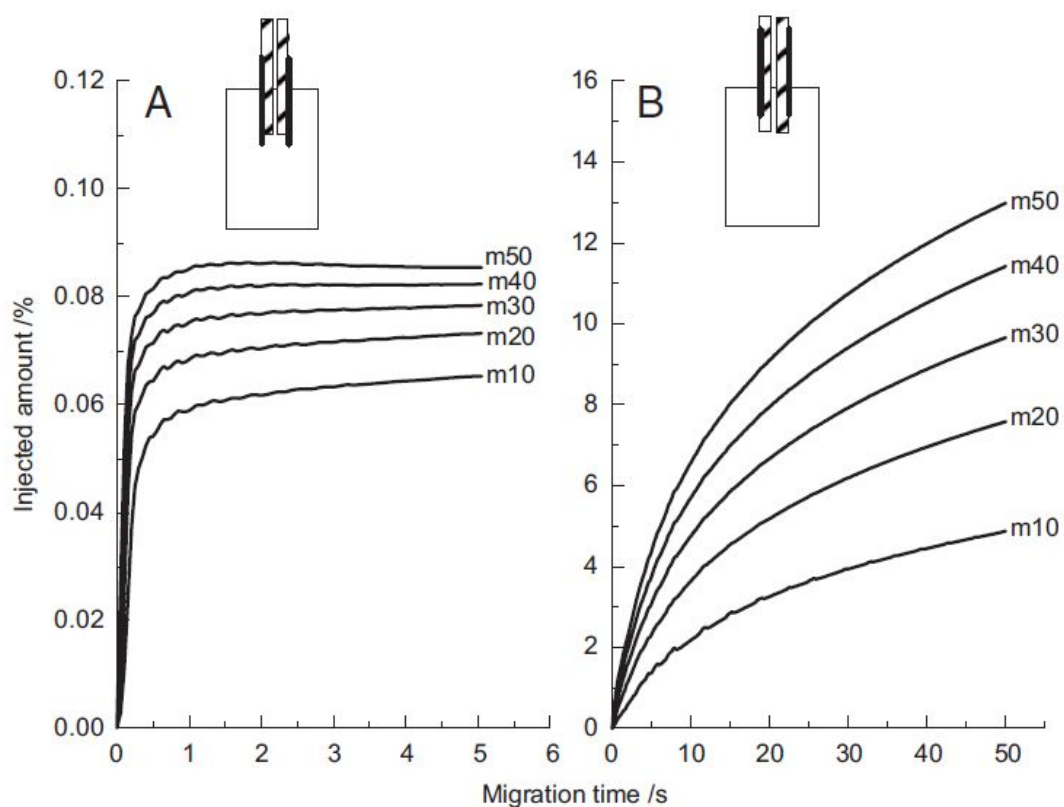**Fig. 2.7:** Sample and BGE compartment of Aglient HP-3D CE system.

Figure 2.8: Simulated results of relative injection amount for a model with a capillary inserted in a hollow electrode: (A) capillary end was 500 mm shorter than electrode, and (B) capillary end was 500 mm longer than electrode. The sample load in the reservoir was 1.25 nmol for each analyte.

2.3 Reference

[1] Breadmore, M. C., *Electrophoresis* 2007, 28, 254-281.

[2] Malá, Z., Křivánková, L., Gebauer, P., Boček, P., *Electrophoresis* 2007, 28, 243-253.

[3] Hirokawa, T., Okamoto, H., Gas, B., *Electrophoresis* 2003, 24, 498-504.

[4] Xu, Z. Q., Timerbaev, A. R., Hirokawa, T., *J. Chromatogr. A* 2009, 1216, 660-670.

[5] Chien, R., Burgi, D. S., *J. Chromatogr. A* 1991, 559, 141-152.

[6] Chien, R., *Anal. Chem.* 1991, 63, 2866-2869.

[7] Hirokawa, T., Koshimidzu, E., Xu, Z. Q., Electrophoresis 2008, 29, 3786-3793.

[8] Hruska, V., Gas, B., *Electrophoresis* 2007, 28, 3-14.

[9] Foret, F., Szoko, E., Karger, B. L., *J. Chromatogr. A* 608 (1992) 3-12.

[10] Foret, F., Szoko, E., Karger, B. L., *Electrophoresis* 1993, 14, 417-428.

[11] Waterval, J.C.M., La Porte, C.J.L., Van't Hof, R., Teeuwsen, J., Bult, A., Lingeman, H., Underberg, W.J.M., *Electrophoresis* 1998, 19, 3171-3177.

[12] Timerbaev, A. R., Buchberger, W., *J. Chromatogr. A* 1999, 834, 117-132.

[13] Petr, J., Maier, V., Horakova, J., Sevcik, J., Stransky, Z., *J. Sep. Sci.* 2006, 29, 2705-2715.

[14] Timerbaev, A. R., Hirokawa, T., *Electrophoresis* 2006, 27, 323-340.

[15] Křivánková, L., Pantuckova, P., Boček, P., *J. Chromatogr. A* 1999, 838, 55-70.

[16] Gebauer, P., Thormann, W., Boček, P., *Electrophoresis* 1995, 16, 2039-2050.

[17] Fukushi, K., Nakayama, Y., Tsujimoto, J., *J. Chromatogr. A* 2003, 1005, 197-205.

[18] Gebauer, P., Thormann, W., Bocek, P., *J. Chromatogr. A* 1992, 608, 47-57.

[19] Křivánková, L., Vrana, A., Gebauer, P., Boček, P., J*. Chromatogr. A* 1997,

772, 283–295.

[20] Stutz, H., Bordin, G., Rodriguez, A. R., *Electrophoresis* 2004, 25, 1071-1089.

[21] Gebauer, P., Křivánková, L., Pantuckova, P., Boček, P., Thormann, W., *Electrophoresis* 2000, 21, 2797-2808.

[22] Hirokawa, T., Okamoto, H., Ikuta, N., Gas, B., *Anal. Sci.* 2001, 17, i185-188.

[23] Hirokawa, T., Okamoto, H., Ikuta, N., *Electrophoresis* 2001, 22, 3483-3489.

[24] Schwer, C., Gaš , B., Lottspeich, F., Kenndler, E., *Anal. Chem.* 1993, 65, 108-2115.

[25] Chien, R., Burgi, D. S., *J. Chromatogr. A* 1991, 559,141-152.

Chapter 3: High sensitive analysis of rare-earth elements

3.1 Introduction

Insufficient concentration sensitivity is an inherent limitation of CE analysis, suffering from minute sample volumes and short light pathways for photometric detection. Various in-line preconcentration techniques, e.g. field-amplified sample injection (FASI) [1], transient ITP (tITP) [2], sweeping [3], and dynamic pH junction [4] have been developed and revealed powerful capabilities of improving detection sensitivity for a wide range of analytes, from small ions to biopolymers [5, 6]. In general, most of the in-line preconcentration approaches are due to the changes in electrophoretic velocity so that the analytes entering the separation capillary stack into a narrow zone. In an excellent review article [7], the principles of stacking were classified as field strength-chemically, and physically induced- and this categorization provides a simplified way to understand the mechanism of sample preconcentration. Applying an individual stacking technique does not always afford a requested increase in sensitivity, especially when the quantification of ultra-low analytes is the target. A few sequential stacking methods based on multiple stacking mechanisms were developed to meet this challenge and offered an impressive enhancement in detectability, as also discussed by Breadmore [7]. To obtain high-concentration sensitivity in CE, it is essential to introduce a large amount of sample to be then well focused into a sharp zone prior to separation. The electrokinetic sample injection has alwaysbeen preferred for introducing large-volume samples in multiple stacking methods. As first reported by Quirino and Terabe, a million-fold increase in sensitivity could be achieved when electrokinetic injection is combined with sweeping for the enrichment of

cationic analytes [8]. Recently, a couple of novel stacking approaches have been proposed [9, 10] which accompanied electrokinetic sample injection to make feasible improvements in LODs over 100,000 times. However, the existing high-sensitivity methodology came across certain critical conditions, e.g. injection of a high-conductivity solution and water plug before sample introduction [8] or an hour-long injection time [9]. These might hinder its practical implementation.

The concept of electrokinetic supercharging (EKS) pioneered by Hirokawa et al. [11] implies an extended electrokinetic injection to introduce a great amount of analyte followed by a tITP stacking step to refocus the injected analytes into a narrow zone. In such an amalgamation, greater increases in sensitivity could be expected than those by using electrokinetic injection or tITP alone. A recent examination of EKS mechanism [12] has resulted inconclusion that much work remains to be done to overcome the current limitations in practical application of EKS. For instance, the movement of stacking boundary was found to worsen the resolution. Our group has been performing a systematic research on improving the concentration power of EKS, using rare-earth metal ions (REs) as model analytes (in a great part due to their extremely low background levels that facilitate high-sensitivity experiments). Typical detectable concentrations of REs in CE with indirect UV detection, after hydrodynamic injection under essentially non-stacking conditions, are at the micromolar level [13, 14]. Using FASI allowed for substantially lower LODs, e.g. 45 mg/L (0.27 mM) for erbium(III) taken as a representative RE [15]. In its basic design, EKS lowered the LOD of Er down to 0.27 mg/L (1.6 nM) [11]. The following studies demonstrated that the electrode configuration and position significantly affect the efficiency and reproducibility of sample injection [16, 17]. Importantly, by increasing the distance between tips of the electrode and the capillary in vertical direction (abbreviated as De/c hereafter), which are located in a typical sample vial, the LOD of erbium was improved to an impressive threshold of 0.02 mg/L (0.12 nM) [16].

In this update, we have shown that it is possible to further improve analyte loading and hence EKS-CZE detectability by modifying sample introduction setting. A simple technical alteration was achieved by replacing the typical 0.7-mL sample vial with a 1.0-mL commercial elongated vial, in which De/c could be extended to 40.0mm to maintain the effective electric field strength over a larger space. The impetus behind such a modification was to allow injection of larger sample volumes for subsequent tITP stacking while keeping the efficiency and resolution intact. Another enhancement of the previous EKS system was due to the possibility of creating the tITP conditions without addition of an external terminating ion but taking advantage of a system-induced terminator (i.e. the hydrogen ion).Fundamental studies to understand the formation of terminator zone upon applying the injection voltage were undertaken through computer simulations, and this information was used to design a simplified EKS mode. The developed approach provided sensitivity enhancements approaching 80,000, which makes EKS-CZE adequate to achieve ultratrace multi-component analysis.

3.2 Materials and methods

3.2.1 Instrumentation

All experiments were conducted on a CAPI-3300 instrument (Otsuka Electronics, Osaka, Japan) fitted with a photodiode array detector set at 214 nm, and placed in an air-conditioned room (251C). Separations were performed using polyimide-coated fused-silica capillaries of 50 cm×75 mm id (effective length 37.7 cm) purchased from Otsuka Electronics. Purified water used to prepare all solutions was delivered by a Millipore Labsystem (Tokyo, Japan).

3.2.2 Reagents and samples

All chemicals for preparation of the BGE [4-methylbenzylamine (4-MB), 2-hydroxyisobutyric acid (HIBA), malonic acid, hydroxypropyl cellulose (HPC), and 2-ethylbutyric acid (2-EB)] were from Sigma-Aldrich Japan. The sample was a mixture of K, Na, Li, La, Nd, Sm, Gd, Y, Er, and Yb chlorides of analytical grade from Mitsuwa Kagaku (Osaka, Japan) prepared in Milli-Q water. The concentration of each analyte in the stock solution was 2.5 mM. The stock solution was diluted with Milli-Q water as required.

3.2.3 Electrophoretic conditions

The BGE was a solution of 10mM 4-MB, 4mM HIBA, 0.4mM malonic acid, and 0.1% HPC, adjusted to pH 4.8 with 2-EB. 4-MB was used as a UV-absorbing probe for indirect UV detection, while HIBA and malonic acid played the role of complexing agents for resolving REs, and HPC was employed as EOF modifier. The fresh capillaries were preconditioned by flushing with 1.0M NaOH, Milli-Q water, and BGE for 10min each. Between separations, the capillary was rinsed with Milli-Q water for 2 min and BGE for 3min. Injections were performed by placing the sample either in the standard or in the novel, elongated vial (commonly used for sedimentation experiments), both detailed in Fig. 1, and applying a voltage of 10 kV (as a positive polarity at the inlet vial) for a designated time. Note that not only the sample volume but also the $D_{e/c}$ could be increased by adopting the elongated vial, notably without modification of a given CE instrument. A constant voltage of +20 kV was applied for separations. Before each injection, the capillary inlet and the working end of the electrode were washed with Milli-Q water in order to avoid contaminations originated from the BGE, which might bring about crossover interferences with ultra-low concentration analyses.
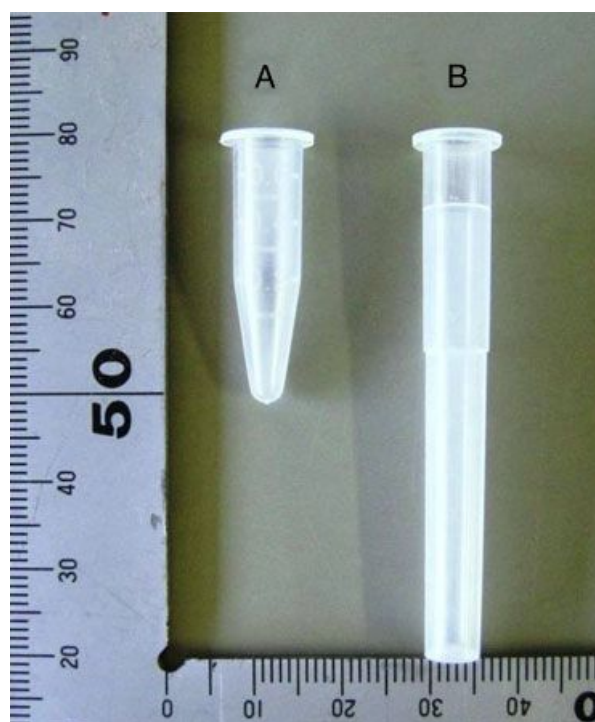
Figure 3.1: Vials used for sample injection: (A) 0.7-mL Eppendorf vial; (B) 1.0-mL elongated vial. Actual sample volumes were 500 and 900 µL, respectively.

3.2.4 Computer simulation

A finite element method was carried out with CFD-ACE1 software (CFDRC, Huntsville, AL, USA) to simulate the concentration profiles for analytes, co-ion, and counter-ion as well as changes in the pH and field strength during sample injection. The software was implemented on a Pentium Xeon 3 GHz processor. The 2-D model with the corresponding dimensions is presented in Fig. 3.2. The electrodes were placed at the walls of the reservoir in parallel with the capillary. An applied voltage for injection was set at 100 V. The sample consisted of five model cations with mobilities 10×10^{-5} ($m10^+$), 20×10^{-5} ($m20^+$), 30×10^{-5} ($m30^+$), 40×10^{-5} ($m40^+$), and 50×10^{-5} ($m50^+$) $cm^2V^{-1}s^{-1}$

and an initial concentration of 1.0 mM. Chloride-ion at 5.0 mM served as the counter-ion, and the initial pH of the sample solution was 7.0. The BGE consisted of 100 mM 2-EB with the pH adjusted to pH 4.8 with KOH (50 mM), in which K1 performed a function of the leader to enable tITP conditions. No EOF was assumed, and in contrast to actual experiments, the complexing agents were not included in the simulated BGE, as simulation of the separation was not the case. To our judgment, such a simplification does not discriminate imitating the sample injection step against formation of the terminator, but provided a great saving of simulation time. All simulations were for a time of 5 s with data collection in 20 000 steps.
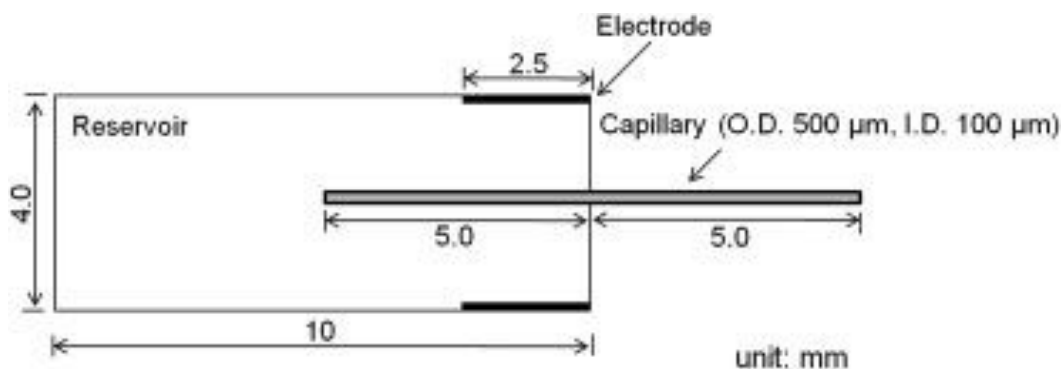

Figure 3.2: An outline of 2-D simulation model of the sample reservoir, electrode, and capillary.

3.3 Results and discussion

3.3.1 Computer simulations of formation of a system-induced terminator

In common EKS arrangement, the electrokinetically injected analytes are sandwiched between the leading and terminating electrolytes purposely added to the system. As a matter of fact, the CE process frequently encounters intrinsic tITP stacking conditions, although the ITP origin of the preconcentration effect observed is sometimes underestimated by practitioners. On the other hand, there are a number of ways how the tITP state can be deliberately induced by employing components of separation medium or the major constituent(s) of the sample [12, 18]. For instance, the co-ion of BGE, namely 4-MB^+, can act as leading ion as its effective mobility is higher than that of REs (La-Yb) under essentially complexing conditions (but lower than the mobility of Li) [19] and hence only a suitable terminating ion is requested to make tITP true. However, while carrying out simulation experiments, we have realized that in the case of very dilute analytes (less than ca. 100 mM), the EKS procedure could be simplified to be performed without an intentionally introduced terminator.
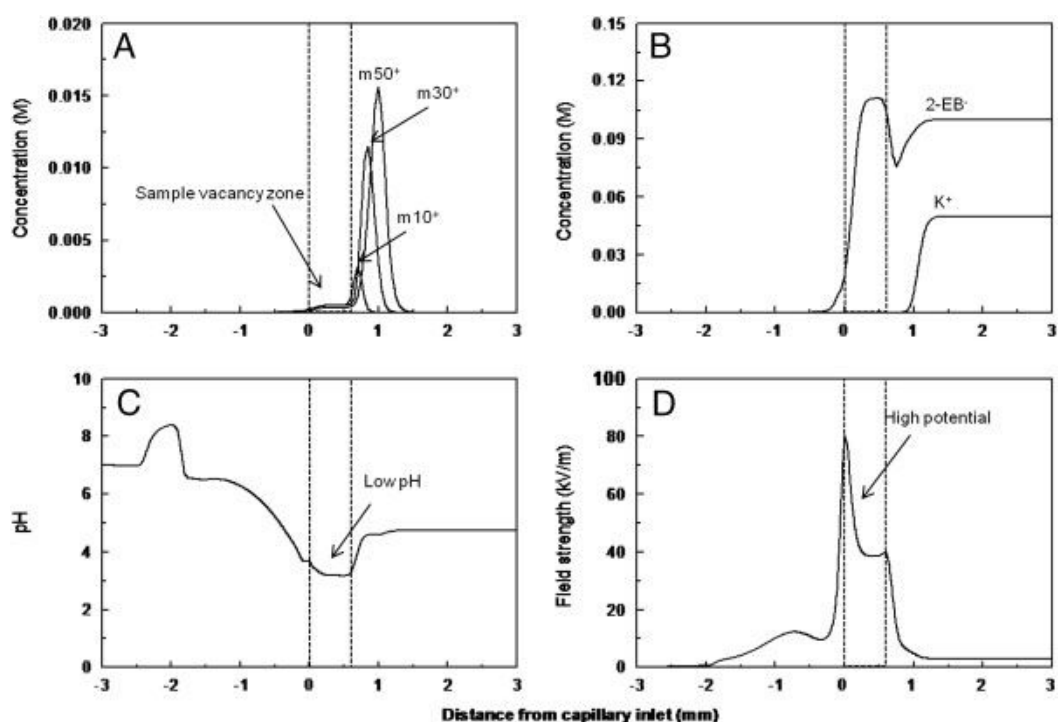

Figure 3.3: Computer simulations of the profiles of (A) supercharged analytes

of different mobility; (B) co- and counter-ion of BGE; (C) pH; and (D) electric field strength. The EKS time simulated was 5.0 s. The zero point at X-axis refers to the capillary inlet.

Fig. 3 presents the simulated profiles of analytes differing in mobility, co-ion (K^+) and counter-ion (2-EB$^-$), as well as the pH and field strength after applying the injection voltage for 5 s (when the stacking is essentially completed). The simulations elucidate the formation of a system-induced terminator upon sample introduction. Once the voltage is applied, the analytes stack at the boundary between the leading co-ion and a sample-vacancy zone (SVZ) marked with two dotted lines. As a result, the m50$^+$ analyte experienced a 15 000-fold increase in its actual concentration (Fig. 3.3A). It should be emphasized that such sensitivity enhancement is superior to that achieved by FASI due to tITP that accompanies electrokinetic injection (i.e. By a virtue of EKS effect). Observed in the SVZ was an increased concentration of the counter-ion 2-EB$^-$, migrating oppositely, in the direction toward the capillary inlet, and no co-ion (K^+) (Fig. 3.3B). It is worth noting that in real experiments, with 4-MB$^+$ as leading ion, its deficiency would produce a massive negative peak. To fulfill the electro neutrality requirement, H$^+$ seems to be the only candidate to overtake the role of the co-ion in the SVZ (to compensate the charge of a highly concentrated 2-EB$^-$) and hence to carry the electric current when the cationic analytes expire. Therefore, one may anticipate a much lower pH in the SVZ, and as shown in Fig. 3.3C, computer simulations unambiguously prove this anticipation. With trace cationic analytes injected, H$^+$ can be easily generated and, consequently, the conductivity of SVZ (containing the anion of a weak acid) turns out to be fairly low, resulting in high field strength, as can be seen in Fig. 3.3D. The hydrogen ion has already been considered as potent terminating ion in cationic ITP analysis where, e.g. HCl solution can work as good terminating electrolyte [20]. In our model system, due to the high mobility of BGE co-ion, the gradually formed H$^+$ (as a product of dissociation of the weak acid, 2-EB) acts as a proper terminating ion, coined

here as a system-induced terminator. The latter creates the tITP state and genuine EKS conditions during sample injection and thus provides a useful understanding of much higher preconcentration effects (than by FASI).

3.3.2 Optimization of injection conditions

It was essential to understand the effect of various factors influencing the performance of EKS, especially those that favor introduction of the largest possible amounts of analytes. Therefore, the potential of EKS was exploited with regard to use of a larger sample vial and optimization of capillary versus electrode configuration. In a previous work [16], it was demonstrated that analytes occurring in an effective electric field can only be introduced into the capillary and the stronger the field strength, the greater the amount of analytes subjected to injection. These findings led to a clear-cut assumption that the position of the electrode relative to the capillary inlet is critical for increasing the amount of the injected analytes. Indeed, with De/c extended to 19.5mm in the typical sample vial, it was possible to increase sample loadings and reach for LODs of REs as low as 0.02 mg/L. However, a configuration of the sample vial has not been much concerned as a factor supporting the introduction of yet a greater amount of sample (at the same injection voltage). A simple replacement of the standard vial by the elongated vial trialed in this study (see Fig. 1) enabled not only the sample volume (from 500 to 900 µL) but also $D_{e/c}$ to be further increased, attaining 40.0 mm (the maximum value for such a vial). This gave rise to increased loadings of target analytes and notably improved detectability of EKS-CZE system, as shown in Fig. 3.4.

One needs no magnifying glass to observe a huge negative peak in electropherograms collected in Fig. 3.4. Such system peaks regularly appear in CE with indirect UV detection [21] as a result of that the concentration of BGE converges toward that of the sample in accordance with Kohlrausch regulating function [22]. Concomitantly, the UV absorbing probe tends to

disappear from the BGE at the site of sample injection. Note that such a system peak is always transported to the detector by the EOF and thereby detected. After tITP preconcentration is completed, the analytes should be destacked out of the stacking boundary. However, the latter migrates in the vicinity to the system peak and, if the length of the capillary available for separation is insufficient, the analytes would remain co-migrated with this peak. As shown in Fig. 3.4 A, this is the case of ytterbium. Advantageously, extending the $D_{e/c}$ to 40.0 mm improved the solution and also moved back the system peak (Fig. 3.4B) due to a lower local velocity of EOF in a more loaded sample zone. The amount injected and preconcentration effect could be further increased with a longer injection time (350 s) but at the expense of resolution (data not shown). The optimal injection time guaranteeing the baseline separation for seven REs was determined to be 300 s.
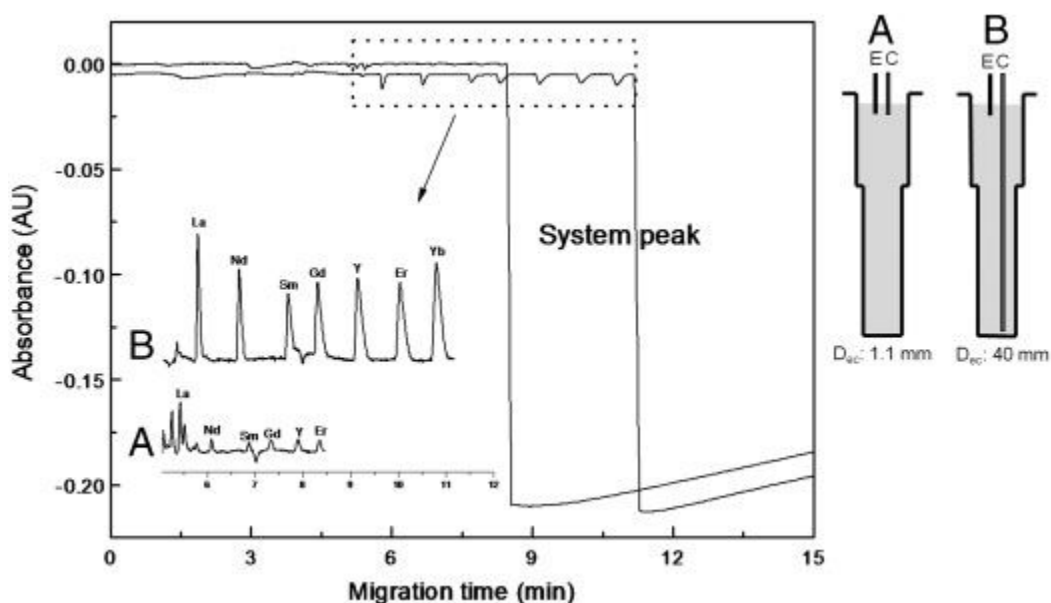

Figure 3.4: Electropherograms obtained at $D_{e/c}$ (A) 1.1mm and (B) 40.0 mm. Capillary: fused-silica, 50 cm×75 mm I.D.. BGE: 10mM 4-MB, 4mM HIBA, 0.4 mM malonic acid, 0.1% HPC, pH 4.8 (adjusted with 2-EB). Injection: 10 kV for 300 s (from the elongated vial). Applied voltage: 20 kV. Indirect UV detection at

214 nm. Sample: 1000-fold diluted at 2.5 nM. Traces A and B show a close-up and reversed peak-polarity view of lower traces A and B.

3.3.3 Sensitivity performance

Fig. 3.5 demonstrates the applicability of the EKS-CZE system to concentrate and separate REs from progressively diluted sample solutions. Even with a dilution factor of 10 000 corresponding to a 0.25 nM level of analytes, the peaks of all REs under scrutiny can be well recorded. LODs for the analytes obtained in Fig. 3.5B are exceptionally low and range from 0.01 to 0.04 nM (1.4-6.8 ng/L). Longer injections to further improve the detectability were deemed to be unreasonable since with injection at 10 kV for 300 s, about 40% of analyte amount existing in the sample vial has been introduced into the capillary (data not shown). Additionally, the resolution might be compromised because of interfering effects of the system peak (see above). Nonetheless, the LODs obtained in this work represent 3–45-fold improvements compared to the previously published data with EKS performed at $D_{e/c}$ of 1.1 [11] or 19.5mm [16]. Furthermore, such sensitivities are much better than those obtained by ICP-AES (0.2-2 µg/L) and comparable to those of ICP-MS (r1 ng/L).

As a further manifestation of the sensitivity gain that can be achieved with EKS-CZE, it was interesting to assess the eventual preconcentration factor. The latter is defined here as the ratio of analyte concentration in the detected zone to that in the original sample. In the detected zone, the electroneutrality relationship is given by the following equation:

$$[2\text{-}EB^-] + [HIB^-] + [OH^-] = (3\text{-}n)[RE(HIB)_n^{(3\text{-}n)+}] + [4\text{-}MB^+] + [H^+]$$
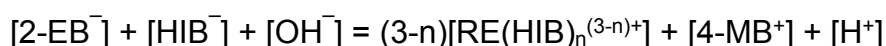
Where HIB^- is the deprotonated form of HIBA. The sum of $[2\text{-}EB^-]$ and $[HIB^-]$

is kept constant as both are supplied by the BGE, while 4-MB$^+$ is replaced by cationic complexed RE analytes, so that the actual concentration of REs can be calculated from a decrease in the probe concentration. The absorbance of a 10mM solution of 4-MB was measured to be 0.36. For the reversed peak of erbium displayed in Fig. 3.5B, the absorbance is 0.00072. For the sake of simplicity, we assumed here that the net positive charge of a complexed metal is equal unity. Therefore, the concentration of Er in the detected zone was assessed as 20 μM. Comparison of this value with the original sample concentration, i.e. 0.25 nM, resulted in a preconcentration factor of 80 000.
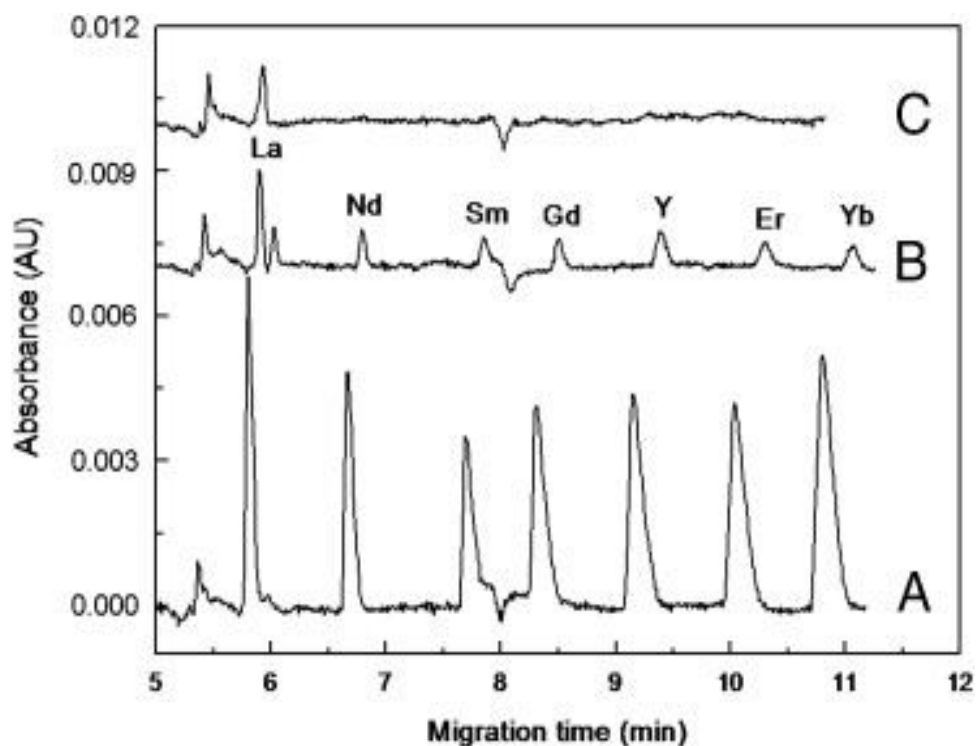

Figure 3.5: Electropherograms obtained under the optimized EKS conditions. Sample: A, 2.5 nM; B, 0.25 nM; C, 0.025 nM. D$_{e/c}$: 40.0mm. Other conditions as in Fig. 3.4.

3.4 Summaries

This is the first successful demonstration of an EKS system for generating the tITP state without the introduction of an external terminator. In contrast, the hydrogen ion produced at an increased concentration during electrokinetic injection plays the role of terminator on condition that the sample contains ultra-low cationic analytes. In combination with the leading ion supplied by the BGE, such system-induced terminator ensures the analytes to be concentrated yet at the stage of sample injection, simplifies the total EKS preconcentration protocol, and makes it particularly useful for ultra-trace multi-component analysis. Computer simulations offered an insight into the stacking mechanism governing the formation of system-induced terminator.

Another advancement of EKS presented in this study is the use of an elongated sample vial. This allows for optimizing the capillary versus electrode configuration with regard to a extended distance between capillary and electrode tips and thus enables enhanced analyte loadings. With the injection time optimized to avoid the analytes from being overlapped by the system peak, 0.25 nM levels of REs could be supercharged and then completely separated. The preconcentration factor attained by using the novel EKS system reached for as much as 80 000 and provided the part per trillion LODs for a mixture of seven REs, which are the lowest ever reported for these ions in CE.

3.5 References

[1] Chien, R. L., Burgi, D. S., *J. Chromatogr. A* 1991, 559, 141-152.

[2] Foret, F., Szoko, E., Karger, B. L., *J. Chromatogr. A* 1992, 608, 3-12.

[3] Quirino, J. P., Terabe, S., *Anal. Chem.* 1999, 71, 1638-1644.

[4] Britz-McKibbin, P., Bebault, G. M., Chen, D. D. Y*., Anal. Chem.* 2000, 72, 1729-1735.

[5] Timerbaev, A. R., Hirokawa, T., *Electrophoresis* 2006, 27, 323-340.

[6] Mala, Z., Slampova, A., Gebauer, P., Bocek, P., *Electrophoresis* 2009, 30, 215-229.

[7] Breadmore, M. C., *Electrophoresis* 2007, 28, 254-281.

[8] Quirino, J. P., Terabe, S., *Anal. Chem.* 2000, 72, 1023-1030.

[9] Breadmore, M. C., *Electrophoresis* 2008, 29, 1082-1091.

[10] Breadmore, M. C., Quirino, J. P., *Anal. Chem.* 2008, 80, 6373-6381.

[11] Hirokawa, T., Okamoto, H., Gas, B., *Electrophoresis* 2003, 24, 498-504.

[12] Xu, Z. Q., Timerbaev, A. R., Hirokawa, T., *J. Chromatogr. A* 2009, 1216, 660-670.

[13] Macka, M., Nesterenko, P., Andersson, P., Haddad, P. R., *J. Chromatogr. A* 1998, 803, 279-290.

[14] Verma, S. P., Garcıa, R., Santoyo, E., Aparicio, A., *J. Chromatogr. A* 2000, 884, 317-328.

[15] Hirokawa, T., Okamoto, H., Ikuta, N., *Electrophoresis* 2001, 22, 3483-3489.

[16] Hirokawa, T., Koshimidzu, T., Xu, Z. Q., *Electrophoresis* 2008, 29, 3786-3793.

[17] Xu, Z. Q., Koshimidzu, E., Hirokawa, T., *Electrophoresis* 2009, 30, 3534-3539.

[18] Krivankova, L., Pantuckova, P., Bocek, P., *J. Chromatogr. A* 1999, 838, 55-70.

[19] Okamoto, H., Hirokawa, T., *J. Chromatogr. A* 2003, 990, 335-341.

[20] Bocek, P., Gebauer, P., Deml, M., *J. Chromatogr.* 1981, 219, 21-28.

[21] Doble, P., Haddad, P. R., *Anal. Chem.* 1999, 71, 15-22.

[22] Macka, M., Haddad, P. R., Gebauer, P., Bocek, P., *Electrophoresis* 1997, 18, 1998-2007.

Chapter 4: High sensitive analysis of DNA fragments by EKS-CGE

4.1 Introduction

Recently, DNA analysis by CGE has become the preferred instrumental technique due to its high resolving power, speed, and quantitative ability in comparison with conventional slab gel electrophoresis [1]. However, the small I.D. of capillaries (25-100 μm) leads to the inside volume and detector cell volume in CE are respectively at μL and nL level, which results in the limitation of concentration sensitivity of CE, especially when CE couples normal UV detection. The low sensitivity of CGE hinders many applications of DNA analysis, since where the sample concentration is usually very low, e.g. in the field of clinical diagnostics, gene therapy, forensic investigations and other biomedical studies [2-4]. In response to the challenge, online preconcentration strategies or advanced sensitive detectors have been proposed in many reports for trace analysis of biosamples [5-8].

The majority of common preconcentration principle is based on a stacking step in which the analytes from a wide diluted sample zone in the capillary accumulate into a stacked narrow zone due to the change of migration velocity, thus become concentrated prior to electrophoretic separation. Among these stacking methods, electrokinetic supercharging (EKS) is a powerful and practical online preconcentration approach combining electrokinetic sample injection (EKI) with transient isotachophoresis (tITP) applied for various analytes [9]. The merit of EKS is that tITP step could remedy the shortcoming of EKI, a overloaded long sample zone could be effectively refocused. Therefore, higher sensitivity is expected than EKI and tITP when applied alone. Subsequent works on EKS for CE and microchip electrophoresis (MCE) have

61

been reviewed with a major focus on theoretical and computer simulation analysis of critical factors that affect the performance of EKI and tITP [10]. As was also highlighted in the recent review [11], research efforts of various groups have proven potentially universal applicability of EKS, including metal ions, pharmaceuticals, peptides, DNA fragments, and proteins, importantly both in capillary and microchip formats.

Researchers prefer to use the soluble polymers as the sieving matrix in place of solid gel in CGE for DNA fragments separation, since the polymer entangles in buffer to form dynamic sieving network and could be replaced after each run. The viscosity of BGE depends on the concentration and molecular weight of the used polymer. Conventionally, the higher viscosity, the better sieving ability is expected. But the high viscosity BGE sometimes means the replacement of gel in capillary would be difficult and not suitable for routine analysis. Han et al. once reported a polymer sieving matrix with ultralow viscosity that consisted of Tris-Boric acid-EDTA (TBE) system and used mannitol as an additive [12,13]. They regarded tetraborate bridge through mannitol and HPMC (Mw of 10,000) chains to form additional sieving network, therefore the developed low viscosity BGE will not deteriorate the resolution power and easy to be operated. We found that not only the sieving ability was kept with the additive of mannitol, but also EKS performance was promoted due to the generated leading ion of borate polyanion in ultralow-viscosity TBE buffer for ITP preconcentration.

The amount of injected analytes is another important contributor to EKS performance. To greatly improve concentration sensitivity, the analytes in the sample vial are expected to be ultimately introduced into the separation capillary prior to stacking. In successive works of our group [14-17], the impact of sample volume, electrode configuration and stirring way on EKS process has been studied. It was demonstrated that the analytes in an effective electric field can only be introduced into the capillary. All the efforts to enhance the effective electric field area in sample vial and to supplement the depleted

analytes would accelerate the sample introduction, consequently benefit the sensitivity in case of online stacking technique. Above, the proposal was just proved for EKS preconcentration and CZE separation of small ions. Herein, the modified electrode configuration was first applied for greatly loading of biopolymer (i.e. dsDNA fragments) that followed with EKS preconcentration and final gel separation. For the type of hollow electrode where the capillary passes through, the original electrode was cut shorter, which resulted in the increasing distance between the tips of electrode and the capillary end in the vertical direction (De/c). The effective electric field in sample vial was maintained over a large space according to the increasing of De/c from the default of 3.6 mm to 16.0 mm and 24.0 mm. At De/c of 24.0 mm, a Pt-ring type electrode was used since the hollow electrode was too short to touch the sample solution. The Pt-ring electrode configuration could significantly increase the space of effective electric field in sample vial which previously verified [17]. In this update, a Pt-ring electrode was positioned near the surface of sample solution around the capillary, meanwhile, the volume of the sample could be increased from 100 μL to 230 μL. Such alteration makes EKS-CGE adequate to perform several ng/mL DNA sample analysis, and the LODs approach several pg/mL only with UV detection.

4.2 Experimental

4.2.1 Instrumentation

All experiments were carried out on the Agilent HP^{3D} CE system (Agilent Technologies, Waldbronn, Germany) fitted with a photodiode array detector. The temperature of capillary chamber was set at 25°C. The default electrode is hollow and cylinder-shaped, therefore, the capillary goes right through the electrode (Fig. 4.1). All separations were performed in the fused-silica capillary

of 50 cm×75 µm I.D. (41.5 cm effective length) purchased from Ostuka Electronics. Purified water used to prepare all solutions was delivered by a Millipore Lab system (Tokyo, Japan).
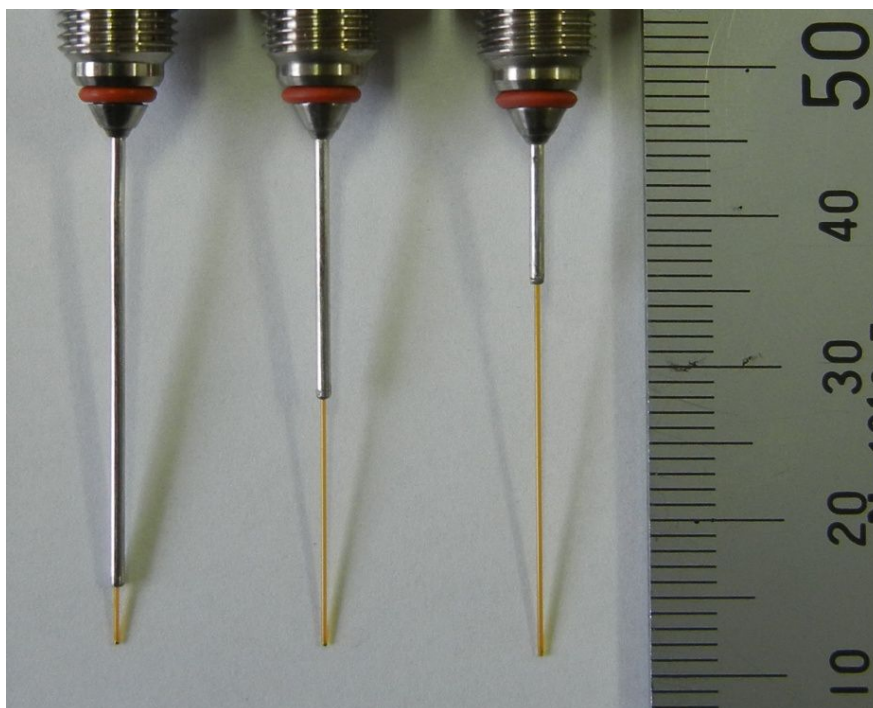

Figure 4.1: Photo of electrode configuration: the hollow electrode with (A) the default $D_{e/c}$ of 3.6 mm, extended $D_{e/c}$ of 16 mm and 23 mm, respectively.

4.2.2 Reagents and samples

The φ×174/HaeIII digest, a standard DNA sample, was purchased from Takara BIO Inc. (Shiga, Japan) and used for DNA studies here. The sample consists of 11 restriction fragments, from 72 to 1353 bp, at the total concentration of 500 µg/ml. Separation behavior with two TBE buffers at different viscosity properties were investigated. The ultralow-viscosity and

high-viscosity TBE buffers were respectively prepared with hydroxypropyl methyl cellulose (HPMC) and hydroxyethyl cellulose (HEC). HPMC, HEC and mannitol were purchased from Sigma-Aldrich (St. Louis, USA). The average molecular weight of HPMC is around 10,000, specified that the viscosity of 2 % aqueous solution is 5 cP. The HEC has high average molecular weight at 250,000. Accordingly, the pH of ultralow-viscosity (5 cP) TBE buffer (consisted of 2 % HPMC, 6 % mannitol, 2 mM EDTA, and 100 mM Tris) was adjusted to 8.0 by boric acid. The high-viscosity (70 cP) TBE buffer solution composed of 2 % HEC in $1 \times$ TBE buffer (89mM Tris-Borate, 89mM Boric acid, and 2 mM EDTA). The $10 \times$ TBE buffer was obtained from Promega (Madison, WI, USA). Other chemicals including Tris, boric acid and EDTA were obtained from Sigma-Aldrich Japan (Tokyo, Japan).

4.2.3 Electrophoretic conditions

New capillaries were washed with Milli-Q water and BGE for 10 min respectively. Between each run, the capillary was flushed with water for 2 min, 1.0 M HCl for 2 min, water for 2 min, and then BGE for 8 min. In order to avoid contaminations originated from BGE, the capillary inlet and the electrode system were washed with Milli-Q water before EKI. A constant voltage of -2.0 kV and -10 kV was applied for EKI and gel separation, respectively. The detection wavelength was set at 260 nm.
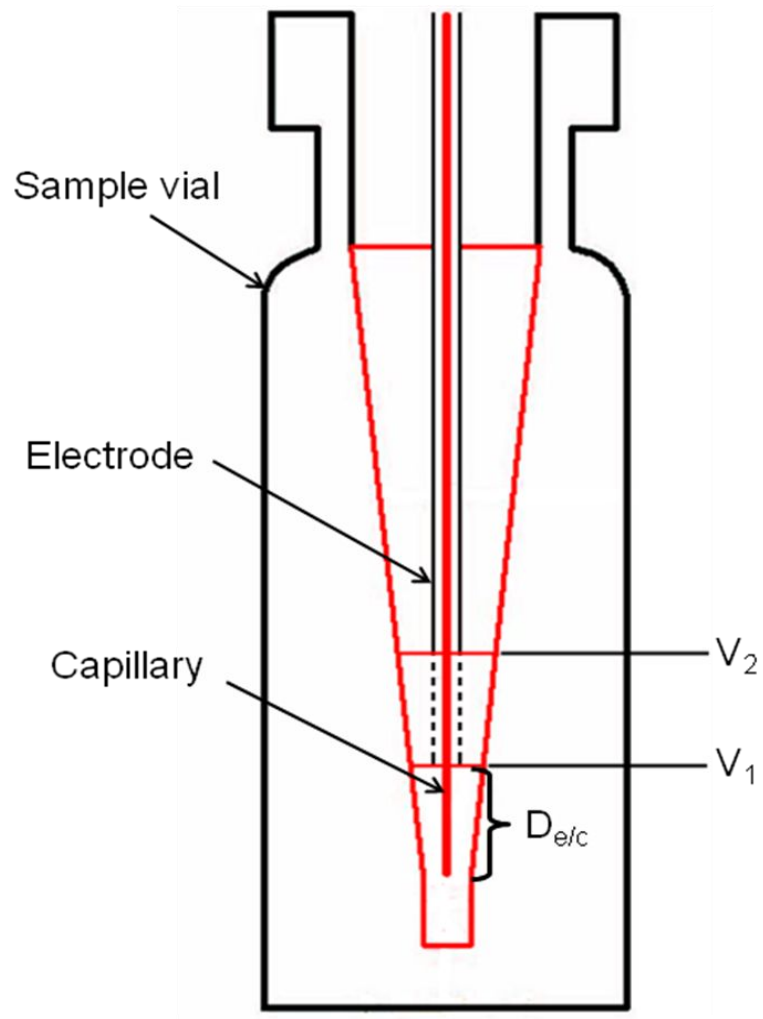
Figure 4.2: Vial of the same dimensions as the real one for computer simulation. When $D_{e/c}$ was at 3.62 mm and 7.24 mm, the volume of V_1 and V_2 were 14.82 µL and 37.16 µL, respectively.

4.2.4 Computer simulation

A finite element method was carried out with CFD-ACE+ software (CFDRC, Huntsville, AL, USA) to simulate the concentration profiles for analytes in a sample vial during EKS. The 2-D model of the sample vial that presented in Figure 4.2 was almost the same dimensions as the real used one. The tapered design of inside vial for sample storage could save sample volume. Herein, we focused on the tapered part, where was filled by sample for simulation with the mesh of 10 μm × 10 μm in the capillary and 12 μm × 17 μm at the tapered part. The cylindrical and hollow electrode surrounds the capillary with $D_{e/c}$ at 3.62 mm and 7.24 mm, respectively. An applied voltage for injection was set at 0 V at electrode and 100 V at capillary. The sample consisted of five model anions with mobilities $10×10^{-5}$ ($m10^-$), $20×10^{-5}$ ($m20^-$), $30×10^{-5}$ ($m30^-$), $40×10^{-5}$ ($m40^-$), and $50×10^{-5}$ ($m50^-$) $cm^2V^{-1}s^{-1}$. Initial concentration was assumed to be 1.0 μM for each analyte. The used BGE was a mixture of 50 mM HCl ($m_0(Cl^-) = 79.1 \times 10^{-5}$ $cm^2V^{-1}s^{-1}$) and 100 mM Tris ($m_0=29.5 \times 10^{-5}$, $pK_a=8.076$). No EOF was assumed. The software was implemented on a Pentium Xeon 3GHz processor. All simulations were for a time of 10 s ~ 17 s with data collection in 40,000 ~ 85,000 steps.

4.3 Results and discussion

4.3.1 Low-viscosity BGE induced leading ion

EKS procedure conventionally has two essential steps of EKI and tITP. To achieve tITP preconcentration, the sample is sandwiched by leading electrolyte (LE) and terminating electrolyte (TE) matching the condition that the mobility of analyte is lower than that of leading ion but higher than that of terminating ion. If the co-ion of BGE takes over the role of leading ion (or

terminating ion), such mode is called separation medium-induced tITP [18,19], which could simplify the LE or TE replacement for tITP. In our recent paper [16], a novel mechanism was elaborated that EKS simultaneously occurred upon EKI when the co-ion acted as leading ion and the system-induced terminator generated from much diluted analytes. This discovery was the significant update of normal EKS concept.
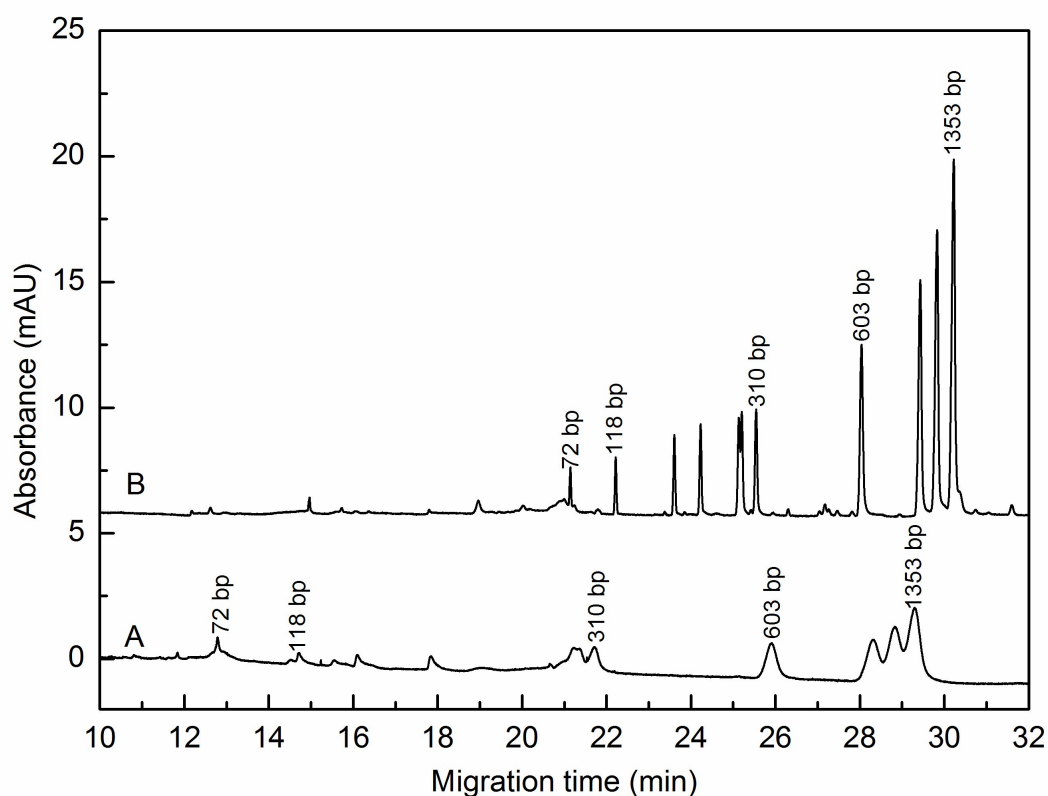

Figure 4.3: Electropherograms of φ×174/HaeIII digest obtained by using different viscosity buffer: (A) 2 % HEC in 1×TBE buffer (89mM Tris-Borate, 89mM Boric acid, and 2 mM EDTA), viscosity is 70 cP; (B) 2 % HPMC, 6 % mannitol, 2 mM EDTA, 100 mM Tris, and pH 8.0 adjusted by boric acid, viscosity is 5 cP. Sample: 2,000-fold diluted at 250 ng/mL. Injection condition: EKS -2.0 kV for 150 s using default setting as Fig. 4.1 A. Separation voltage: -10kV. UV detection: 260 nm.
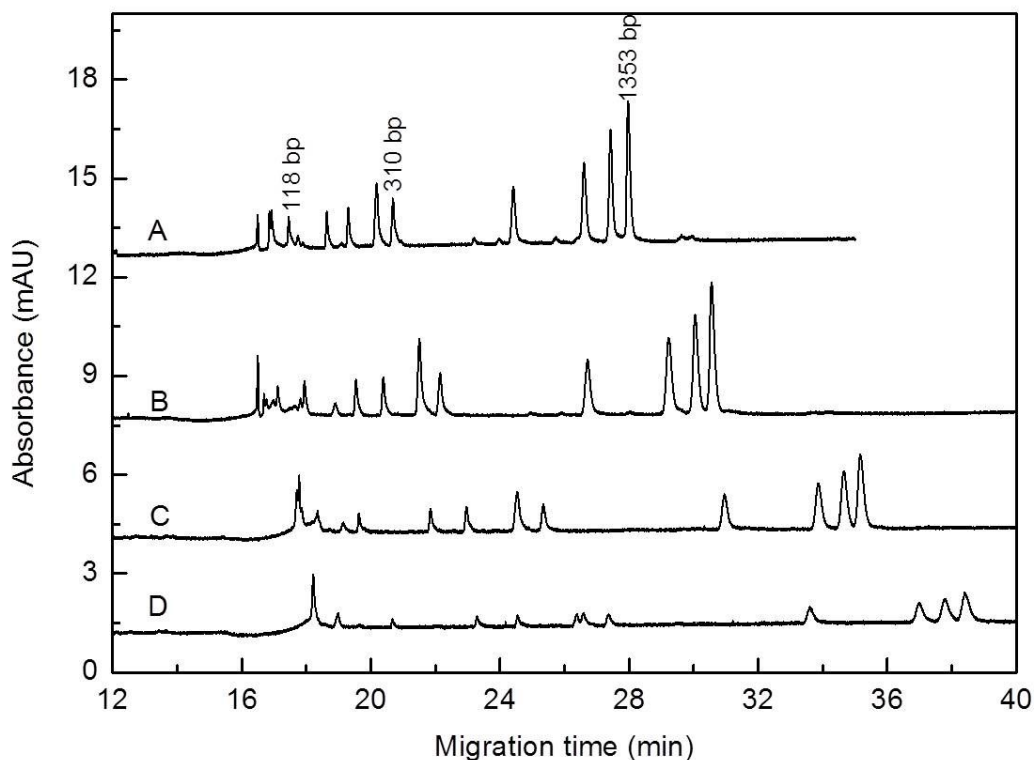
Figure 4.4: Electropherograms of X174/HaeIII digest obtained by using different HEC concentration: (A) 0.8% HEC, (B) 1.0% HEC, (C) 1.5% HEC, and (D) 2.0% HEC in 1 × TBE buffer (89 mM Tris, 89mMBoric acid, and 2mMEDTA), with 6% mannitol, viscosities are 18 cP, 26 cP, 49 cP, and 70 cP, respectively. Sample: 10 000- fold diluted at 50 ng/mL. Others as in Fig. 4.3.

Fig. 4.3 presents the DNA sample was 2000-fold diluted (at 250 ng/mL) that was analyzed by two different viscosity BGEs. At the same EKI conditions (-2.0 kV for 150 s), the obtained electropherograms in Fig. 4.3 A and B display much different peak profiles. In our opinion, simple EKI stacking effect issued in high-viscosity TBE buffer as Fig. 4.3 A. Here, the diluted sample was only stacked due to the difference of field strength between sample zone and BGE. Apparently, Fig. 4.3B exhibits much better stacking efficiency in low-viscosity TBE buffer. We regarded such sensitivity enhancement (Fig. 4.3 B) was superior to that achieved by EKI (Fig. 4.3 A) due to tITP that accompanied by

EKI (i.e. by a virtue of EKS effect). The hydroxyl ion (OH^-) in sample vacancy zone acted as the system-induced terminator when analytes were introduced from a diluted sample. If some co-ions in ultralow-viscosity TBE buffer could be leading ions, EKS process was possibly achieved. The pH of ultralow-viscosity BGE was 8.0 that adjusted by boric acid which is a kind of Lewis acid (pK_a = 9.24). In presence of mannitol, the complex acid must arise due to tetrahydroxyborate complexes mannitol. The dissociation of complex acid (pK_a around 4.0) will lead to form borate polyanion (negatively charged) at pH 8.0. However, in high-viscosity TBE buffer (2 % HEC), the mobility of co-ion (a small number of tertrahydroxyborate fraction at pH 8.3) significantly decreased which resulted in deteriorated function as leading ion. The generation of borate polyanion was already verified in some studies, where the boron complexed with other polyhydroxy compounds [20,21]. Consequently, the ultralow-viscosity TBE buffer benefited EKS enrichment, since the leader of co-ion (borate polyanion) and system-induced terminator (hydroxyl) for tITP process.

4.3.2 EKS process simulated in a tapered vial

Computer simulation has already been adopted in our study to explore the relationship between EKS performance and the electrode configuration [14,15]. The simulated components of BGE and sample are the typical model for achieving EKS process, thus it well describes the movement and preconcentration behaviors of the analytes. The capillary surrounded by the cylindrical electrode owns one unique feature that $D_{e/c}$ in Fig. 4.1 can be varied a bit. And the efficiency of sample introduction amount was significantly determined by configuration of electrode and capillary [14]. When the capillary was shorter than electrode and hidden inside, few analytes was injected [22]. On the other hand, the configuration with capillary-tip longer than that of electrode leads to a wider distribution of the electric potential in the solution.

Herein, two factors were expected to be understood from the simulation: one was the influences of $D_{e/c}$, another was the non-uniform potential distribution in a tapered vial.
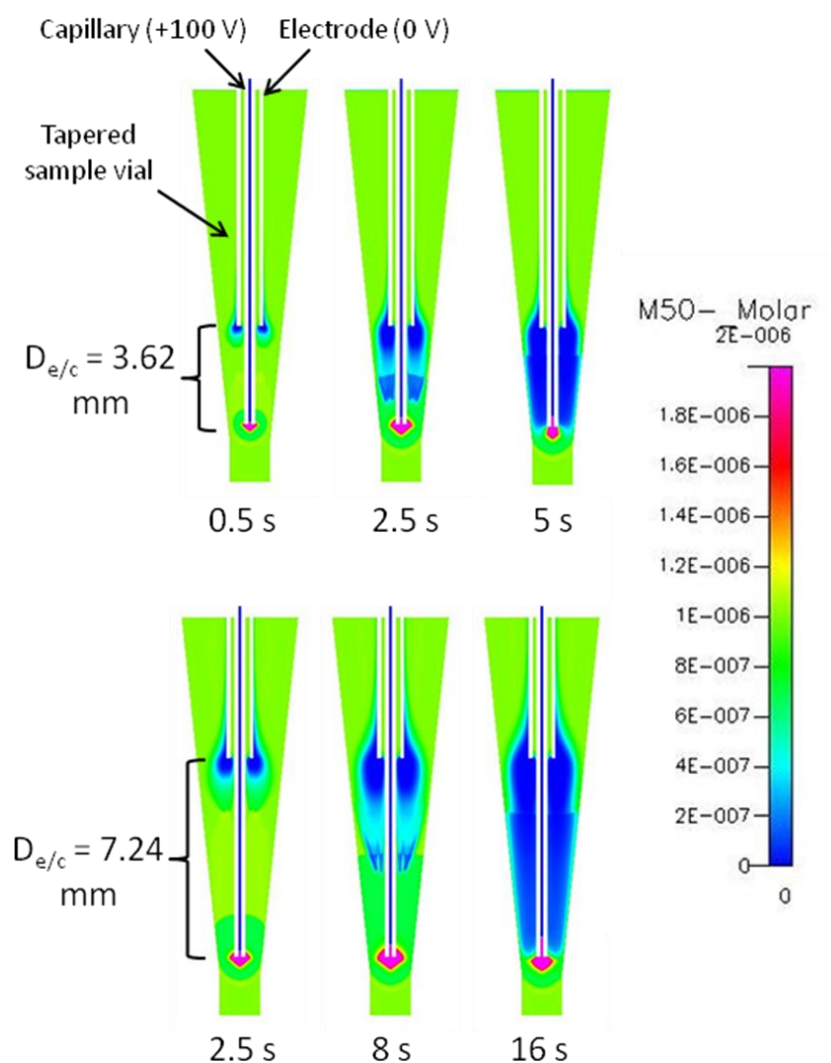

Figure 4.5: Illustration of m50⁻ concentration profile varied with time after applying migration voltage according to $D_{e/c}$ at 3.62 mm and 7.24 mm, respectively. The time represented the analyte depletion speed by simulation. The color corresponds to the concentration values as scaled.

Visual simulation of Figure 4.5 illustrates the concentration profiles of m50$^-$, including the different time for short and long simulated $D_{e/c}$ after applying the same voltage (100 V). It should be noted that the same voltage leaded to much different field strength in the vial due to the different $D_{e/c}$, so the simulated time (i.e. depletion velocity of analytes) was different. Consequently, the effective potential distribution depended on $D_{e/c}$, and would determine the injected sample amount then influence the sensitivity. In Fig. 4.5, we knew the effective potential distributed between the tips of electrode and capillary, which resulted in the most of injected analytes were from this area. Figure 4.6 puts another way to verify the injected amount significantly depended on $D_{e/c}$. As in Fig. 4.6, the $D_{e/c}$ was doubled from 3.62 mm to 7.24 mm, the final injected amount of m30$^-$ and m50$^-$ were more than double, although the EKS time was longer since the field strength decreased. Besides such previous known conclusion, it was concluded that the tapered vial is more suitable for EKS than straight-bucket sample vial. Fig. 4.5 gives the same conclusion that the sample vacancy zone almost reached the boundary of the tapered area. A tapered vial means small volume used, however, the ratio of injected amount to initial sample amount was high. For the analyte of m50- at De/c of 3.62 mm, about 88 % of the initial amount (14.82 pmol) contained in the volume that below the tip of electrode (V1 = 14.82 µL as shown in Fig. 4.2) can be injected after 10 s. When the De/c increased to 7.24 mm, more analytes can be injected due to the initial amount of m50- in V2 (V2 =37.16 µL as in Fig. 4.2) was increased to 37.16 pmol. After 16 s simulation, 78 % of m50- was injected and still going up. The conclusion implies a Pt-ring electrode setting at the upper of vial and inserting the capillary to the bottom (i.e. maximum De/c), the contained sample would almost be introduced for EKS preconcentration. The hypothesis was verified in the next section.
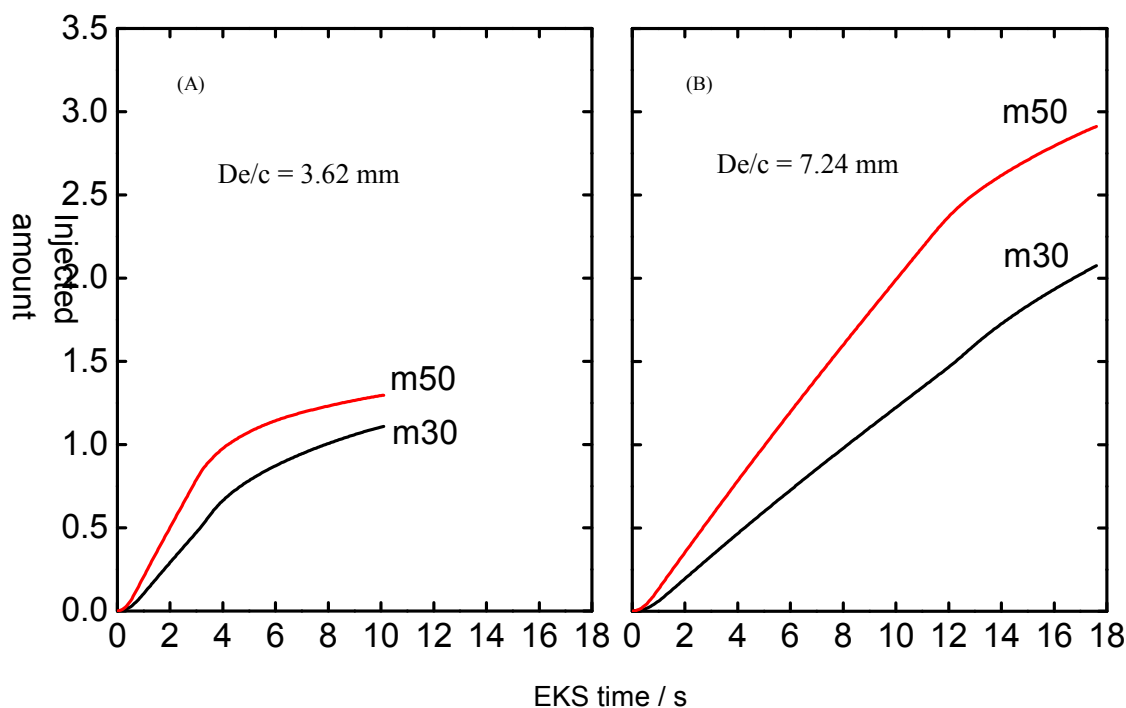
Figure 4.6: Simulated results of the injected amount by using the hollow electrode with different $D_{e/c}$ of (A) 3.62 mm and (B) 7.24 mm. Sample: 2 anions (m50$^-$ and m30$^-$), each at 1.0 μM. BGE: 50 mM HCl and 100 mM Tris. Others as in Fig. 4.4.

4.3.3 Optimization of electrode configuration for injection

Figure 4.1 presents our strategies to increase $D_{e/c}$ for improving the efficiency of EKS according to simulation. The default $D_{e/c}$ is 3.6 mm. Based on the electrode design of Agilent HP^{3D} CE system, a simple way of cutting the hollow electrode shorter resulted in extending $D_{e/c}$ of 16 mm. At $D_{e/c}$ of 16 mm, the LOD of 72 bp (weakest peak) was improved from 0.15 ng/mL to 0.08 ng/mL. The obtained electropherograms are presented in Figure 4.7A and B. Here, the sample was 10,000-fold diluted at the concentration of 50 ng/mL, the

used volume was increased from 100 µL to 230 µL with the $D_{e/c}$ increasing from 3.6 mm to 16 mm. The implemented EKS condition was the same at -2 kV for 150 s.
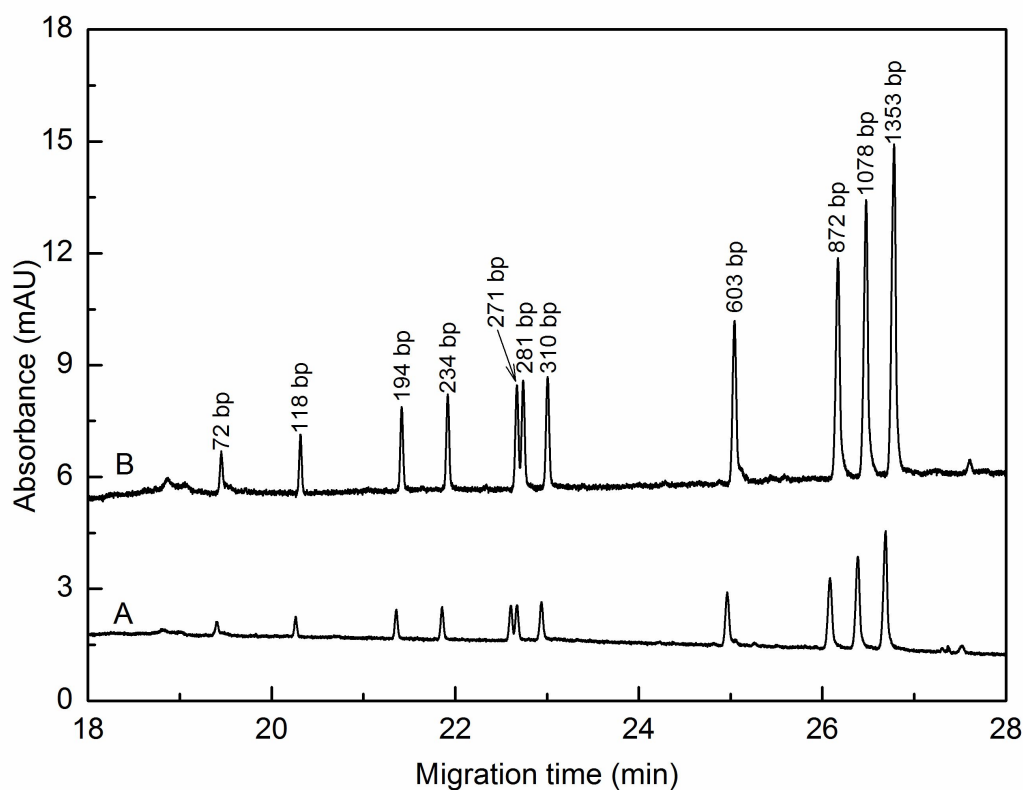

Figure 4.7: Electropherograms of φ×174/HaeIII digest obtained by using hollow electrode: (A) default $D_{e/c}$ of 3.6 mm (as Fig. 4.1 A); (B) cut electrode with extended $D_{e/c}$ of 16 mm (as Fig. 4.1 B). Sample: 10,000-fold diluted at 50 ng/mL. BGE: 2 % HPMC, 6 % mannitol, 2 mM EDTA, 100 mM Tris, and pH 8.0 adjusted by boric acid. Others as in Fig. 4.3.

Although the LOD was improved about 2-fold by such an easy way (increasing $D_{e/c}$ from 3.6 mm to 16 mm), it's still a possibility to pursue higher sensitivity by enlarging the area of effective electric field in the tapered vial.

First, the hollow electrode is replaced by ring type around capillary (Fig. 4.8). For this aim, the conductive function of original electrode should be abandoned. As shown in Fig. 4.8 B, the electrode was cut and the $D_{e/c}$ at 24 mm resulted in contactless of solution in sample vial. Thus the original electrode is only for fixing the capillary. Fig. 4.9 shows the photos of a simple Pt-ring electrode was made and positioned around the capillary at the bottleneck of the vial. Based on previous result [17], the used sample amount was also increased. The added volume to the bottleneck is around 230 µL (almost the maximum of tapered vial). All these modifications gave rise to increased loading of analytes and notably improved detectability of EKS-CGE system as detailed in next section.
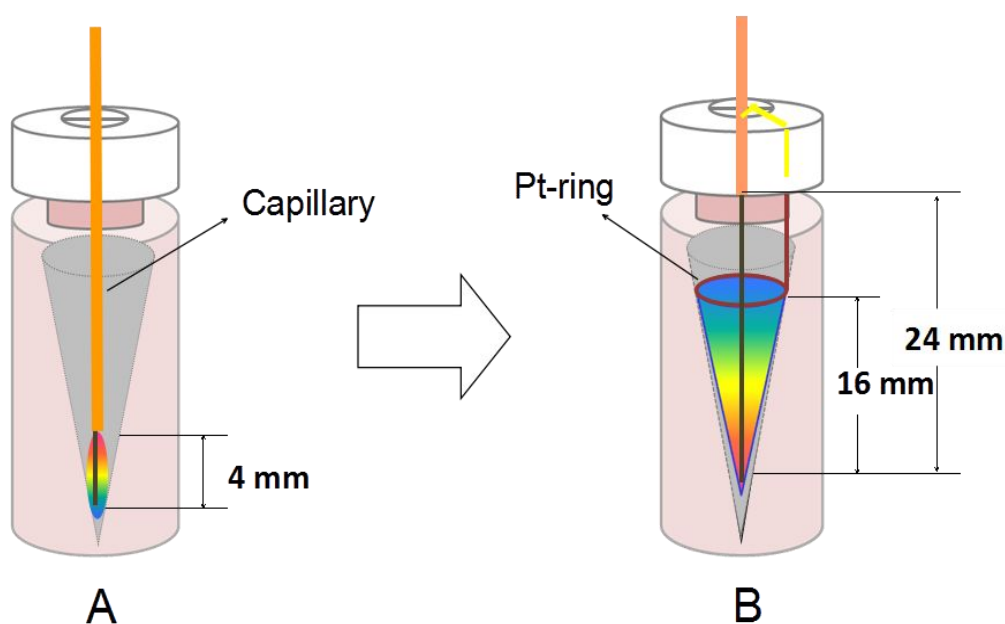

Figure 4.8: Schematic diagram of electrode setting: (A) is the default electrode configuration with the $D_{e/c}$ of 4 mm; (B) is the short electrode ($D_{e/c}$ = 24 mm) modified by a Pt-ring electrode fixed in the sample vial was positioned around the capillary.
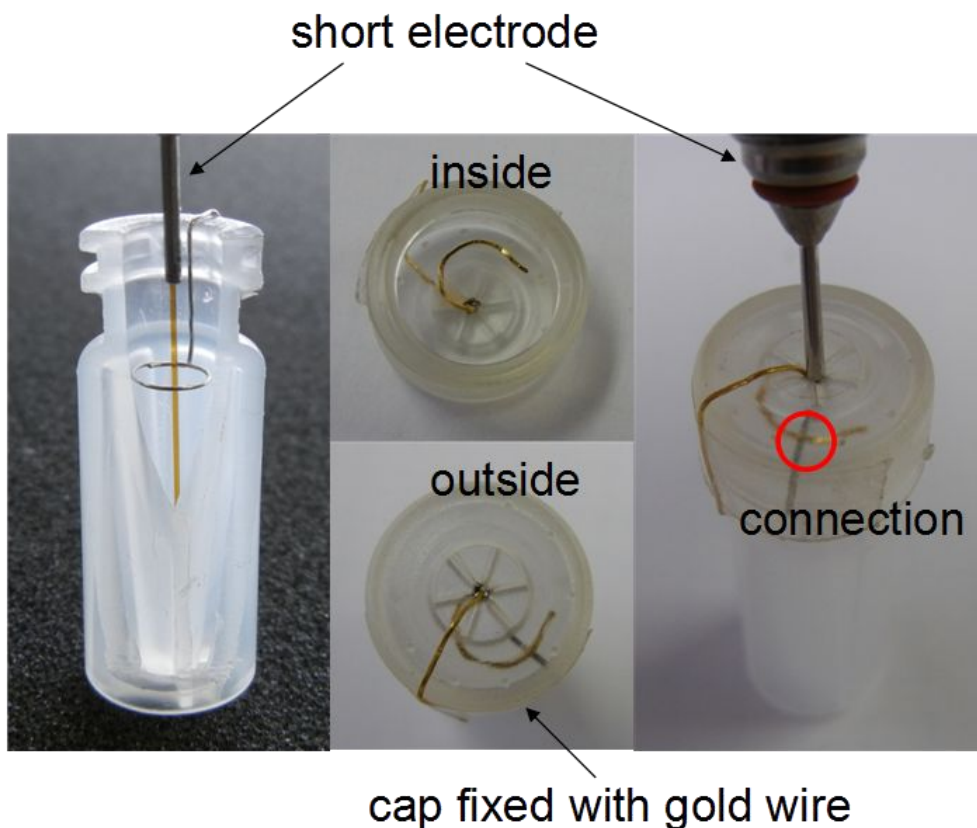
Figure 4.9: Photos of electrode setting which modified by a Pt-ring electrode fixed in the sample vial was positioned around the capillary. The gold wire fixed on the cap was used for conducting.

4.3.4 Optimization of injection conditions

For the default $D_{e/c}$ of 4 mm, the peak area of DNA almost keep constant after the injection time was longer than 150 seconds while the injection voltage was fixed at -2kV and injection last too long will broaden the peaks which is unfavorable to sensitivity. This could be explained that most of the sample occurring in the effective electrical filed had been introduced into the capillary end during 150 seconds, but the sample being outside of the effective electrical field cannot be injected due to its diffusion can be neglected during EKI process. The rate of sample diffusion is significantly smaller than the rate of EKI, so it is useless to continue to increase the injection time in this case.

But for modified Pt-ring electrode, it is necessary further increase the injection time because the lower electric field owing to the longer De/c even at the same injection voltage as original electrode. Besides, more samples occurring in a larger space of the effective electric field needs more time to move toward the capillary end. Thus, 150 seconds is inadequate for Pt-ring electrode with the injection voltage of -2kV. As displayed in Fig. 4.10, the peak area of DNA increased gradually with the injection time increasing from 150 s to 450 s and they increased slowly after 450s and the peak become wide. So, 450 s is optimal injection time for Pt-ring electrode.
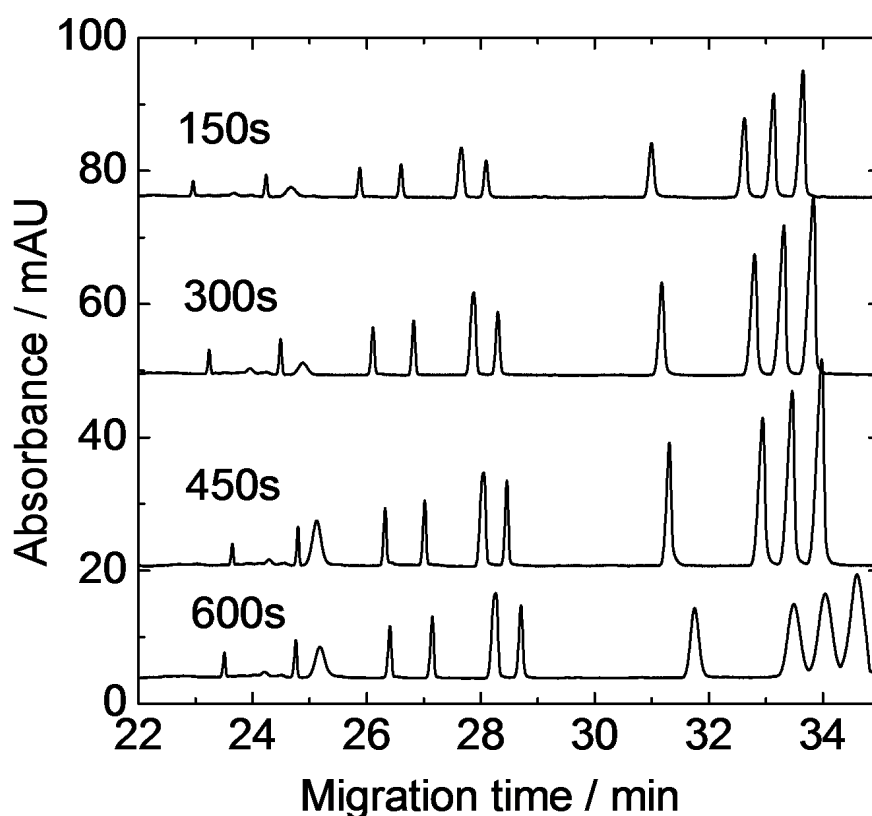

Figure 4.10: Electrophoregrams of φ X 174-Hae III digest obtained by using Pt-ring electrode at concentration of 50 ppb. The sample was injected by -2 kV for 150 s to 600 s that list in the figure.

4.3.5 Sensitivity and reproducibility for DNA analysis

The standard DNA marker, φX174/HaeIII digest, was 10,000-fold diluted in water (total concentration, 50 ng/mL) and injected by using Pt-ring type electrode and large sample volume (230 μL). Fig. 4.11 presents the electropherograms that preconcentrated by EKS and gel separated in ultralow-viscosity TBE buffer at different EKS strategies. The fragments from 72 to 1353 bp were well separated within 30 min. However, the fragments of 271 and 281 bp still kept co-migrating (insert part in Fig. 4.7) because the buffer is without 10 bp sieving ability. We investigated the RSD (n=3) of the migration time and peak area followed the conditions in Fig. 4.7C. The migration time had a very good precision with the RSD 0.09 %. For the peak area, the RSD was still acceptable as 8.6 %, which was caused by long time EKS. We previously reported the LOD of same DNA sample was 0.09 ng/mL (for 72 bp components), which was achieved by tITP stacking combined high-sensitive fluorescence detection [23]. Herein, the sample was enriched by novel EKS proposal and only with normal UV-Vis detection. The 170,000-fold highly diluted sample was analyzed at the optimal conditions (electropherogram not shown), the obtained LOD was down to 7.7 pg/mL (for the weakest peak of 72 bp at S/N=3). It is much better than fluorescence detection. Therefore, the represented LOD was about 20-fold improved than the original hollow electrode configuration as described in Fig. 4.7A. Furthermore, such sensitivity is more than 10,000 times better than those obtained by normal CGE with UV-Vis detection. It was found that the peak intensity was significantly decreased after the first injection if take three successively injection from the same sample vial using Pt-ring electrode. When the injection time increased to 450 s, the peak intensity of the first run was accounted for more than 70 % of the total intensity of three run. That is to say, the optimal injection at -2kV for 450 s by Pt-ring electrode introduced about 70% of analytes amount existing in the sample vial into the capillary.
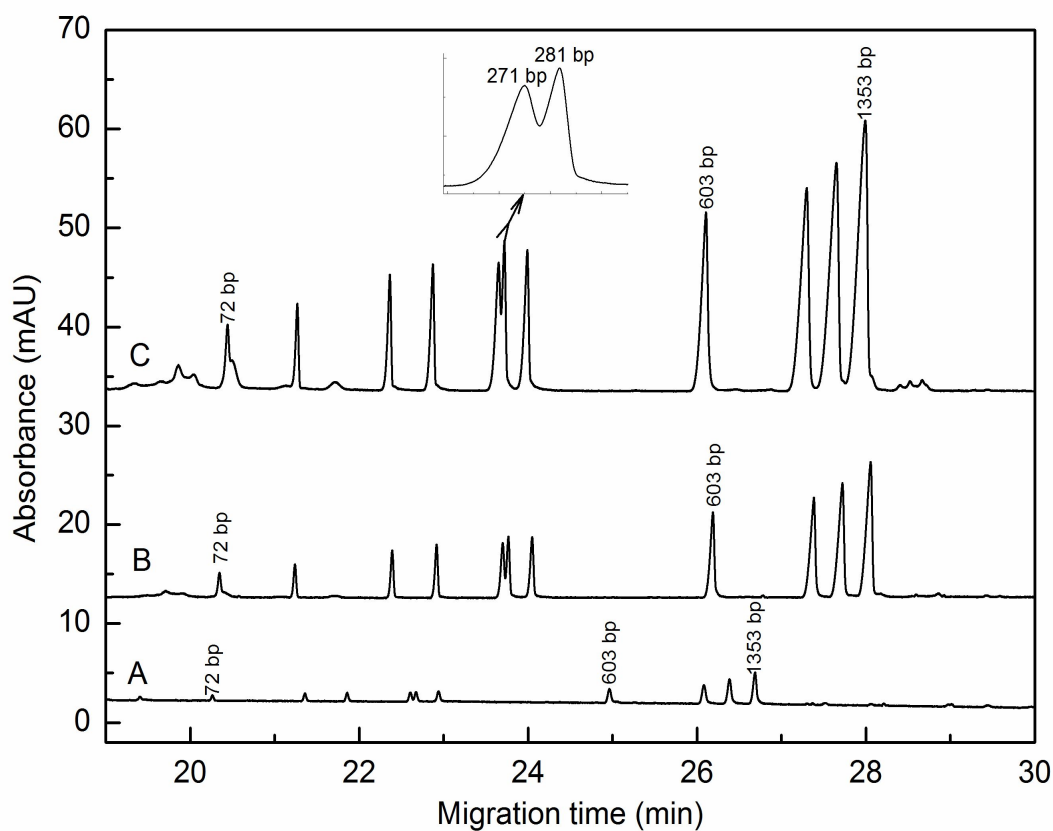
Figure 4.11:. Electropherograms were obtained by using different protocols: (A) hollow electrode with $D_{e/c}$ at 3.6 mm, EKS at -2.0 kV for 150 s; (B) Pt-ring electrode, EKS at -2 kV for 150 s; (C) Pt-ring electrode, EKS at -2.0 kV at 450 s. Others as in Fig. 4.6.

4.4 Summaries

The proposed strategy has a great promise for carrying CGE analysis of DNA fragments with high sensitivity, due to EKS preconcentration achieved by using developed buffer and at the modified electrode configuration. The

additive of mannitol will lower the buffer viscosity and complex with boric acid, which resulted in generating borate ployanion for tITP. A Pt-ring type electrode and large sample amount were adopted and optimized to improve EKS performance. To our best knowledge, the LOD of CGE analysis of dsDNA with UV-Vis detection is always at μg/mL (ppm) level, which could be improved to a few pg/mL (ppt) by our method. Advantageously, the simple and inexpensive alteration of EKS preconcentration procedure presented here, easily adopted with commercial Agilent instrumentation. The simulation and experiments will be also useful for any other online preconcentration protocol based on electrokinetic sample injection given a complementary enrichment technique that has the potential to effectively stack the injected analytes.

4.5 References

[1] Mitnik, L., Novotny, M., Felten, C., Buonocore, S., Koutny, L., Schmalzing, D., *Electrophoresis* 2001, 22, 4104-4117.

[2] Sato, K., Hosokawa, K., Maeda, M., *J. Am. Chem. Soc.* 2003, 125, 8102-8103.

[3] Lian, W., Litherland, S. A., Badrane, H., Tan, W., Wu, D., Baker, H. V., Gulig, P. A., Lim, D. V., Jin, S., *Anal. Biochem.* 2004, 334, 135-144.

[4] Elghanian, R., Storhoff, J. J., Mucic, R. C., Letsinger, R. L., Mirkin, C. A., *Science* 1997, 277, 1078-1081.

[5] Breadmore, M. C., *Electrophoresis* 2007, 28, 254-281.

[6] Malá, Z., Krivánková, L., Gebauer, P., Bocek, P., *Electrophoresis* 2007, 28, 243-253

[7] Chien, R. L., *Electrophoresis* 2003, 24, 486-497.

[8] Simpson, Jr. S.L., Quirino, J.P., Terabe, S., *J. Chromatogr. A* 2008, 1184, 504-541.

[9] Hirokawa, T., Okamoto, H., Gas, B., *Electrophoresis* 2003, 24, 498-504.

[10] Xu, Z. Q., Timerbaev, A. R., Hirokawa, T., *J. Chromatogr. A* 2009, 1216, 660-670.

[11] Dawod, M., Chung, D. S., *J. Sep. Sci.* 2011, 34, 2790-2799.

[12] Han, F. T., Huynh, B. H., Ma, Y. F., Lin, B. C., *Anal. Chem.* 1999, 71, 2385-2389.

[13] Han, F., Xue, J., Lin, B. C., *Talanta* 1998, 46, 735-742.

[14] Hirokawa, T., Koshimidzu, T., Xu, Z. Q., *Electrophoresis* 2008, 29, 3786-3793.

[15] Xu, Z. Q., Koshimidzu, E., Hirokawa, T., *Electrophoresis* 2009, 30, 3534-3539.

[16] Xu, Z. Q., Kawahito, K., Ye, X. X., Timerbaev, A. R., Hirokawa, T., *Electrophoresis* 2011, 32, 1195-1200.

[17] Xu, Z. Q., Nakamura, K., Timerbaev, A. R., Hirokawa, T., *Anal. Chem.* 2011, 83, 398-401.

[18] Gebauer, P., Thormann, W., Boček, P., *Electrophoresis* 1995, 16, 2039-2050.

[19] Fukushi, K., Nakayama, Y., Tsujimoto, J., *J. Chromatogr. A* 2003, 1005, 197-205.

[20] Shao, C. Y., Matsuoka, S., Miyazaki, Y., Yoshimura, K., Suzuki, T. M., Tanaka, D. A. P., *J. Chem. Soc., Dalton Trans.* 2000, 3136-3142.

[21] Shao, C. Y., Miyazaki, Y., Matsuoka, S., Yoshimura, K., Sakashita, H., *Macromolecules* 2000, 33, 19-25.

[22] Boer, T. D., Ensing, K., *J. Chromatogr. A* 1997, 788, 212-217.

[23] Xu, Z. Q., Esumi, T., Ikuta, N., Hirokawa, T., *J. Chromatogr. A* 2009, 1216, 3602-3605.

Chapter 5: DNA aggregation and cleavage during EKI

5.1 Introduction

In recent years, CGE has become a preferred instrumental technique for DNA analysis due to its advantages over conventional slab gel electrophoresis including high resolving power, short separation time, ease of automation, and good sensitivity [1,2]. In DNA analysis, electrokinetic injection (EKI) is usually considered as one of the useful approaches to improve sensitivity of CGE. Furthermore, higher sensitivity could be obtained by combining CGE with preconcentration strategies such as field amplified sample injection, transient isotachophoresis (tITP) and electrokinetic supercharging (EKS) [3]. Consequently CGE found wide applications in clinical diagnostics [4], gene therapy [5] and forensics [6] for DNA separations, where high-sensitive analysis was needed in these fields.

In our previous research [7-9], we successfully achieved high-sensitivity detection of DNA fragments by using EKS in microchip gel electrophoresis using conventional UV detection. We also tried LIF detection in combination with tITP achieving the LOD for φ×174/HaeIII digest down to 90 ng/L for 72 bp fragment (S/N=3) [10]. For rare-earth metal ions, to improve the sensitivity, the relationship between electrode position and sample amount injected was explored using EKS. We found that analytes occurring only in an effective electric field could be introduced into the capillary while the other analytes remaining outside of the field were hardly injected because of slow diffusion [11]. Based on these results, we proposed an EKS method using a long vial with a distance between tips of electrode and capillary ($D_{e/c}$) of 40 mm, which afforded the LODs of rare-earth metal ions at single-digit part per trillion (ppt) level [12]. Thus EKS could contribute to high sensitivity analysis even for DNA fragments by using UV detection when a longer $D_{e/c}$ was applied. In our recent

work, the EKS approach was adopted for the analysis of DNA fragments by using an ultralow-viscosity buffer solution with good sieving ability and a modified electrode configuration (a Pt ring placed around the capillary). This led to efficient sample introduction from a large volume of the sample (230 µL). The obtained LOD was 7.7 ng/L (for the weakest peak of 72 bp at S/N=3), so that apparently improved by a factor of more than 10,000-fold in comparison with conventional CGE [13,14].

However, along with this, it was found that the peak areas of DNA fragments decreased with increase of injection voltage (V_{inj}) from 2 to 10 kV at a $D_{e/c}$ of 16 mm, and some unexpected peaks occasionally appeared when the V_{inj} was e.g. 10 kV. This phenomenon might be attributed to the aggregation of the fragments, since aggregates would be formed at high electric field (>= 400V/cm) as described for DNA with high molecular weight (4.3 - 48 kbp) [15]. On the other hand, no aggregation was observed at low electric field strength (< 50 V/cm) [15]. Our observation might be caused due to aggregation similarly, but might suggest DNA decomposition during EKI as described in the later section. It is well known that not only high-energy ionized particles may cause DNA cleavage in the solid state [16], but also low energy electrons (0-20 eV) induced single- and double-strand breaks in DNA via dissociative electron attachment [17]. The authors suggested that the damage involved initial electron attachment to nucleobase moieties, followed by electron transfer to the sugar-phosphate backbone and subsequent dissociation of the phosphodiester bond [18], as described in the supplementary Fig. 5.5-1. Therefore, by analogy we assumed that chemical bonds in DNA in aqueous solution could also be damaged by high electric field even during EKI process although low energy electrons do not exist in an aqueous solution.

In order to show the possibility of such DNA damage, in this paper, DNA step-ladder samples were injected and analyzed by applying different V_{inj} from 2 to 30 kV. Then the samples that were intentionally voltage-affected (200 V/cm) yet before injection were analyzed to explore the effect. We also

investigated the effects of $D_{e/c}$ and DNA concentration on the degree of DNA damage.

5.2 Materials and methods

5.2.1 Instrumentation

All experiments except for 40 mm $D_{e/c}$ were carried out on the Agilent HP^{3D} CE system (Agilent Technologies, Waldbronn, Germany) fitted with a photodiode array detector. The default electrode was hollow and cylinder-shaped, therefore, the capillary went right through the electrode. The separations were performed in the fused-silica capillary with 50 cm × 75 μm I.D. (41.5 cm effective length). If not specified, HP3D was used.

The experiments for 40 mm $D_{e/c}$ were conducted on a CAPI-3300 instrument (Otsuka Electronics, Osaka, Japan) and with fused-silica capillaries of 75 μm I.D. with a length of 50 cm (37.7 cm to the detector). All the capillaries were purchased from GL sciences (Tokyo, Japan). The temperature of capillary chamber was set at 25 ° C. All the voltage applied was negative against electrode near the detector, but we used positive value to describe the applied voltage throughout this paper for convenience.

5.2.2 Reagents and samples

The standard DNA sample of 50 bp DNA step-ladder was purchased from Promega Co. (Madison, USA). The sample consists of 16 DNA fragments ranging from 50 to 800 bp in exactly 50 bp increments and an original 1800 bp fragment, the total concentration was 340 mg/L, where 90 μg step- ladders were contained according to the specification (original sample volume was calculated as 265 μL). The original sample was diluted by pure water for the

CGE experiments. The sample was used only once in the EKS-CGE analysis. An ultralow-viscosity sieving buffer [14] with pH of 7.0 was used throughout this study, which was prepared to contain 2 % hydroxypropyl methyl cellulose (HPMC), 6 % mannitol, 2 mM EDTA, 0.1 M boric acid and 0.1 M Tris. The HPMC with average molecular weight around 10,000 was purchased from Sigma-Aldrich (St. Louis, USA). They specified that the viscosity of 2 % aqueous solution was 5 cP. Other chemicals including phosphoric acid, Tris, boric acid and EDTA were obtained from Sigma-Aldrich Japan (Tokyo, Japan). Mannitol is from Sigma-Aldrich USA (St. Louis, USA). Purified water used to prepare all solutions was delivered by arium® pro DI Ultrapure Water System produced by Sartorius Stedim Biotech GmbH (Goettingen, Germany). The step-ladder sample (1000 times dilution, 0.34 mg/L) used for intentionally damaged sample was prepared by applying 200 V DC in a glass vial.

5.2.3 Electrophoretic conditions and data analysis

New capillaries were washed with deionized water for 5 min and 1.0 M HCl for 30 min. Between each run, the capillary was flushed with water for 2 min, 1.0 M HCl for 2 min, water for 2 min, and then BGE for 5 min. In order to avoid contaminations originated from BGE, the capillary inlet and the electrode system were washed with deionized water before EKI. The injection voltage was ranged from 2.0 to 30 kV. A constant voltage of 10 kV was applied for gel separation of analytes. The detection wavelength was set at 260 nm. The peak area and migration time were obtained by homemade software. For accurate analysis, the value of peak area (mAU) in each figure and table was calculated as the quotient, the peak area (mAU · min) divided by migration time (min) of individual peaks.

5.2.4 Computer simulation

A finite element method was carried out with CFD-ACE+ software (CFDRC, Huntsville, AL, USA) to simulate the concentration and potential gradient profiles in a tapered-vial model similar to the real vial used for Agilent HP^{3D} CE system, which is shown in later section. The used model was two-dimensional, which can be extended to three dimensional by rotation. The size of meshes in the vial and a capillary was varied from 10 μm × 10 μm up to 50 μm × 50 μm for convenience. The cylindrical electrode (700 μm I.D., 1000 μm O.D.) surrounded the capillary with $D_{e/c}$ of 3.6 mm. The voltage applied for injection was set at 0 V at the electrode and 100 V at the end of capillary (30 mm length, 100 μm I.D., 400 μm O.D.). The sample consisted of five model anions with mobilities of 10×10^{-5} (m10$^-$), 20×10^{-5} (m20$^-$), 30×10^{-5} (m30$^-$), 40×10^{-5} (m40$^-$), and 50×10^{-5} (m50$^-$) cm^{2}V^{-1}s^{-1}. Initial concentration was assumed to be 1.0 μM for each analyte (counter ion, 5.0 μM Na$^+$). The used BGE was a mixture of 50 mM HCl (m_0(Cl$^-$) = 79.1×10^{-5} cm^{2}V^{-1}s^{-1}) and 100 mM Tris (m_0=29.5×10^{-5} cm^{2}V^{-1}s^{-1}, pK$_a$=8.076). No EOF was assumed. The software was implemented on a PC with dual Pentium Xeon 3GHz processors. All simulations were for a time of 10 s ~ 17 s with data collection in 40,000 ~ 85,000 steps (time interval, dt, was 0. 25 ms).

5.3 Results and Discussion

5.3.1 DNA damage in aqueous solution during EKI

 Fig. 5.1 As can be seen from Fig. 5.1, the peak shape of DNA fragments was always very sharp owing to EKS and good sieving ability of the BGE used. But it should be noted that the height of the peaks remarkably decreased with the increase of V_{inj}, which might imply that the DNA fragments were partly damaged (aggregated or cleaved) and converted into snowballs [15] or smaller fragments.
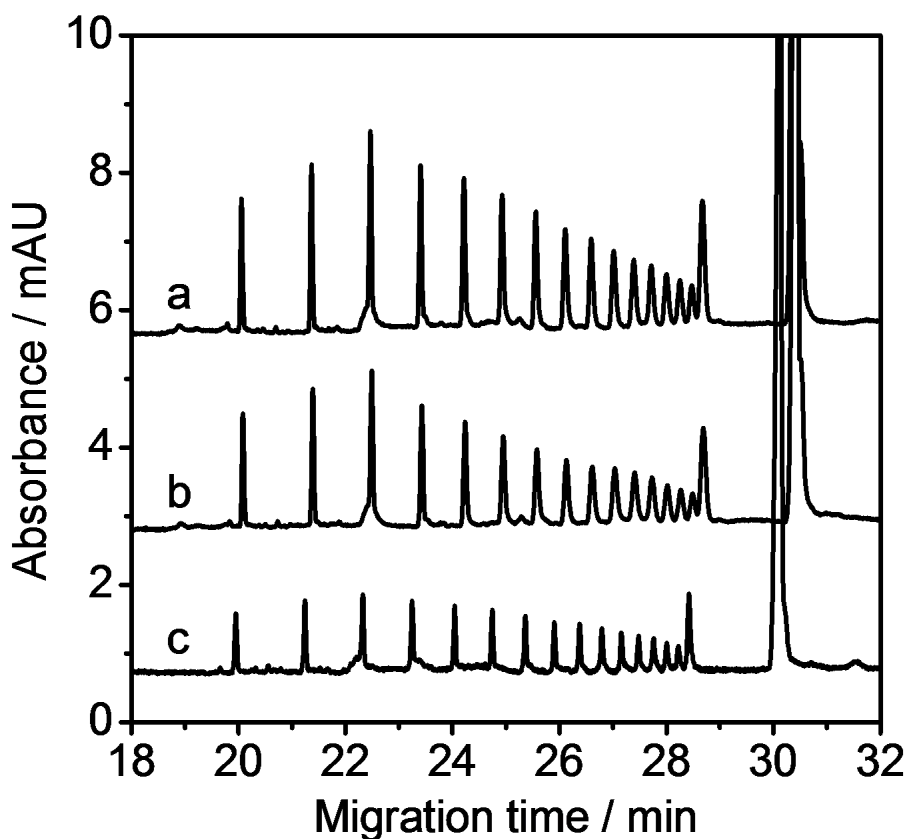
Figure 5.1: Electropherograms of 50 bp step-ladder samples obtained by using different injection conditions: (a) 10 kV for 30s, (b) 20 kV for 15 s, (c) 30 kV for 10 s. Sample concentration: 170 µg/L. $D_{e/c}$ was 4 mm. Separation voltage: 10 kV.

It is well known that such DNA transformation can be induced by low energy electrons when the DNA samples are solid. Low-energy electrons may attach directly to phosphate groups and induce strand breaks (a summary was given in the supplementary Fig. 5.1) [17,18]. In refs 17 and 18, the possible fragmentation shown in Fig. 5.2 was suggested. If the number of phosphate groups in the damaged fragments are not enough, they remained as cations or neutral, which are difficult to observe in the present CGE experiments observing anionic components. Phosphate might be observed depending on the position of cleavage of chemical bonds.
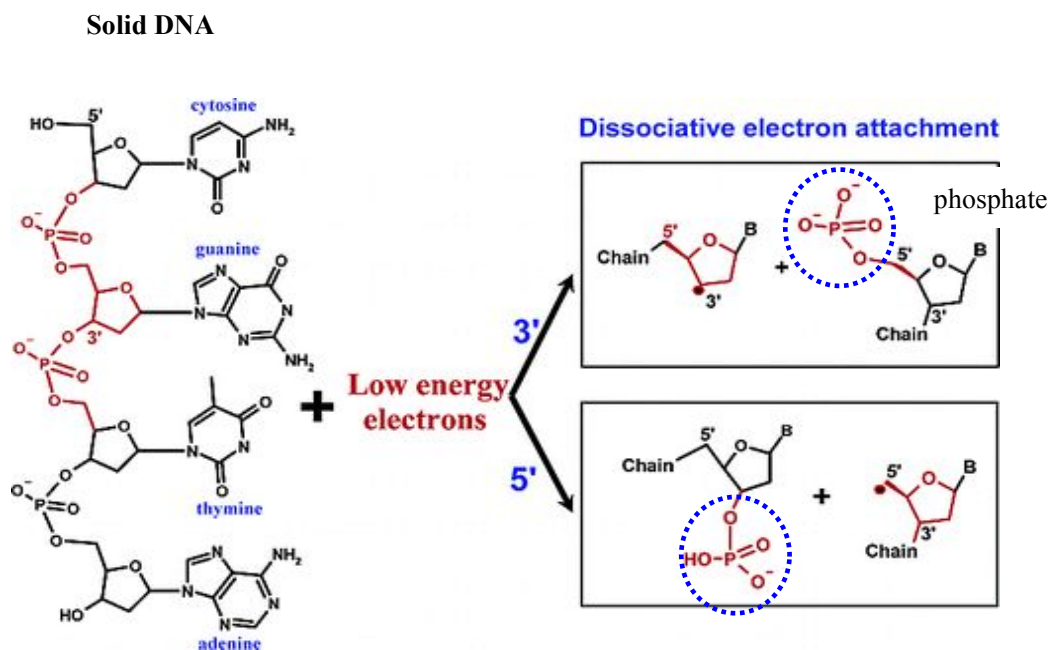
Solid DNA

Figure 5.2: Fragmentation of 3' or 5' O-C σ bonds in phosphate-centered anions.

If phosphate groups were dissociated, damaged DNA would not migrate and be detected. So we speculated that a high V_{inj} might lead to the cleavage of DNA fragments even in aqueous solution besides aggregation. However, the mechanism of cleavage is still not very clear at present and the ratio of aggregated DNA and cleaved DNA is not explored, although many undetermined decomposed fragments were detected by HPLC for the solid samples [17]. In our CGE analysis, the peaks of DNA fragments (50 - 800 bp) became smaller and smaller with increasing V_{inj}, but no other significant anionic peaks appeared when $D_{e/c}$ was 4 mm. This might be due to the fact that the ionic property of the originally electronegative DNA fragments at pH 7.0 was not imparted under high V_{inj}. In that case, the damaged fragments could not be introduced into the capillary. We also tried to use lower V_{inj}, such as 2 or 5 kV (the injection time was 150 and 60 s, respectively) to check if the

DNA would be damaged or not. It was found that at such low V_{inj}, there was no significant change in the peak heights and areas (data not shown). In other words, the DNA damage (aggregation and cleavage) was so slight that could be ignored at low V_{inj}.

In order to test our hypothesis, the same experiments were performed on CAPI-3300 CE system that could make the $D_{e/c}$ as 40 mm. Fig. 5.3A shows electropherograms obtained for the step ladder samples in Fig. 5.3A at detection wavelength of 260 nm, where V_{inj} was varied from 2 to 15 kV (the injection time was kept constant at 80 s). Fig. 5.3B shows those obtained at detection wavelength of 200 nm for the same runs in Fig. 5.3A. The peak at ca. 14 min in Fig. 5.3A might be attributed to cleaved fragments since the peaks of 50 step-ladder samples started from 19 min. Obviously, when the V_{inj} increased from 2 kV (a) to 10 kV (c), the peak areas increased with the V_{inj}, but when the V_{inj} reach 15 kV (d), the peak area slightly increased (for 50 bp and 100 bp peaks) or decreased (after 100 bp peaks). Ideally, the peak areas should increase with injection voltage since the injection time is constant. As shown in Fig. 5.3B, however, the negative peak appeared at 12 min referred to phosphate, which was confirmed by the standard sample (data not shown). The formation of phosphate could support the possibility of DNA cleavage, because these phosphate groups might be released from strand breaks. Of course aggregation could happen simultaneously.
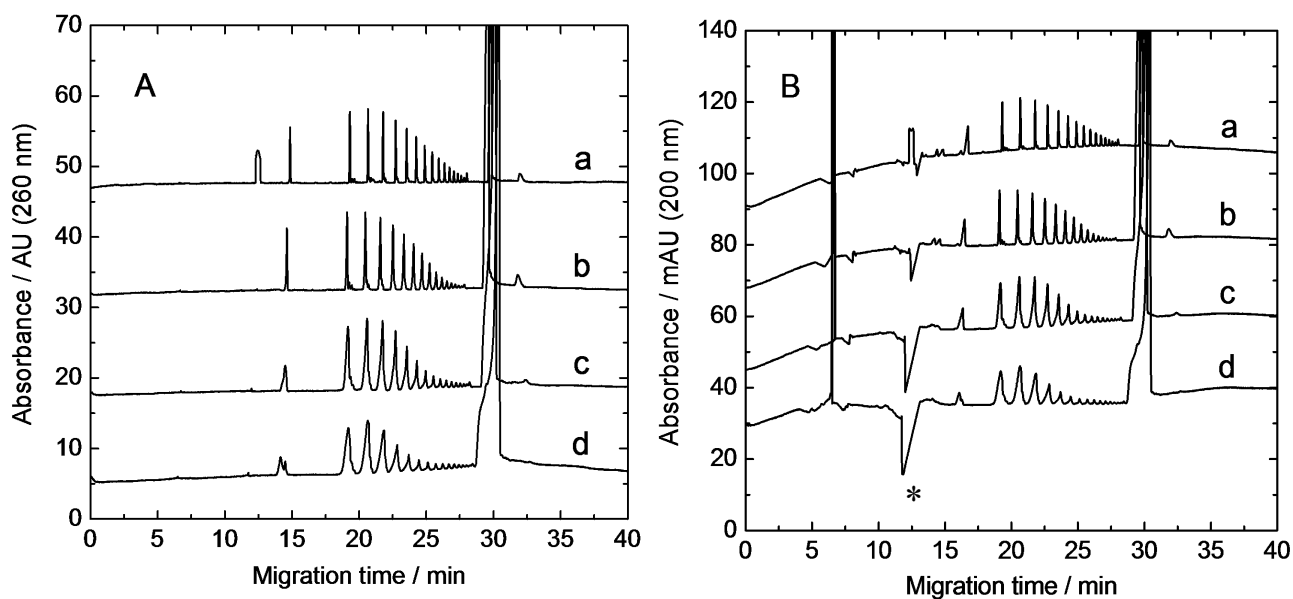
Figure 5.3: Electropherograms of 50 bp step-ladder samples at UV absorption (A) 260 nm and (B) 200 nm. The DNA sample introduced by using different injection voltage of (a) 2 kV, (b) 5 kV, (c) 10 kV and (d) 15 kV, respectively, and the injection time was keep constant at 80 seconds. DNA Sample concentration: 170 µg/L. $D_{e/c}$ was 40 mm. Separation voltage: 10 kV. The peak marked with asterisk (appeared around 12 min) referred to phosphate.

Fig. 5.4 here shows the peak area dependence on the injection voltage taken from the Fig. 5.3A. Obviously, the increment of peak area was not very much proportional to the voltage As shown in Fig. 5.4, the peak areas of small step ladders like 50 and 100 bp increased with increase of the injection time, but the larger base pairs in the range 400-800 bp are almost constant, suggesting that the DNA fradments were anyway damaged (aggregated or cleaved).
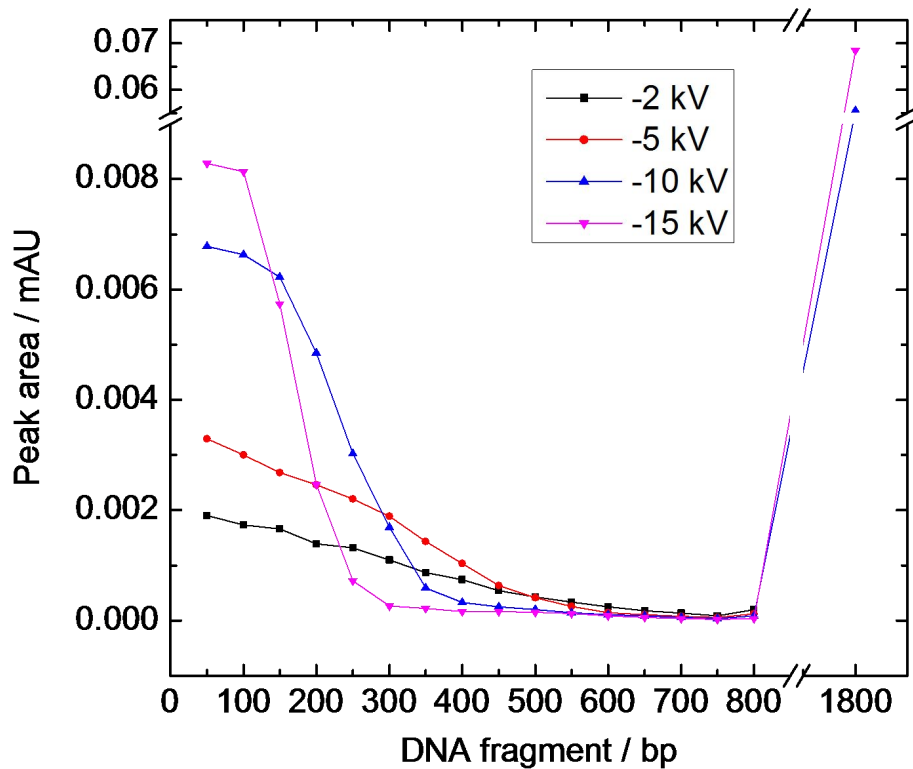
Figure 5.4: Peak areas of all the fragments measured by varying V_{inj}. Others as in Fig. 5.3.

Fig. 5.5 demonstrates the peak areas of DNA fragments observed at varied V_{inj} and injection time. The peak area is referred to the sum of all the peak areas of DNA fragments existing in the standard sample except for the 1800 bp fragment. The degree of the peak area change for the 1800 bp fragment was different from the other 16 step-ladder fragments as discussed later. From Fig. 5.5, the peak areas were linearly increasing in the range of 120 to 300 kVs even at three different injection voltages, but almost no increment of the area was observed at 450 kVs. At V_{inj} of 10 kV, the peak areas increased quickly, whereas the increment of peak area was smaller at higher V_{inj}. This can be interpreted as the result of the DNA damage at high V_{inj}. As the Vt

increased, the amount of injected DNA fragments was increased, but the amount of damaged fragments also increased when the V_{inj} was as large as 20 kV or more.
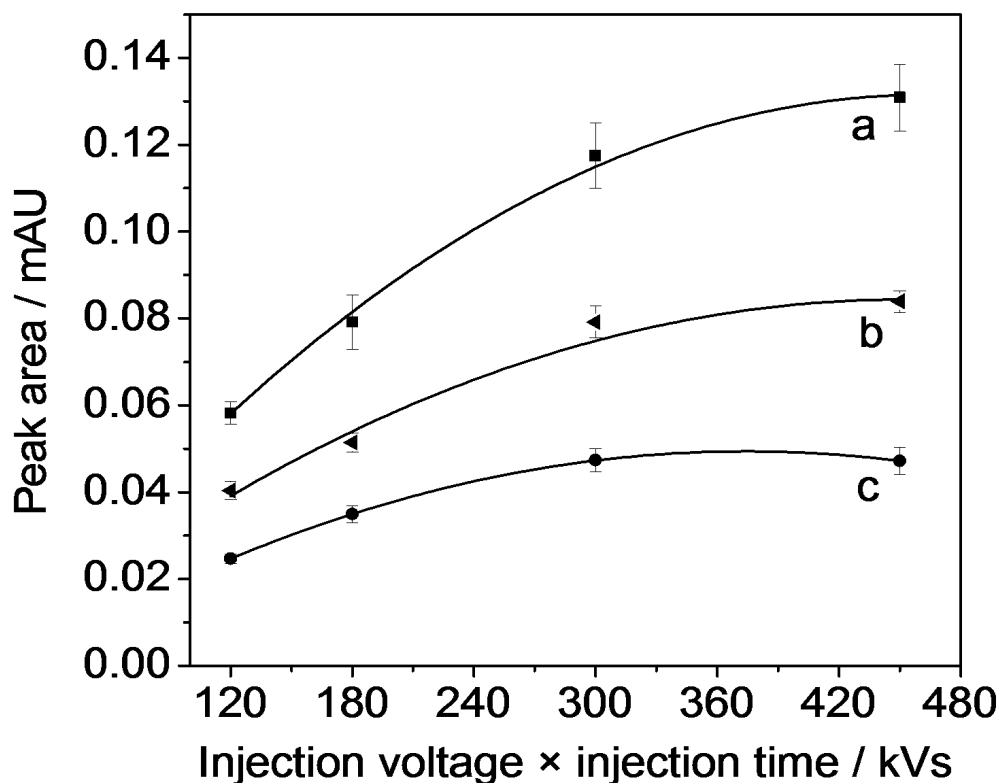

Figure 5.5: Sum of all the peak areas (except for 1800 bp) increased with Vt increasing (average of three experiments). The sample was injected by (a) 10 kV, (b) 20 kV and (c) 30 kV. Injection time was changed to give Vt in the range from 120 to 450 kVs. Sample concentration: 340 µg/L. Others as in Fig. 5.1.

The plateau between 300 and 450 kVs suggested that almost all the DNA fragments occurring in the effective electric field between the tips of electrode and capillary ($D_{e/c}$, 4 mm) were introduced into the capillary but considerable amount was damaged at higher V_{inj}. The DNA fragments existing outside of the effective electric field could not be injected in spite of increase of the injection

time because of slow diffusion. Consequently, if there was no DNA damage caused by high V_{inj}, the sum of the peak areas in Fig. 5.5 should reach the same plateau but this was not the case. The results obtained at low V_{inj} (no damage at 2 and 5 kV) also suggested the validity of our assumption (data were not shown). It should be noted that the observed peak area decrease was not due to electrode reaction, since the DNA fragments originally migrated toward the counter electrode.

5.3.2 Intentional damage of DNA fragments before EKI

From in-depth investigation of the influence of injection voltage shown in the previous section, we analyzed the same DNA samples (step-ladders) by applying voltage before EKI and CGE. As shown in Fig. 5.6A, two platinum wire electrodes set with distance of 1 cm were inserted in a small glass vial, and 2 mL of step-ladder sample with the concentration of 0.34 mg/L were filled into the vial. After preliminary experiments, a voltage of 200 V was applied to the electrodes for up to 20 s. In CGE analysis, in order to avoid the damage induced by V_{inj}, we used a low voltage of 2 kV for the injection of the obtained sample. Fig. 5.6B shows the electropherogram change depending on the voltage application time (0-20 s). Obviously, the DNA fragments were affected by intentionally applied voltage, and the effects increased with time. Although we could not deny the possibility of aggregation during high electric field, but according to the reference [15], the aggregates would start to dissociate just after 10 seconds when the field was turned off. Even if the aggregation would occur in our experiments shown in Fig. 5.6A, there was enough time for its dissociation before CE analysis (at least a few hours and sometimes overnight). So we believed the decrease of peak areas in Fig. 5.1 and 2 was not only due to a transient aggregation but also an irreversible cleavage. Another interesting point was that, in comparison with Fig. 5.1, the peak shape of 1800 bp fragment changed obviously by applying voltage in this simple

device. The injection electrode of Agilent HP^{3D} CE system was hollow and with a cylindrical shape, so that the capillary passed right through the electrode, whereas the electrodes in the simple device were parallel. From the above experiments, we estimated that the damage of DNA fragments was caused by the applied voltage and the damage depended on the electrode configuration.
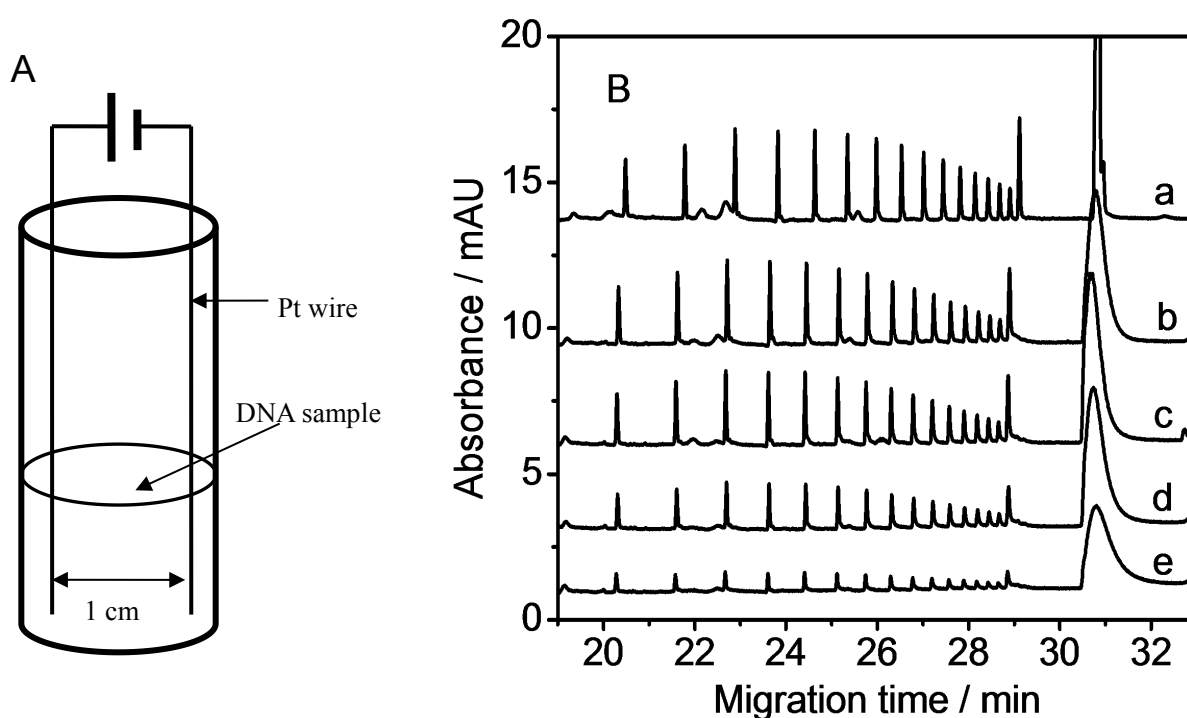

Figure 5.6: (A) Schematic of a device for applying voltage (D.C. 200 V) to step-ladder samples. The distance between the two platinum electrodes was 1 cm. (B) Electropherograms of 50 bp step-ladder DNA samples that were applied by the voltage before EKI. The voltage-applying time were (a) 0 s, (b) 2.5 s, (c) 5 s, (d) 10 s and (e) 20 s. Sample concentration: 340 µg/L. Injection condition: 2kV for 150s. Others as in Fig. 5.1.

5.3.3 Computer simulation of possible electric field during EKI

The computer simulation using CFD-ACE+ was adopted to verify the possibility of generation of high electric field during EKI. Since the mobility of the step-ladders and their interaction with sieving material are unknown, we could not simulate the real case. However, the following simulation is expected to be useful to estimate probable high potential gradient during injection process. The BGE was 0.1 M HCl buffered by 0.2 M Tris. Five dilute analytes (1 µM each) were m50$^-$ to m10$^-$ (mobility, 50～10×10^{-5} cm^{2}V^{-1}s^{-1}). The capillary was surrounded by the cylindrical electrode with a $D_{e/c}$ of 3.6 mm, which was similar to the real condition (4.0 mm). The injection voltage was applied at +100 V between the end of 3 cm capillary and the electrode, which caused ca. 30 V/cm on the assumption of uniform electric field in the current path. As mentioned in the practical experiments, 200 V/cm would cause damage of DNA fragments to a certain degree, and by applying 500 V/cm, almost all of the DNA could be damaged (data are not shown). If the potential gradient was uniform between the two electrodes in the real CE apparatus, a voltage of 10 kV would create in a 50cm capillary of ca. 200V/cm. Unfortunately the situation was not so simple: The uniform assumption was not held, since the conductivity of the BGE filled in a capillary was significantly different from that of the sample solution (in other words, electric resistance of the sample solution was significantly higher than that of the BGE).

Fig. 5.7 shows the model used for computer simulation and the potential gradient profile. Fig. 5.7A and 7C shows a part of the potential gradient profile in the vial along an assumed line that was 500 µm apart from the line penetrating capillary center (it should be noted the outer radius of the electrode was 500 µm) 1 s and 10 s respectively, after starting the injection. The sample volume roughly defined by the tips of capillary and electrode was important, because most of the injected analytes existed there. At the beginning of EKS, as we can see in Fig. 5.7A, the potential near the inlet of capillary was much

higher (>400 V/cm for applying only 100 V at the inlet) than that of other position, which caused by the lower analyte concentration due to the analytes in this area was very quickly introduced into the capillary. After 10 s of EKS, the analytes near the electrode migrated into the capillary and the counter-ion migrated out to the vial from the capillary. As a result, the potential near the inlet was decreased, simultaneously, the potential near the electrode increased. Fig. 5.7B shows the potential gradient profile along the capillary center. Obviously there was a very short zone but with very high potential (> 600 V/cm) at the capillary end, which corresponded to so-called system induced terminator [13]. Accordingly, when DNA fragments migrated across this zone, they might possibly be damaged when the applied voltage was high. In the real experiments, 10 kV or higher voltage was applied for injection, so the potential gradient corresponding to Fig. 5.7 must be several times higher than that of the present simulation depending on the sample concentration and applied voltage. That is, the highest potential in the practical EKI could be over applied voltage (a few kV/cm or more). Thus, the DNA migrating in such high electric field might be damaged in this process.

Furthermore, we assumed that the necessary time to travel across the high potential gradient zones was the other key to cause the damage of the fragments: The damage should be a kind of chemical reaction that needed a reaction time (although we do not know how long), therefore if the traveling time was very short, the sample damage was not so significant. To discuss about the assumption, we made the other experiments using the different electrode configuration ($D_{e/c}$) in the following section.
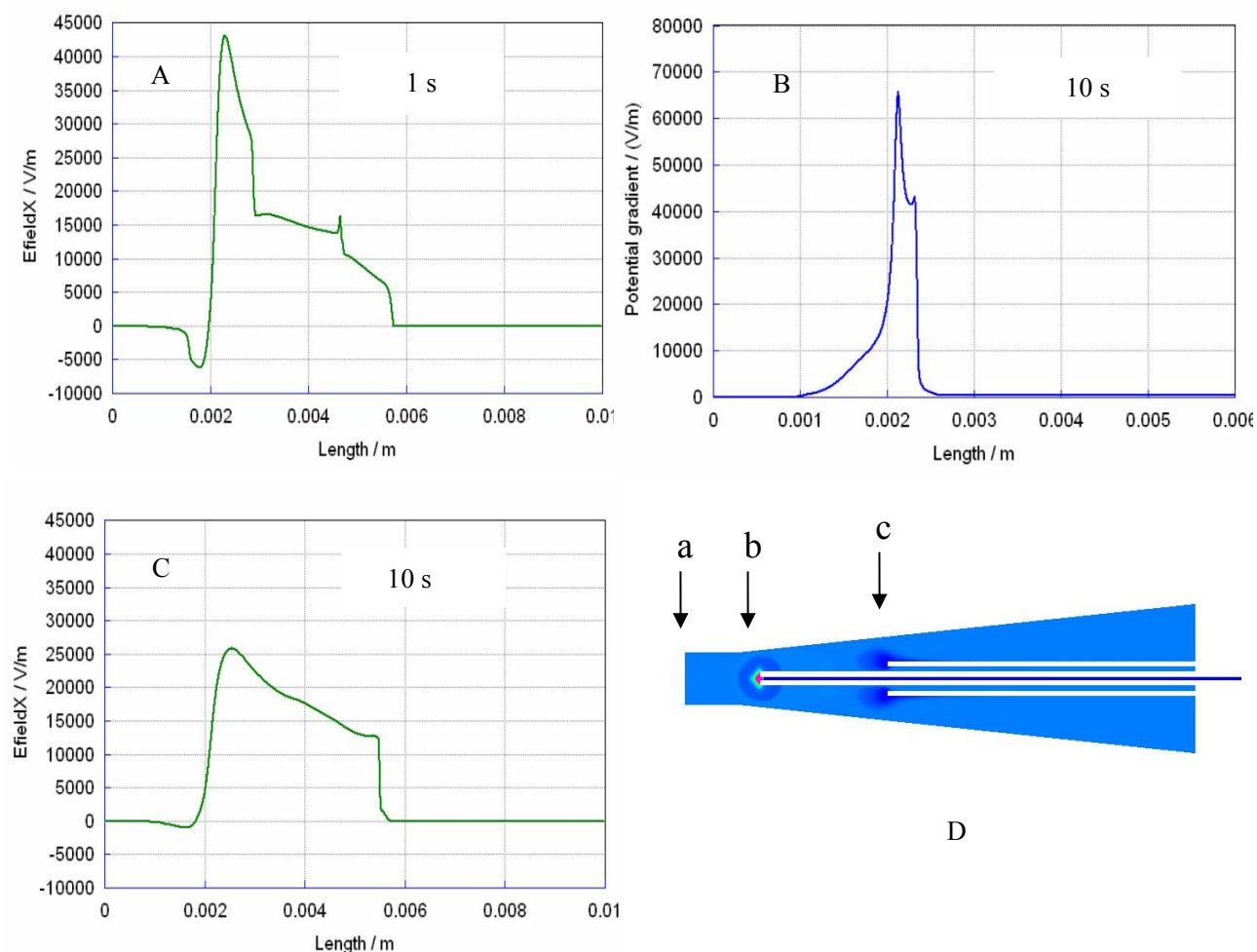
Figure 5.7: Computer simulation of the potential gradient along the assumed line (10 mm in length) that was 500 μm apart from the capillary center starting from the vial bottom, (A) 1 s and (C) 10 s after starting EKS; and along the central line (6 mm in length) of the inner capillary (B) 10 s after EKS. Samples: 5 anions (m10⁻ to m50⁻) 1.0 μM each with 5 μM Na⁺. BGE: 0.1 M HCl buffered by 0.2 M Tris. (D) Simulation model; the capillary was 3 cm long and 100 μm I.D., and the injection voltage applied was 100 V at the end. Distance from the bottom of the vial; (a) 0 mm, (b) 2.13 mm (capillary end), (c) 5.75 mm (electrode end).

5.3.4 DNA damage affected by $D_{e/c}$ and sample concentration

As we already demonstrated in our previous papers [19,20], $D_{e/c}$ was an important factor to improve the amount of injected analytes for high sensitivity. When $D_{e/c}$ and V_{inj} was 4 mm and 2 kV respectively, we assumed that there was no decomposition of the fragments. Fig. 5.8A shows the observed peak area for all fragments. For convenient comparison, we set the sum of the observed peak areas of all fragments (Fig. 5.8B) except for 1800 bp under the above condition as 100 %. If V_{inj} increased to 5 and 10 kV, there was just a little decrease in peak areas (within 10 %). As the V_{inj} increased to 20 kV, DNA damage became obvious, and the sum of peak areas was decreased to 81 %. Furthermore, when V_{inj} reached to 30 kV, more than half of the fragments were damaged maintaining only 42 % of the original peak area.

When we extended the $D_{e/c}$ to 10 mm but keeping the injection voltage at 2 kV, the sample peak areas increased even with the same Vt (e.g. 300 kVs), as shown in Fig. 5.9A. This was because the analytes were efficiently introduced owing to the effective electric field being increased as discussed in our previous paper [21]. In fact, the sum of all fragments peaks was about three times larger than that of the 4 mm case. Anyway, this condition ($D_{e/c}$ was 10mm, V_{inj} was 2 kV) was used as the standard (sum of the peak areas was 100 %) to evaluate the damage shown in Fig. 5.9B: When V_{inj} was even 10 kV, we found the fragments were significantly damaged and the sum of peak area was 48 %. With the V_{inj} increasing to 20 and 30 kV, only 20 and 13 % of DNA fragments were detected, respectively.
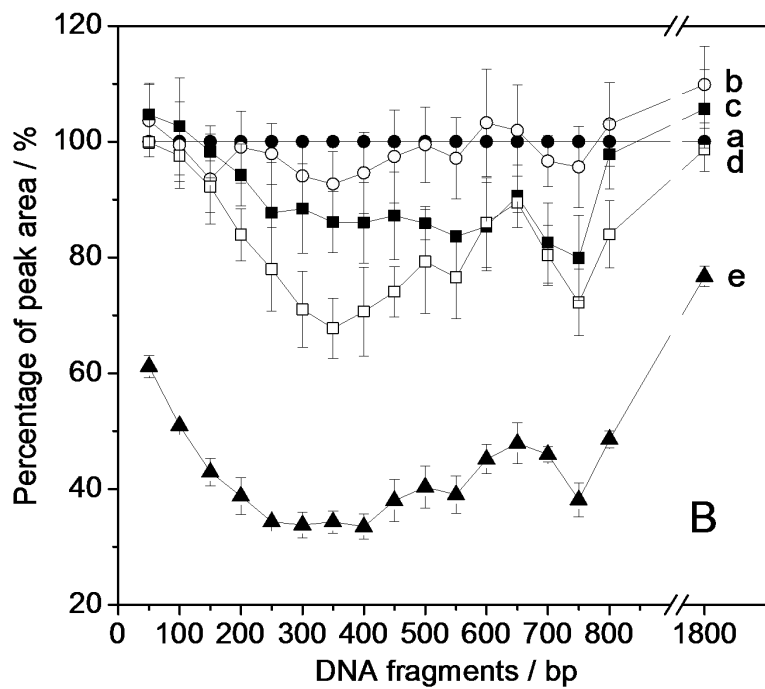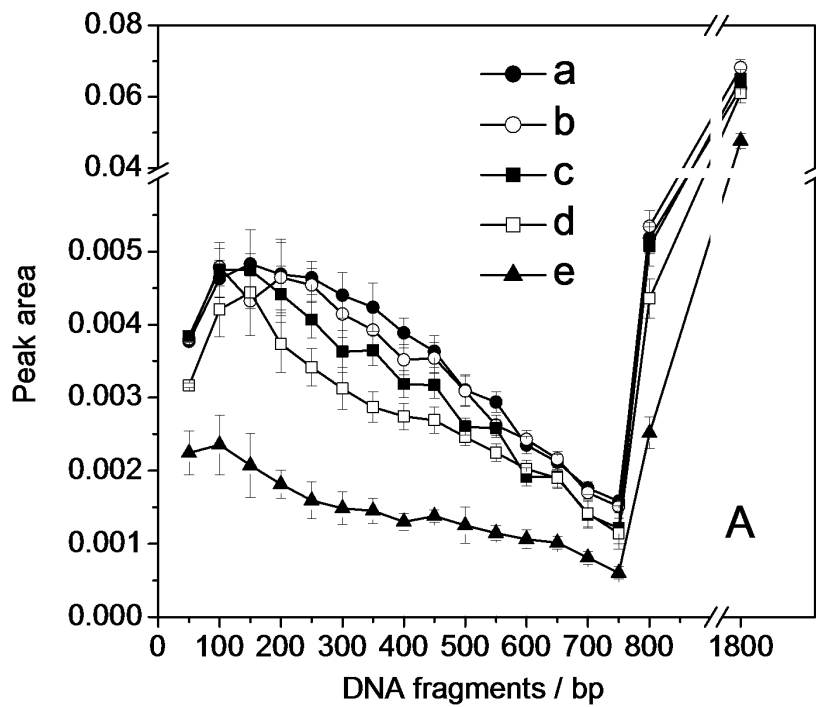
Figure 5.8: (A) Peak areas of all the fragments changed with V_{inj} (Vt was kept constant as 300 kVs); (B) percentage of peak area obtained by varied injection voltages when set the peak area injected by 2 kV for 150 s as 100 %. From curve a to e, the injection conditions were 2 kV for 150 s, 5 kV for 60 s, 10 kV for 30 s, 20 kV for 15 s, and 30 kV for 10 s, respectively. Sample concentration: 170 µg/L. Others as in Fig. 5.1.
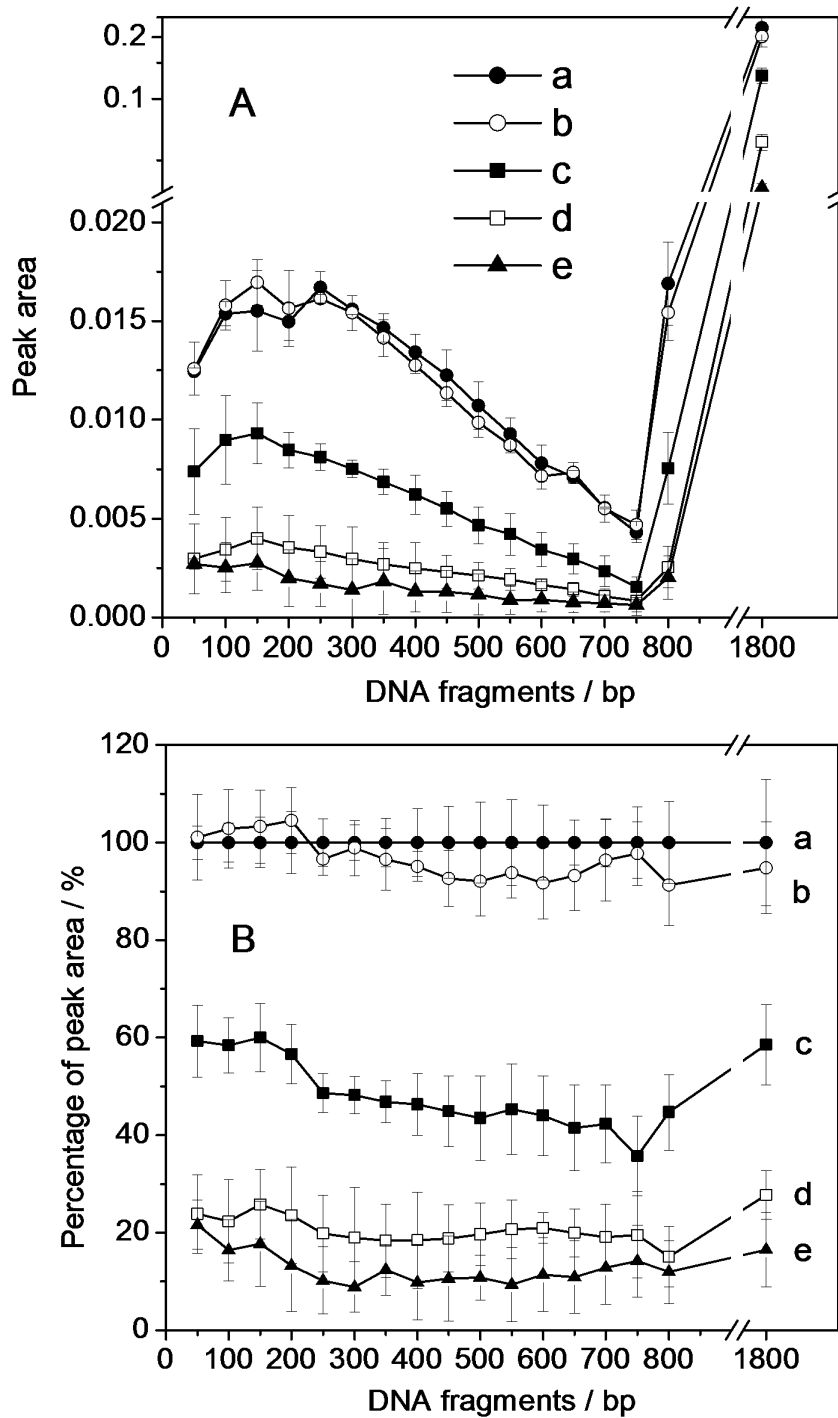
Figure 5.9: (A) Peak areas of all the fragments changed with the V_{inj}; (B) percentage of peak area obtained by varied injection voltages when set the peak area injected by 2kV for 150 s as 100 %. From curve a to e, the injection condition were 2 kV for 150 s, 5 kV for 60 s, 10 kV for 30 s, 20 kV for 15 s, and 30 kV for 10 s, respectively. $D_{e/c}$ was 10 mm. Others as in Fig. 5.8.

It can be seen from Fig. 5.8B that the decrement of peak areas along with the V_{inj} was different for every fragment. In the step-ladder sample, middle size of fragments (200 to 500 bp) were easy to be damaged, and the largest fragment of 1800 bp and minimum fragment of 50 bp in $D_{e/c}$ of 4 mm were hard to be damaged by the electric field. However, as shown in Fig. 5.9B, whatever the size of DNA fragments, the extent of damage caused by V_{inj} was similar when the $D_{e/c}$ increased to 10 mm. According to the computer simulation of potential gradient, we estimated that it might be related with traveling time of the fragments in the high electric field. While the $D_{e/c}$ increased, the velocity of DNA fragments decreased and the fragments near the electrode had to migrate a longer distance to the capillary end, which resulted in a longer traveling time. Therefore, the fragments would be more seriously damaged during traveling across the high potential gradient zone. It should be noted that the short passing time needs high electric field and thus they are closely correlated with each other.

The $D_{e/c}$ of Agilent HP^{3D} CE system could not be longer than 16 mm due to length limitation of electrode and vial. With the aim of longer $D_{e/c}$, we used a CAPI-3300 with a modified electrode, where $D_{e/c}$ could be up to 40 mm [12]. Fig. 5.8 shows the elecropherograms that obtained by using various V_{inj} (2 to 25 kV) but keep the Vt be constant as 1000 kVs. As shown in Fig. 5.10, at such a long De/c of 40 mm, the peak areas of 50 bp step-ladder were significantly decreased with the increasing of V_{inj} from 2 to 20 kV, and other unexpected peaks sometimes could be found between the original DNA peaks. When the V_{inj} increased to 25 kV, the original DNA peaks almost disappeared, occasionally, a huge unexpected peak appeared at 19.5 min. In fact, we had done some experiments to remove the possibility that these peaks were caused by impurities. However, we were still not sure these unexpected peaks came from DNA decomposition due to the poor reproducibility and the unclear mechanism of DNA cleavage by high electric field in aqueous solution until now.
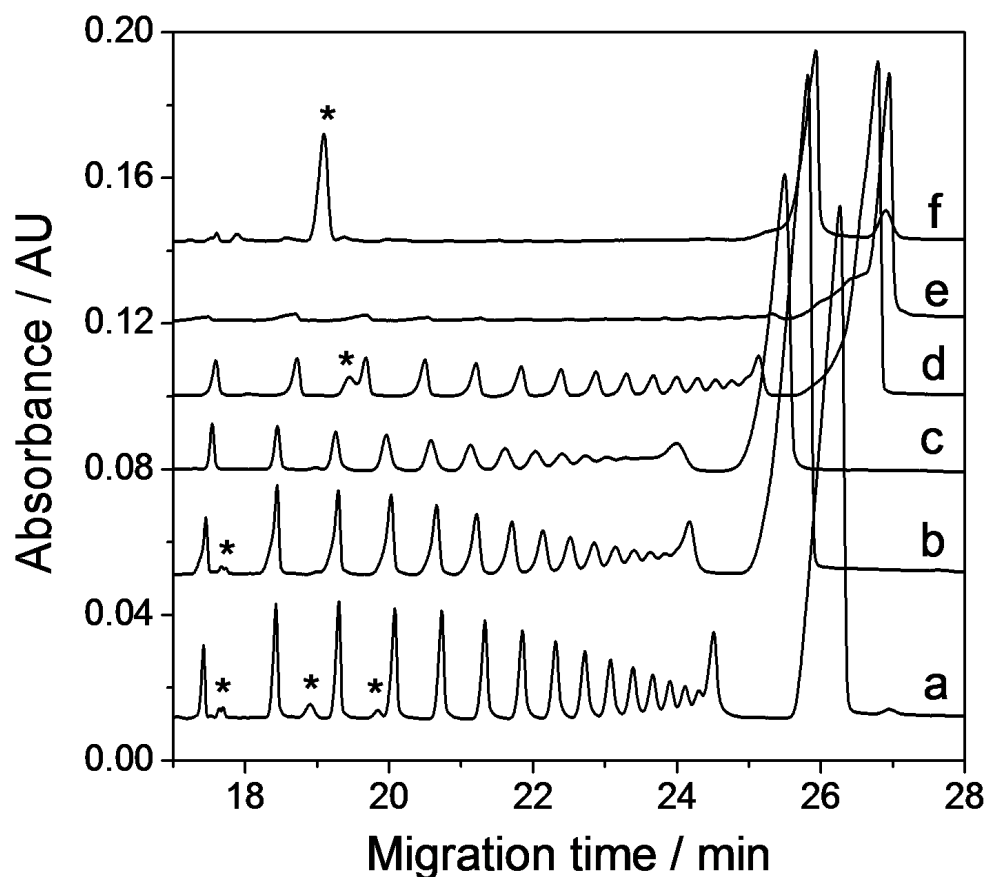
Figure 5.10: Electropherograms of 50 bp step-ladder obtained by CAPI-3300 with the $D_{e/c}$ of 40 mm. Injection conditions: (a) 2 kV for 500 s, (b) 5 kV for 200 s, (c) 10 kV for 100 s, (d) 15 kV 67s, (e) 20 kV for 50 s and (f) 25 kV for 40 s. The peaks marked with asterisks were unknown peaks. Others as in Fig. 5.8.

Another factor might be the sample concentration. Table 1 listed the percentage of peak areas of three V_{inj} obtained by two different concentrations of DNA sample ($D_{e/c}$ = 4 mm). When we set the peak areas obtained by 10 kV as 100 %, as the V_{inj} increased to 30 kV, the percentage of peak areas was 53 % and 39 % for the two concentrations of 3.4 mg/L and 0.17 mg/L, respectively. Such tendency was reproducible within errors. This indicated that DNA

fragments with lower concentration were damaged more easily, since the electric field in a dilute sample was higher than that of concentrated sample.

Table 5-1 The sum of the peak areas[a] depending on the sample concentration and Vt.

Concentration (mg/L)	Vt (kV·s)		
	10kV 30s	20kV 15s	30kV 10s
3.4	100 %	86 %	53 %
0.17	100 %	75 %	39 %

[a] The sum of peak areas obtained by 10 kV for 30 s was set as the comparison standard ($D_{e/c}$, 4 mm). The sum did not contain the peak area of 1800 bp.

5.4 Summaries

The study presented here highlighted that the DNA fragments were affected by high V_{inj} during EKI. In addition to the aggregation phenomena already confirmed by Song et al., we have shown the possible DNA cleavage under high potential field for the first time owing to high-sensitivity of EKS-CGE. However, the mechanism of such DNA fragmentation in aqueous solution is still not clear until now. Nonetheless some recommendations for avoiding this unwanted process could be given: Although longer $D_{e/c}$ could cause a larger space of effective electric field in a sample vial with the objective to increase sensitivity, it also brought about a stronger damage for DNA fragments, since the time for which the analytes travel across high electric field during EKI increased. At $D_{e/c}$ of 4 mm, the V_{inj} of 20 kV resulted notable damage (about 20

%) of DNA in comparison with 2 kV. When $D_{e/c}$ was increased to 10 mm, half of fragments was affected at V_{inj} of 10 kV, furthermore, at $D_{e/c}$ of 40 mm, we could find significant damage even at 5 kV. The factors that affected the potential field in sample vial during EKI would affect the DNA damage, thus, low sample concentration resulted in a high potential field during EKI, which would make DNA fragments easily to be damaged. Therefore, the injection voltage should be thoughtfully chosen, especially for diluted DNA samples. However, even at high electric field, not all of the DNA fragments were affected in our experiments. Our result is also applicable to the situation when the DNA sample contains matrix ions, which may protect the DNA fragments from serious damage by decreasing the electric field. Furthermore, in the usual gel-format separation, such damage might not happen as far as the sample concentration is not very low (see Fig. 5.5-3 in Supplementary for gel electrophoresis).

5.5 References

[1] Mitnik, L., Novotny, M., Felten, C., Buonocore, S., Koutny, L., Schmalzing, D., *Electrophoresis* 2001, 22, 4104-4117.

[2] Righetti, P. G., Gelfi, C., D'Acunto, M. R., *Electrophoresis* 2002, 23, 1361-1374

[3] Hirokawa, T., Okamoto, H., Gaš, B., *Electrophoresis* 2003, 24, 498-504.

[4] Righetti, P. G., Gelfi, C., *Electrophoresis* 1997, 18, 1709-1714.

[5] Baba,Y., *J. Chromatogr. B* 1996, 687, 271-302

[6] Butler, J. M., Buel, E., Crivellente, F., McCord, B. R., *Electrophoresis* 2004, 25, 1397-1412.

[7] Xu, Z. Q., Hirokawa, T., Nishine, T., Arai, A., *J. Chromatogr. A,* 2003, 990, 53-61.

[8] Xu, Z. Q., Nishine, T., Arai, A., Hirokawa, T., *Electrophoresis,* 2004, 25, 3875-3881.

[9] Hirokawa, T., Takayama, Y., Arai, A., Xu, Z. Q., *Electrophoresis,* 2008, 29, 1829-1835.

[10] Xu, Z. Q., Esumi, T., Ikuta, N., Hirokawa, T., J. *Chromatogr. A,* 2009, 1216, 3602-3605.

[11] Hirokawa, T., Koshimidzu, T., Xu, Z. Q., *Electrophoresis,* 2008, 29, 3786-3793.

[12] Xu, Z. Q., Kawahito, K., Ye, X. X., Timerbaev, A. R., Hirokawa, T., *Electrophoresis,* 2011, 32, 1195-1200.

[13] Ye, X. X., Mori, S., Yamada, M., Inoue, J., Xu, Z. Q., Hirokawa, T., *Electrophoresis*, 34, 2013, 583-589.

[14] Han, F. T., Huynh, B. H., Ma, Y. F., Lin, B. C., *Anal. Chem.,* 1999, 71, 2385-2389.

[15] Song, L., Maestre, M. F., *J. Biomol. Struct. Dyn.* 1991, 9, 525-536.

[16] Sonntag, C. V., *Taylor & Francis, London* 1987.

[17] Berdys, J., Anusiewicz, I., Skurski, P., Simons, J., *J. Am. Chem. Soc.,* 2004, 126, 6441-6447.

[18] Zheng, Y., Cloutier, P., Hunting, D. J., Sanche, L., Wagner, J. R., *J. Am. Chem. Soc.,* 2005, 127, 16592-16598.

[19] Xu, Z. Q., Koshimidzu, E., Hirokawa, T., *Electrophoresis,* 2009, 30, 3534-3539.

[20] Xu, Z. Q., Nakamura, K., Timerbaev, A. R., Hirokawa, T., *Anal. Chem.,* 2011, *83*, 398-401.

[21] Xu, Z. Q., Timerbaev, A. R., Hirokawa, T., *J. Chromatogr. A,* 2009, 1216, 660-670.

Chapter 6: Impact of BGE carry-over during injection

6.1 Introduction

Samples are introduced into the capillary for separation by electrokinetic injection (EKI) and hydrodynamic injection that both having advantages and disadvantages. EKI is widely used to enrich a low concentration sample in a very simple and effective way when the conductivity of sample is much lower than that of BGE. Chien and Burgi contributed many initial studies on EKI to elucidate the stacking mechanism and to quantify the injected amounts [1, 2]. In EKI, the sample introduction process is driven by a combined effect of electrophoretic mobility and EOF and has an intrinsically stacking character when the sample is dilute (as in field amplified sample injection). Being dependent on the applied voltage and ionic strength of the sample solution and the BGE [3], EKI is always regarded as having a poorer repeatability than hydrodynamic injection. Regarding the repeatability of peak area during EKI process, Boer and Ensing earlier reported [4] the influence of the sample volume and the position of electrode and concluded that good repeatability could be obtained by using such a configuration in which the capillary end stood back in the cylindrical electrode, although with no great improvement of sensitivity.

For analysis of very diluted sample, electrokinetic injection combined with on-line preconcentration technology such as electrokinetic supercharging (EKS) [5] is most to improve the sensitivity. In EKS-CZE like in other CE methods using electrokinetic injection, the repeatability of peak areas is generally inferior to that attained with hydrodynamic or hydrostatic injection. This is mainly due to variations of the distance between an electrode and the capillary end, as well as minor effects related to the temperature changes and the convection of the sample solution in sample reservoir. The impact of

distance variation might be most serious, when the sample volume is small and the electrode configures a thin Pt wire that could be accidentally bent during sampling [6]

In DNA analysis, the high diluted sample contamination by a viscous background electrolyte (BGE) [7], carried unintentionally by the capillary or the electrode (along with the contamination from laboratory environment), impairs injection efficiency. To reduce the contamination, the capillary and the electrode should be rinsed thoroughly by pure water. The application of voltage while rinsing was shown to wash off the BGE components more effectively. In this chapter, our considerable research into addressing these issues and the optimized experimental procedure to improve injection efficiency and gain good EKS repeatability will be discussed. To underscore experimental results, a 2D simulation using CFD-ACE+ software will be undertaken under the assumption that the capillary and the electrode are covered by a thin film of the BGE.

6.2 Materials and methods

All experiments were carried out on the Agilent HP^{3D} CE system (Agilent Technologies, Waldbronn, Germany). Other conditions as described in Chapter 4. All the DNA sample and reagents were the same as in Chatper 5.

6.3 Results and discussion

6.3.1 Impact of BGE carry over on injection efficiency

EKI is performed by applying the voltage between the ends of capillary. Usually, analyte enters the capillary by both migration and pumping action of

the EOF. A unique property of EKI is that the quantity loaded is dependent on the mobility of the individual solutes. Discrimination occurs for ionic species since the more mobile ions are loaded to greater extent than those that are less mobile. The quantity injected, Q (g or moles), can be calculated by the equation:

$$Q = \frac{(\mu_e + \mu_{EOF})V\pi r^2 Ct}{L}$$
(6.1)

Where μ_e represents the electrophoretic mobility of the analyte, μ_{EOF} is EOF mobility, V is voltage, r is capillary radius, C is analyte concentration, t is injection time and L is the total length of capillary. Variations in conductivity, which can be due to matrix effects such as a large quantity of an undetected ions such as sodium or chloride, results in differences in voltage drop and quantity loaded. Due to these phenomena, electrokinetic injection is generally not as reproducible as its hydrodynamic injection.

In the case of DNA analysis, migration of solutes predominated the injection. Since the capillary is usually dipped into the BGE vial for filling before injection, the BGE may produce liquid film on both the capillary and the electrode. This film is rather stable in the case of DNA analysis due to a viscous BGE fortified with a sieving material is typically used in CGE. If the inlet of the capillary and electrode is placed into the sample vial for sampling without any cleaning steps, the diluted sample will be contaminated by the attached BGE, then reduce the efficiency of the injection. To remove this BGE film, the capillary and the electrode are usually dipped into a vial filled with pure water. Electropherograms in Fig. 6.1 were obtained by using different washing methods before injection: a shows the impact of residual BGE to injection efficiency, As the result of BGE carry-over, the injection current would be carried mainly by the BGE (not analyte) ions so that injection efficiency for the analytes inevitably decreases.
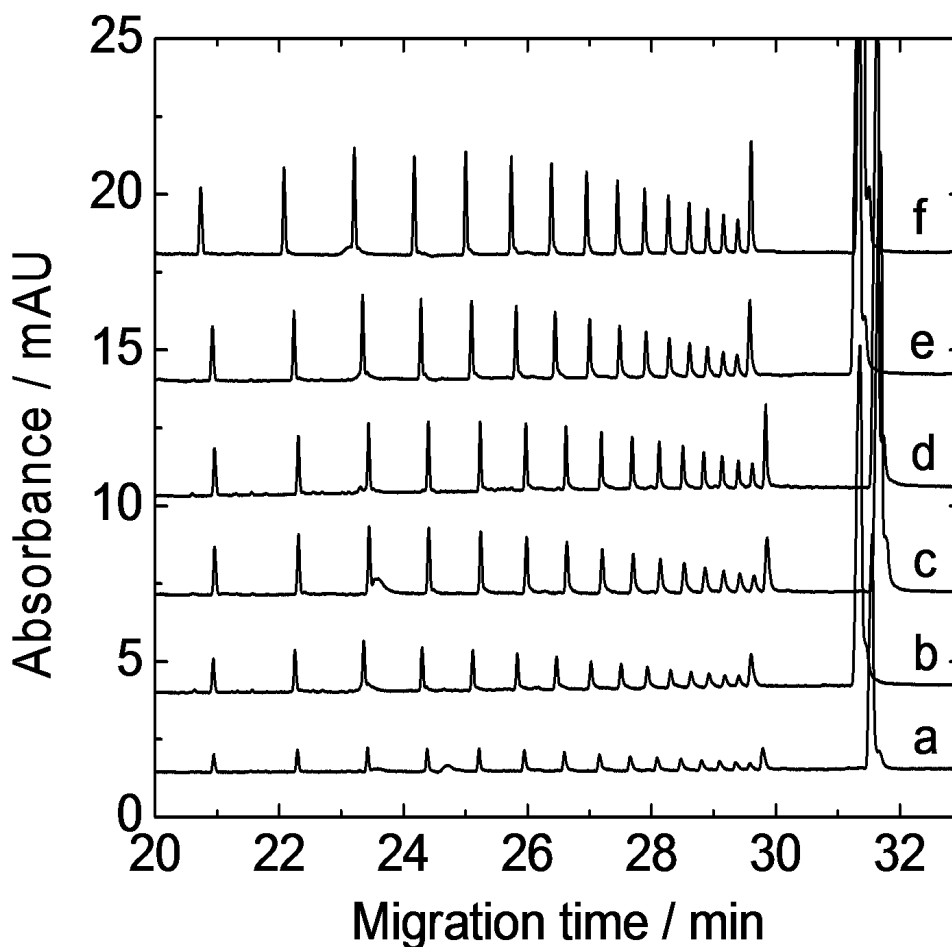
Figure 6-1: Electropherograms of 50 bp step-ladder samples obtained by using different washing method before injection conditions: dip the electrode in in water vial for (a) 0 min; (b) 0.1 min; (c) 0.5 min (d) 1 min; (e) 2 min; and (f) was applied -10 kV for 10 s after dipped in to water for 1 min. Sample concentration: 170 µg/L. $D_{e/c}$ was 4 mm. Separation voltage: -10 kV.

The most common cleaning method was to dip the inlet of the capillary and electrode into a water vial for a while. However, it is doubtful that only immersion is enough to eliminate impact, since the viscous BGE used in DNA

analysis was not easy to completely remove. Therefor, two cleaning methods were used for comparison: (A) dip into water vial for 0-2 min; (B) dip into water vial for 1 min and then applied voltage of -10 kV for 10 s. Fig.6.2 illustrate the influence of cleaning methods on peak areas. The sum of peak areas was the average of eight parallel determinations, which obtained by peak area (mAU·min) divided by migration time (min). It is obvious that the peak area increased with the washing time. The peak area referred to latter method (dip into water vial for 1 min and applied -10 kV for 10 s) was more than two times lager than that of no washing step (dip in to water vial for 0 min), which indicated that the application of voltage while rinsing was shown to wash off the BGE components more effectively.
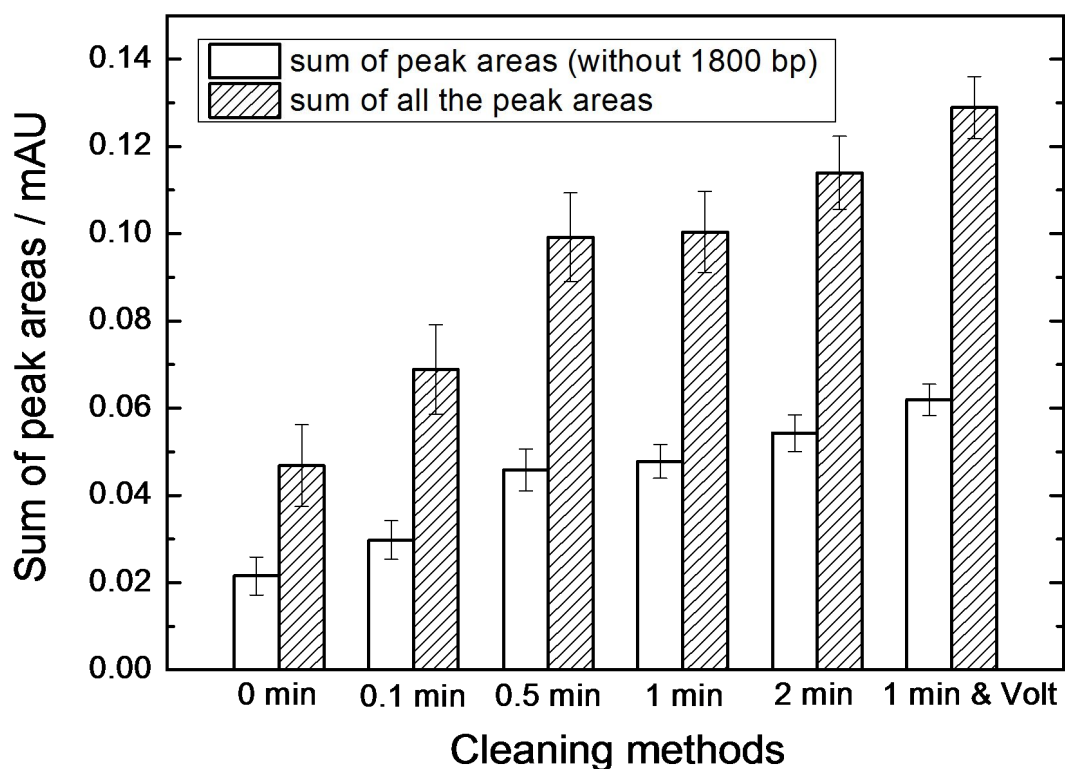

Figure 6.2: Sum of Peak area of 50 bp step-ladder samples obtained by using different washing method before injection conditions. The washing methods were shown in the figure. Other as in Fig. 6-1
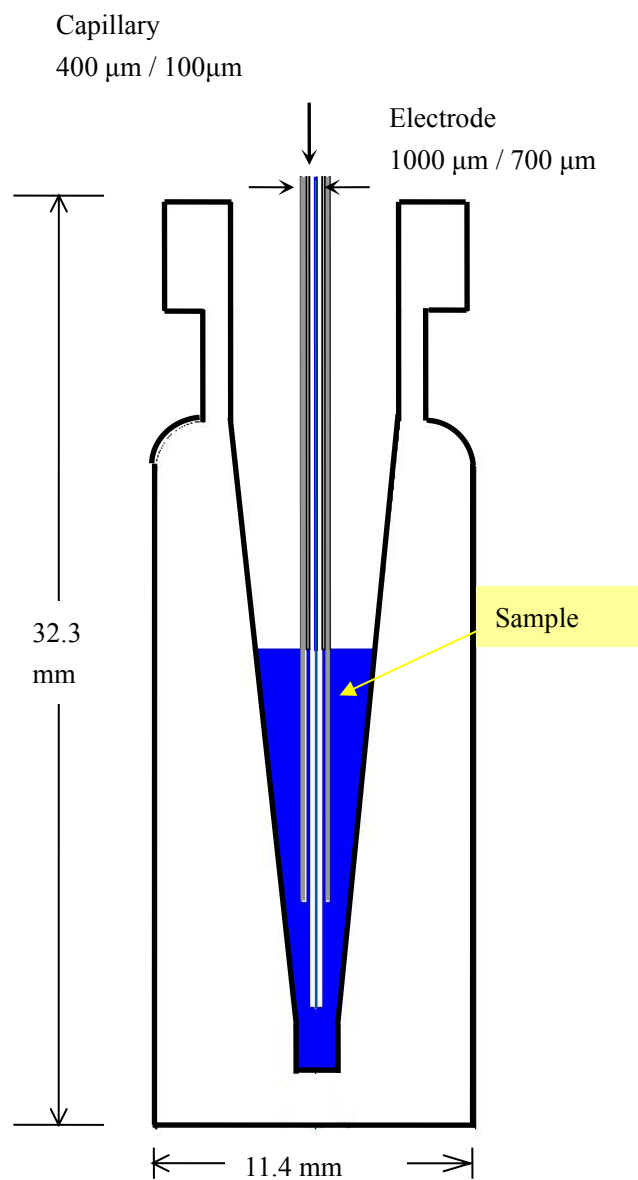
Figure 6.3: Vial of the same dimensions as the real one for computer simulation. The $D_{e/c}$ was at 3.62 mm and the volume of sample is 100 µL.

6.3.2 Computer simulation for BGE carry-over

Computer simulation was adopted in our study to explore the condition that a thin film was attached to the electrode and capillary end. At the step of filling capillary with BGE, the end of electrode and capillary should dip into the BGE vial, so there was some residual BGE attached to the electrode and capillary when we take them out. Here, we assumed the thickness of attached BGE film was 20 µm. The simulated components of BGE and sample are the typical model for achieving EKS process, thus it well describes the movement and preconcentration behaviors of the analytes. The capillary surrounded by the cylindrical electrode owns one unique feature that $D_{e/c}$ in Fig. 6.3

Visual simulation of Figure 6.4 illustrates the concentration profiles of m50-, including the different time for two conditions: with and without attached BGE film. It should be noted that the same voltage leaded to much different sample introduction in the vial due to BGE carry-over. In the case of BGE carry-over, the co-ions of BGE will injected with sample, simultaneously. As shown in equation 6.1, the quantity of injected analytes is proportional to mobility, if the mobility of co-ion was higher than that of sample, the co-ions will be introduced prior to sample ions.

Fig. 6.5 puts another way to verify the injected amount significantly affected by BGE carry-over. As in Fig. 6.5A, the $D_{e/c}$ was doubled from 3.62 mm to 7.24 mm, the final injected amount of five model ions were more than double, although the EKS time was longer since the field strength decreased. Compare with Fig. 6.5A and B, when the $D_{e/c}$ was 3.62 mm, the injected amount with BGE carry-over was about 1 % of that of without BGE effect. The BGE carry-over not only decreased the injected amount of sample, but also hindered the EKS efficiency.
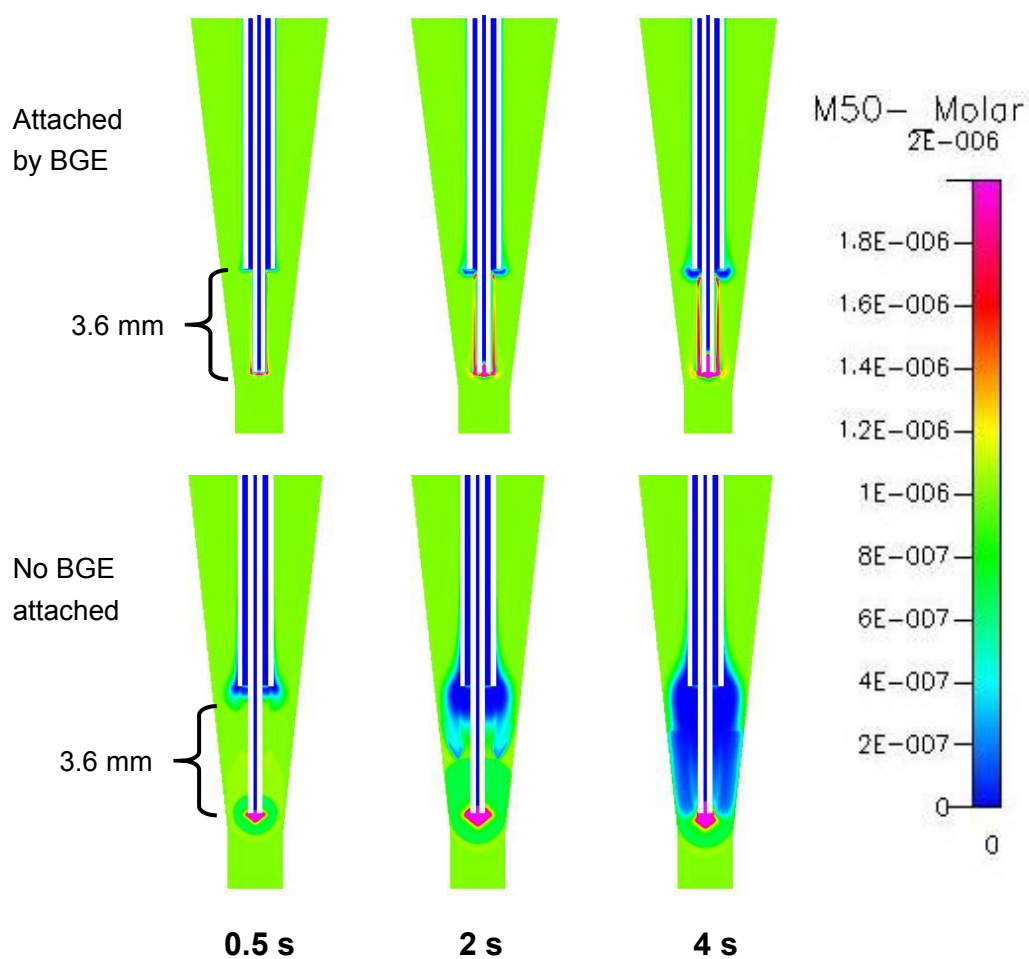
Figure 6.4: Illustration of m50$^-$ concentration profile varied with time after applying voltage when the $D_{e/c}$ was 3.62 mm. The time represented the analyte depletion speed by simulation. The color corresponds to the concentration values as scaled.
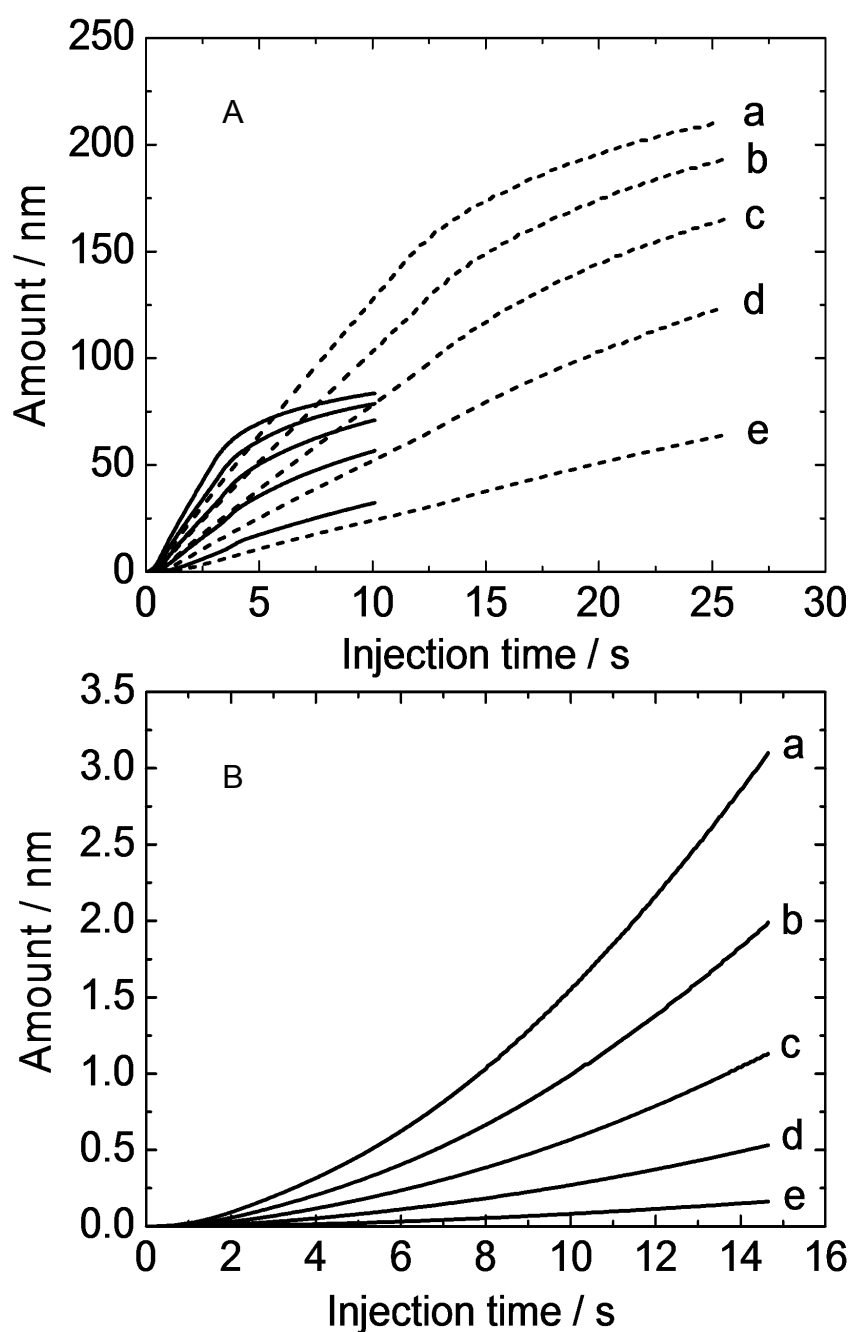
Figure 6.5: Simulated results of the injected amount by using the hollow electrode: (A) without BGE carry-over effect; (B) with BGE carry-over effect. The solid and dotted lines represent the $D_{e/c}$ were 3.62 mm and 7.24 mm, respectively. in Fig. 6.4 The Samples: the curve from top to bottom (curve a to e) represents model anions with five different mobility (m10⁻, m20⁻, m30⁻, m40⁻ and m50⁻), each at 1.0 µM. BGE: 50 mM HCl and 100 mM Tris. Others as in Fig. 6.4.

6.3.3 Repeatability of peak areas in EKI

BGE carry-over not only greatly reduces the sensitivity, but also lowers reproducibility. The quantitative repeatability was tested for the standard DNA sample by using different washing methods before injection: (A) dip in water vial for 0-2 min; (B) apply voltage of -10 kV for 10 s after dipped in water vial for 1 min. As shown in Table 6.1, the obtained RSD of the peak areas (n=4) was improved from 18.9 % to 6.2 % when the washing time increased from 0 to 2 min. By applying voltage to clean the electrode and capillary ends, the RSD of peak areas can be improved to 6.4 %.

Table 6.1: RSD of DNA fragments (n = 8)

		Method A				Method B
Cleaning methods	no washing	0.1 min	0.5 min	1 min	2 min	1 min & Volt
RSD (n=4)	18.9 %	13.5 %	9.7 %	7.3%	6.2 %	6.4 %

Method A: dip in water vial for 0-2 min;

Method B: apply voltage of -10 kV for 10 s after dipped in water vial for 1 min.

In fact, the same water vial was used in a continuous experiment. However, the efficiency of washing step will impair due to repeated use. In order to discuss the influence of water vial on reproducibility and optimize the cleaning method, the repeatability of four washing methods were compared in

Table 6.2: a) Wait for 1 min in the same vial; b) wait for 1 min and applied voltage of -10 kV for 10 s in the same water vial; c) wait for 1 min in respective vial; d) wait for 1 min and applied voltage of -10 kV for 10 s in the respective water vial. Certainly, the method of applying voltage was superior to the method of only dip into water. And using respective vial for each injection could greatly improve the repeatability.

Table 6.2: Repeatabilities for the same water vial and respective water vial

Cleaning conditions	1 min	1 min & Volt
Same water vial	16.4 %	13.9 %
Respective water vial	8.6 %	7.4 %

6.3 Summaries

In our continuing research on using EKS-CGE for high sensitivity DNA analysis, it was demonstrated that the relative injected amount of analytes can be increased by optimized the washing method before EKI, and thereby the LODs were apparently improved. Such a viscous BGE used in DNA separation seriously affected the injection efficiency and quantitative repeatability. The proposed washing method could improve the sensitivity and repeatability, especially for the very dilute sample with small conductivity which was easily contaminated.

6.4 References

[1] Chien, R., Burgi, D. S., *J. Chromatogr. A* 1991, *559*, 141-152.

[2] Chien, R., *Anal. Chem.* 1991, *63*, 2866-2869.

[3] Gaspar, A., Gabor, L., *J. Chromatogr. A* 2005, *1091*, 163-168.

[4] Boer, T. D., Ensing, K., *J. Chromatogr. A* 1997, *788*, 212-217.

[5] Hirokawa, T., Okamoto, H., Gas, B., *Electrophoresis* 2003, *24*, 498-504.

[6] Hirokawa, T., Koshimidzu, T., Xu, Z. Q., *Electrophoresis,* 2008, 29, 3786-3793.

[7] Ye, X. X., Mori, S., Yamada, M., Inoue, J., Xu, Z. Q., Hirokawa, T., *Electrophoresis*, 34, 2013, 583-589.

Chapter 7: Conclusions

High performance analytical method for DNA fragments by capillary electrophoresis has been developed in this dissertation. By adopting EKS preconcentration and modifying the electrode configuration, the sensitivity of both REs and DNA fragments were greatly improved in spite of use of direct UV detection. It was assessed that EKS was an effective technique to increase the concentration detection limit of DNA fragments when an ultralow-viscosity sieving buffer was used. We also explored some important phenomenon such as DNA aggregation and cleavage during high electric field and BGE carry-over during electrokinetic sample injection, which greatly affected the performance of DNA analysis.

EKS-CZE for rare-earth metal ions

A further improvement of electrokinetic supercharging (EKS) methodology has been proposed, with the objective to enhance the sensitivity of the conventional CZE-UV method down to a single-digit part per trillion (ppt) level. The advanced EKS procedure is based on a novel phenomenon displaying the formation of a zone with an increased concentration of the hydrogen ion, capable to perform the function of a terminator, behind the sample zone upon electrokinetic injection. In combination with a visualizing co-ion of BGE, protonated 4-methylbenzylamine, acting as the leading ion, such a system-induced terminator effected the transient ITP state to efficiently concentrate cationic analytes prior to CZE. Furthermore, to amass more analyte ions within the effective electric field at the injection stage, a standard sample vial was replaced with an elongated vial that allowed the sample volume to be increased from 500 to 900 mL. Alongside, this replacement made the upright distance between the electrode and the capillary tips extended to

40.0mm to achieve high-efficiency electrokinetic injection. The computer simulation was used for profiling analyte concentration, pH, and field strength in order to delineate formation of the terminator during sample injection. The proposed preconcentration strategy afforded an enrichment factor of 80 000 and thereby the LODs of rare-earth metal ions at the ppt level, e.g. 0.04 nM (6.7 ng/L) for erbium(III).

EKS-CGE for DNA fragments

Aiming to high sensitivity DNA analysis by CGE, electrokinetic supercharging (EKS) approach was adopted in this article. EKS is known as an online preconcentration technique that combines electrokinetic sample injection (EKI) with transient ITP (tITP). Herein, two factors of buffer viscosity and electrode configuration were studied to further improve EKS performance. An ultralow-viscosity Tris-Boric acid-EDTA (TBE) buffer solution, consisted of 2% low-molecular-weight hydroxypropyl methyl cellulose (HPMC) and 6% mannitol and with pH 8.0 adjusted by boric acid, was applied. The boric acid wouldmake a complex with mannitol and generates borate polyanion, which acts as the leading ion for tITP process. The new electrode configuration, a Pt ring around capillary, was modified on Agilent CE system to lead large amount sample introduction during EKS. The standard DNA sample of X174/HaeIII digest was used to evaluate the qualitative and quantitative abilities of the proposed strategy. The 170 000-fold highly diluted sample at concentration of 3.0 ng/mL was enriched by EKS and detected by normal UV detection method. The obtained LOD of the weakest peak of 72 bp fragment was around 7.7 pg/mL, apparently improved more than 10 000-fold in comparison with conventional CGE with UV detection.

DNA aggregation and cleavage during EKI

The phenomenon of peak area decrease due to high injection voltage (V_{inj}, e.g., 10 to 30 kV, 200–600 V/cm in the 50 cm capillary) was found in the analysis of very dilute DNA fragments (below 0.2 mg/L) by using high-sensitive electrokinetic supercharging (EKS)-CGE. The possibility of DNA cleavage in aqueous solution was suggested, in addition to the aggregation phenomenon that is already known. The analysis of intentionally voltage-affected fragments (at 200 V/cm) also showed decreased peak areas depending on the time of the voltage being applied. Computer simulation suggested that a high electric field (a few kV/cm or more) could be generated partly between the electrode and the capillary end during electrokinetic injection (EKI) process. After thorough experimental verification, it was found that the factors affecting the damage during EKI were the magnitude of electric field, the distance between tips of electrode and capillary ($D_{e/c}$), sample concentration and traveling time during EKI in sample vials. Furthermore these factors are correlating with each other. A low conductivity of diluted sample would cause a high electric field (over a few hundred volts per centimeter), while the longer $D_{e/c}$ results in a longer traveling time during EKI, which may cause a larger degree of damage (aggregation and cleavage) on the DNA fragments. As an important practical implication of this study, when the dilute DNA fragments (sub mg/L) are to be analyzed by CGE using EKI, V_{inj} should be kept as low as possible.

Impact of BGE carry-over during EKI

In our continuing research on using EKS-CGE for high sensitivity DNA analysis, it was demonstrated that the relative injected amount of analytes can be increased by optimized the washing method before EKI, and thereby the LODs were apparently improved. Such a viscous BGE used in DNA separation seriously affected the injection efficiency and quantitative repeatability. The proposed washing method could improve the sensitivity and repeatability,

especially for the very dilute sample with small conductivity which was easily contaminated.

In conclusion, EKS-CGE for high-sensitive analysis of DNA fragments has been developed in this dissertation. EKS is an effective preconcentration method to improve the sensitivity for dilute samples even by UV detection. Comparing with LIF detection, there are many advantages such as low cost and simple procedure.

ACKNOWLEDGMENTS

CURRICULUM VITAE

Name: Xiaoxue Ye

Date of Birth: November 20, 1984

Place of Birth: Chongqing City, China

E-mail: yexiaoxue@hotmail.com

Education:

1. Octorber, 2010-November, 2013

Doctor of Engineering, Hiroshima University (Japan), major in Applied Analytical Chemistry (this dissertation).

2. September, 2007-June, 2010

Master of Science, Central China Normal University (China), major in Analytical Chemistry.

3. September, 2007-June, 2010

Bechelor of Science, Central China Normal University (China), major in Chemistry.

RELATIVE PUBLICATIONS

(1) Zhongqi Xu, Kouji Kawahito, Xiaoxue Ye, Andrei R. Timerbaev,Takeshi Hirokawa, Electrokinetic supercharging with a system-induced terminator and an optimized capillary versus electrode configuration for parts-per-trillion detection of rare-earth elements in CZE, *Electrophoresis*, Vol.32, 1195-1200, April, 2011.

(2) Xiaoxue Ye, Satomi Mori, Mihoro Yamada, Junji Inoue, Zhongqi Xu, Takeshi Hirokawa, Electrokinetic supercharging preconcentration prior to CGE analysis of DNA: Sensitivity depends on buffer viscosity and electrode configuration, *Electrophoresis*, Vol.34, 583-589, January, 2013.

(3) Xiaoxue Ye, Satomi Mori, Zhongqi Xu, Shinjiro Hayakawa, Takeshi Hirokawa, DNA aggregation and cleavage in CGE induced by high electric field in aqueous solution accompanying electrokinetic sample injection, *Electrophoresis*, accepted, August, 2013.